SANDIA REPORT

DUPLICATE

Hydrogeochemical Studies of the Rustler Formation and Related Rocks in the Waste Isolation Pilot Plant Area, Southeastern New Mexico

M. D. Siegel, S. J. Lambert, K. L. Robinson, Editors

Hydrogeochemical Studies of the Rustler Formation and Related Rocks in the Waste Isolation Pilot Plant Area, Southeastern New Mexico

M. D. Siegel, S. J. Lambert, and K. L. Robinson, Editors
Sandia National Laboratories
Albuquerque, New Mexico 87185

ABSTRACT

Chemical, mineralogical, isotopic, and hydrological studies of the Culebra dolomite member of the Rustler Formation and related rocks are used to delineate hydrochemical facies and form the basis for a conceptual model for post-Pleistocene groundwater flow and chemical evolution. Modern flow within the Culebra in the Waste Isolation Pilot Plant (WIPP) area appears to be largely north-to-south; however, these flow directions under confined conditions are not consistent with the salinity distribution in the region surrounding the WIPP Site. Isotopic, mineralogical, and hydrological data suggest that vertical recharge to the Culebra in the WIPP area and to the immediate east and south has not occurred for several thousand years. Eastward-increasing $^{234}U/^{238}U$ activity ratios suggest recharge from a near-surface Pleistocene infiltration zone flowing from the west-northwest and imply a change in flow direction in the last 30,000 to 12,000 years.

Culebra groundwaters are in chemical equilibrium with gypsum and are undersaturated with halite and anhydrite. A partial-equilibrium model for the chemical evolution of the groundwater suggests that Na, Cl, Mg, K, and SO_4 are added to the Culebra by dissolution of evaporite salts in adjacent strata. Equilibrium is maintained with gypsum and calcite, but dolomite supersaturation increases as the salinity of the water increases. Stable-isotope compositions of carbonates are consistent with this model and indicate that no recrystallization of dolomite in equilibrium with the groundwater has occurred. Major and minor element correlations are consistent with several plausible mechanisms of water/rock interaction, including sorption of lithium and boron by clays and dissolution of Mg-rich clays.

ACKNOWLEDGMENTS

GENERAL CONTENTS

iv

EXECUTIVE SUMMARY

An understanding of the geological history of the Rustler Formation in the northern Delaware Basin of southeastern New Mexico is considered fundamental to the evaluation of the ability of the bedded evaporite environment at the Waste Isolation Pilot Plant (WIPP) to isolate waste radionuclides from the accessible environment for long periods of time. The Rustler is deemed important because it (1) is the uppermost evaporite-bearing unit in the Ochoan (Permian) sequence, (2) is experiencing active dissolution where it outcrops west of the WIPP Site, (3) immediately overlies the Salado Formation, where the WIPP Facility is being mined, and (4) contains interbeds of brittle fractured rock that contain the most abundant and regionally persistent occurrences of groundwater associated with the evaporites.

The US Department of Energy agreed to carry out several supplementary geotechnical studies as part of the WIPP Site characterization program. This report has been prepared to satisfy part of that agreement, as specified in Appendix II to the November 1984 Modification to the Working Agreement.

An extensive geochemical data base, including analyses of major and minor solutes, redox data, mineralogical studies of intact core samples, and isotopic studies of waters, carbonates, and sulfates, has been assembled for the Rustler Formation and adjacent units in the northern Delaware Basin. These data were evaluated to compare the aqueous geochemistry with host rock mineralogies, to delineate hydrochemical facies in the Culebra member of the Rustler Formation, and to determine the consistency of these facies with groundwater flow patterns derived from site stratigraphy and hydrology. The resulting synthesis of data and current hypotheses concerning the origin, composition, and history of waters in the Culebra member of the Rustler Formation and related units provides a tentative conceptual model for groundwater flow in the Rustler during the last 12,000 to 16,000 years. This model can form part of the basis for assessing the long-term performance of the geological containment

system at the WIPP, which is developed in the underlying evaporites of the Salado Formation.

Based on the available hydrological data, modern flow within the Culebra at and near the WIPP Site is interpreted to be largely north-to-south, except in relatively low-transmissivity areas directly affected by either a high-transmissivity zone in the southeastern portion of the WIPP Site or by Nash Draw west of the WIPP Site. The amount of modern vertical flow into and out of the Culebra near site-center remains indeterminate; however, with the exception of the region in and near Nash Draw, this flow may be negligible, making the assumption of confined flow within the Culebra adequate for modeling purposes on some limited time scale. Specifically, it is assumed that the steady-state confined flow is adequate on the time scale of hydro-logical testing and disturbances due to the sinking of the WIPP shafts, probably 100 years or less. This does not preclude a limited amount of localized downward flow through the Tamarisk member from the Magenta to the Culebra over longer time periods, as facilitated by higher potentiometric levels in the Magenta than in the Culebra.

The measurement of modern head potentials, transmissivities, and/or fluid densities, however, does not give any direct indication of time scales on which the system might be transient. The geochemical and isotopic data suggest that inferences about flow direction and velocity based on present hydrologic conditions and modeling alone may not be uniformly applicable to directions and velocities during the past 10,000 years. In particular, present-day steady-state (north-to-south) regional water flow directions under confined conditions are not consistent with the salinity distribu-tion at the WIPP Site, if the salinity distribution itself is assumed to be at steady state (i.e., fixed in place). For example, a hydrochemical facies having low salinity, with element ratios inconsistent with ongoing halite dissolution, lies downgradient along the modern flow directions from more saline water to the north.

Arguments that the observed solute distribution is generally consistent with the current hydrological flow field must rely heavily on the assumption of extensive vertical recharge and on the resultant subsurface mixing of at least two solute assemblages, especially in the southern part of the site. This would be required to provide fresher fluids to dilute the saline brines entering from the less permeable, halite-rich strata east of the sixteen-square-mile area delineating the WIPP.

Isotopic data, however, indicate that vertical recharge to the Culebra in the WIPP area and to the east and south has not occurred for several thousand years. Specifically, the three available radiocarbon dates in the Culebra are in excess of 12,000 to 16,000 years in both northern and southern portions of the study area, with no apparent regionally consistent or statistically significant age gradient.

Mineralogical and isotopic studies of sulfates in overlying layers also show that no significant amounts of either solutes or water have permeated vertically downward from the surface to recharge the Culebra. Specifically, much of the anhydrite in the Tamarisk member between the Magenta and Culebra members has not been hydrated to gypsum by recrystallization in the presence of fresh water, D/H ratios in gypsum throughout the Rustler are not consistent with a pervasively large water/rock ratio accompanying such hydration, and comparison of $^{87}Sr/^{86}Sr$ ratios of gypsums and carbonates in Rustler, Dewey Lake, and surface rocks shows that secondary sulfates and carbonates in the Rustler did not form in a hydrological regime that was uniformly interconnected with overlying rocks and the surface. Thus, the available mineralogical, hydrological, and isotopic data indicate no significant vertical connection between the Culebra and overlying strata.

The apparent discrepancy between modern flow direction and solute distribution can be explained by a change in flow direction in the last 30,000, or perhaps 12,000 years. Such a model is consistent with generally eastward-increasing $^{234}U/^{238}U$ activity ratios that indicate recharge from a near-surface Pleistocene infiltration zone,

flowing from the west-northwest. The model is also consistent with the cessation of recharge in the late Pleistocene, as indicated by the radiocarbon dates. A likely explanation for the less saline waters south of the WIPP Site is that at the time of influx of the present generation of Culebra groundwater from the west-northwest, Rustler halite was absent adjacent to the Culebra in that area, and did not provide a source of NaCl. Thus, the postulated paleoflow direction (from the west-northwest) is consistent with both flow perpendicular to the $^{234}U/^{238}U$ contours and flow parallel to the hydrochemical facies boundary between more saline water in the north and less saline water south of the WIPP.

A model for the chemical evolution of waters in the Culebra tentatively identifies the major sources and sinks for many of the solutes. It is proposed that: (1) solutes are added to the Culebra by dissolution of evaporite minerals; (2) the solubilities of gypsum and calcite increase as the salinity increases, and these minerals dissolve as chemical equilibrium is maintained between them and the groundwater; (3) equilibrium is not maintained between the waters and dolomite, and sufficient Mg is added to the waters by dissolution of accessory carnallite or polyhalite so that the degree of dolomite supersaturation increases with ionic strength; (4) clays within the fractures and rock matrix exert some control on the distribution of Li, B, Mg, and Si via sorption, ion exchange, and dissolution.

Increase of salinity in Culebra waters due to dissolution of evaporite salts in adjacent rock units is an irreversible chemical process affecting the water chemistry. The solubilities of gypsum, dolomite, and calcite increase with salinity up to 3 molal ionic strength and then decrease. Thus, even if the saturation indices for gypsum and calcite are near zero, the waters may still be capable of dissolving significant amounts of these phases if the salinity increases. Computer modeling of several hypothetical reaction paths shows that addition of solutes (Mg, SO_4, K, and Cl) to the Culebra from evaporite minerals such as polyhalite and carnallite in a

partial equilibrium system is consistent with the observed groundwater compositions, if dolomite does not precipitate from supersaturated solutions.

Isotopic studies of minerals and waters provide some support for this model. Stable-isotope compositions of carbonate minerals indicate that calcite has precipitated in equilibrium with the groundwater now found in the Culebra in some areas, but that dolomite has not extensively recrystallized or exchanged isotopes with meteoric groundwater of any age. There is also isotopic evidence that calcium sulfate has recrystallized (dissolved and reprecipitated) in the presence of Rustler ground-waters.

The results of principal component analysis (PCA) suggest that reactions with clay minerals may exert an observable influence on the water's minor-element chemistry throughout the study area. When the effects of solute addition associated with halite dissolution are factored out prior to the PCA, a $Mg\text{-}SiO_2$-alkalinity association is left that is negatively correlated with a pH-B-Li association. These correlations are consistent with several plausible mechanisms, including uptake of Li by vacant octahedral sites in a clay lattice, sorption of B by surface sites of clays, and dissolution of a reactive amorphous Si-Mg-rich layer in corrensite, the dominant Culebra clay mineral.

Investigations that could further elucidate the hypotheses proposed here include collection and analysis of isotopic and chemical data from additional boreholes, systematic examination of the mineralogy of samples from highly transmissive zones (containing core rubble rather than intact core), and more rigorous calculations of the extent of mass transfer that could result from precipitation, dissolution, ion exchange, and sorption.

CHAPTER 1:

SUMMARY OF HYDROGEOCHEMICAL CONSTRAINTS ON GROUNDWATER FLOW AND EVOLUTION IN THE RUSTLER FORMATION

Malcolm D. Siegel and Steven J. Lambert
Sandia National Laboratories

ABSTRACT

Chemical, mineralogical, isotopic, and hydrological data from the Culebra dolomite member of the Rustler Formation and related rocks were evaluated to delineate hydrochemical facies in the Culebra dolomite, to compare these facies with host rock mineralogies and hydrological flow patterns, and to formulate a conceptual model for post-Pleistocene groundwater flow and chemical evolution in the Rustler. Modern flow within the Culebra at and near the Waste Isolation Pilot Plant (WIPP) Site appears to be largely north-to-south; however, these inferences about flow direction and velocity may not be uniformly applicable to directions and velocities during the past 10,000 years. Present-day regional water flow directions are not consistent with the salinity distribution at the WIPP Site, assuming confined hydrological flow. In particular, a hydrochemical facies with low salinity and element ratios inconsistent with halite dissolution lies downgradient from more saline water to the north.

Isotopic, mineralogical, and hydrological data suggest that vertical recharge to the Culebra in the WIPP area and to the immediate east and south has not occurred for several thousand years. These data are consistent with the view that the apparent discrepancy between modern flow direction and solute distribution can be explained by a change in flow direction during the last 30,000, or perhaps 12,000 years. This model is consistent with generally eastward-increasing $^{234}U/^{238}U$ activity ratios that

suggest recharge from a near-surface Pleistocene infiltration zone, flowing from the west-northwest. Culebra groundwaters are in chemical equilibrium with gypsum and undersaturated with respect to halite and anhydrite. A partial-equilibrium model for the chemical evolution of the groundwater suggests that Na, Cl, Mg, K, and SO_4 are added to the Culebra by dissolution of evaporite salts in adjacent strata. Equilibrium is maintained with gypsum and calcite, but dolomite supersaturation increases as the salinity of the water increases. Isotopic studies of minerals and waters provide some support for this model. Stable-isotope compositions of carbonates indicate no recrystallization of dolomite in equilibrium with the groundwater now found in the Culebra, but local precipitation of calcite has apparently occurred. There is isotopic as well as mineralogical indication that calcium sulfate has recrystallized (dissolved and reprecipitated) in the presence of Rustler groundwaters.

Controls on the distribution of minor and trace elements are more problematic. Reactions with clay minerals may exert an observable influence on the water's minor-element chemistry. Major and minor element correlations are consistent with several plausible mechanisms, including sorption of lithium and boron by clays and silicate dissolution.

CONTENTS

CONTENTS (Continued)

FIGURES

FIGURES (Continued)

TABLES

CHAPTER 1.0

1.1 INTRODUCTION

1.1.1 Purpose and Scope

In the "Agreement for Consultation and Cooperation between [the] Department of Energy and the State of New Mexico on the Waste Isolation Pilot Plant," the United States Department of Energy (DOE) agreed to conduct geotechnical studies as part of its site characterization program for the Waste Isolation Pilot Plant (WIPP). The Agreement was enacted on July 1, 1981 and was subsequently modified in November 1984 and August 1987. The DOE agreed to provide the State with a report entitled "Hydrogeochemical Facies in the Rustler Formation at the WIPP." The report was to "compare the solutes with host rock mineralogies at and between various well sites" and "... attempt to delineate hydrochemical facies in the Rustler Formation." In addition, "comparison of these facies with flow patterns derived solely from physical hydrology [was to] be made for the purpose of examining internal consistency" (United States Department of Energy and the State of New Mexico, 1988).

This report synthesizes current data and hypotheses concerning the origin of the composition of waters in the Culebra member of the Rustler Formation. Progress is described in attempts to compare the aqueous geochemistry with host rock mineralogies and geochemistry at and between various well sites and to delineate hydrochemical facies in the Culebra member. These facies are then compared to modern groundwater flow patterns derived from site stratigraphy and hydrology. Although the emphasis is on the properties of waters in the Culebra member, preliminary results from work dealing with the Magenta member, Rustler/Salado contact zone, and the Dewey Lake Red Beds are also included where relevant.

The area included in this study is shown in Figures 1-1 and 1-2. As shown in Figure 1-1, the WIPP Site is located in southeastern New Mexico, in the northern portion of the Delaware Basin. As used in this report, the term "WIPP Site" refers to the 16 square miles of T22S, R31E contained within WIPP Zone 3 as shown in these Figures. Figure 1-2 shows the locations of all wells and boreholes from which water and/or rock samples were taken and described in this report. Table 1-2 describes the kinds of data available from each of these locations.

The information collected in the independent studies described in Chapters 2 through 6 has been integrated in this chapter. The techniques used and specific data examined by the different research groups have led to alternative interpretations and hypotheses concerning the origins of solutes and water in the Culebra. The primary purpose of this chapter is to summarize the results of these investigations, present these differing views, point out the areas of disagreement, and discuss investigations that might resolve the controversies.

1.1.2 Geological Setting

The general stratigraphy in the vicinity of the WIPP Site has been described in detail, particularly in relation to occurrences and manifestations of groundwater, by Powers et al. (1978) and Lambert (1983). The need to consider groundwater geochemistry in its geological context warrants the following brief discussion of the stratigraphy (Figure 1-3) and geological features relevant to the geochemical results subsequently presented. The chemical formulae of minerals mentioned in this section are given in Table 1-2.

The Delaware Basin became a distinct structure by the late Pennsylvanian Period to early Permian Period, around 280 million years (Ma) ago. About 250 Ma ago, fringing reef-type structures began to grow around the margins of the developing basin. Now termed the Goat Seep Dolomite and Capitan Limestone, these carbonates interfinger with the basinal deposits of sandstones, shales, and carbonates now called the Delaware Mountain Group, the uppermost of which is the Bell Canyon Formation. The Bell Canyon contains
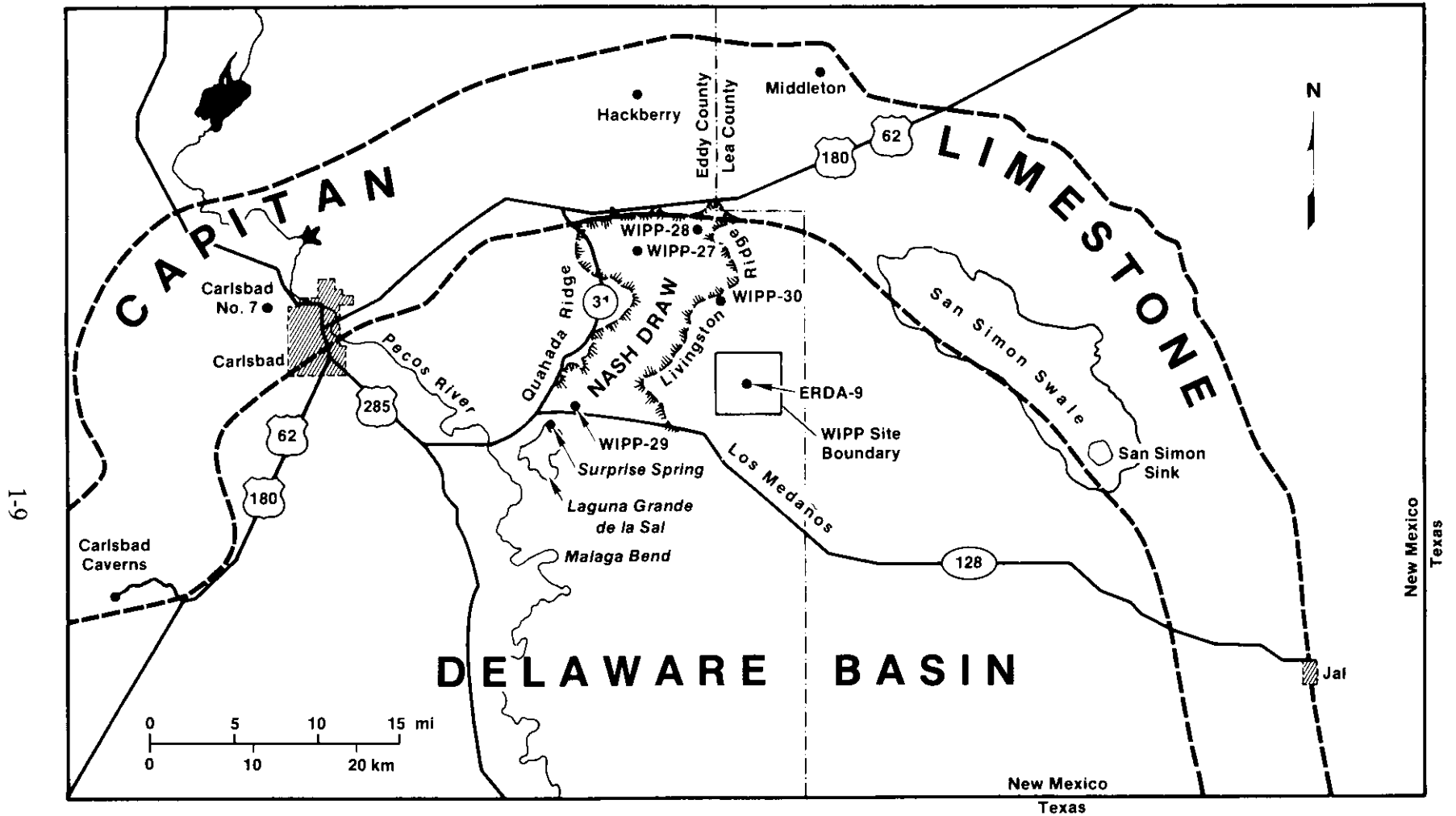
Figure 1-1. Setting of the WIPP Site relative to the northern Delaware Basin, including selected geomorphic features and boreholes (modified by Lappin [1988] from Figure 6-1 of Lambert [1983]).

TRI-6330-72-1

Figure 1-2. Map showing location of wells mentioned in this document.

Table 1-1. Chapters in This Report Containing Discussion of Various Types of Data Available at Each Well

Well	Unit[1]	Waters								Rocks					
		Solutes	Eh	TOC	PMC	^{3}H	δD	δ^{18}O	A.R.	Mnrlgy	$^{87/86}$Sr	δ^{13}C	δ^{18}O	δD	Δ Head[2]
Zone A:															
DOE-1	Mag														+
DOE-1	Cul	2,4	6	6			5	5							
H-5	Mag	2,4													+
H-5	Cul	2,4	6	6		5		5	5			5	5		
H-5	R/S	4					5	5							
P-18	Cul	4					5	5							
P-18	R/S	4					5	5							
H-11	Cul	2,4	6	6				5		3					
H-12	Cul	2,4	6	6		5		5							
Zone B:															
ENGLE	Cul	2,4	6	6		5	5	5							
H-7	Mag														+
H-7	Cul	2,4	6	6						3					
H-7	R/S	4													-
H-8	Mag	4													+
H-8	Cul	2,4	6	6											
H-8	R/S	4													0
H-9	Mag	4													+
H-9	Cul	2,4	6	6	5		5	5							
H-9	R/S	4													

Table 1-1. Chapters in This Report Containing Discussion of Various Types of Data Available at Each Well (Continued)

Well	Unit[1]	Waters								Rocks					
		Solutes	Eh	TOC	PMC	^{3}H	δD	δ^{18}O	A.R.	Mnrlgy	$^{87/86}$Sr	δ^{13}C	δ^{18}O	δD	Δ Head[2]
FR-10	Cul						5	5							
Ranch	DL	2					5								
Twin P.	DL	2,4													
Indian	Cul	4													
Two Mile	Cul	4													
Pocket	DL	4			5		5								
Windmill	Cul	4													
Gnome-SH	Cul	4													
Gnome-1	Cul	4													
Gnome-4	Cul	4													
Gnome-5	Mag	4													
Gnome-5	R/S	4													
Gnome-8	Cul	4													
Unger	DL						5								
South	Cul	4													
Fairview	DL						5								

Table 1-1. Chapters in This Report Containing Discussion of Various Types of Data Available at Each Well (Continued)

Well	Unit[1]	Waters								Rocks					
		Solutes	Eh	TOC	PMC	^{3}H	δD	δ^{18}O	A.R.	Mnrlgy	$^{87/86}$Sr	δ^{13}C	δ^{18}O	δD	Δ Head[2]
Zone C:															
AEC-8	DL										5			5	
AEC-8	Tam													5	
AEC-8	BC											5	5		
DOE-2	49r														0
DOE-2	Mag														+
DOE-2	Cul	2,4	6	6			5	5							
DOE-2	BC	2													
H-1	Mag	4					5	5							+
H-1	Cul	4					5	5							
H-1	lwr														
H-1	R/S	4					5	5							
H-2	Mag	4					5	5							+
H-2	Cul	2,4		6			5	5							+
H-2	R/S	4					5	5							+
H-3	49r														-
H-3	Mag	2,4					5	5							+
H-3	Cul	2,4	6	6		5	5	5		3					
H-3	R/S	4					5	5							
H-4	Mag	2,4													+
H-4	Cul	2,4	6	6	5	5	5	5	5	3		5	5		
H-4	R/S	4					5	5							
H-6	Mag	2,4													0
H-6	Cul	2,4	6	6	5		5	5	5	3		5	5		
H-6	R/S	4					5	5							-

Table 1-1. Chapters in This Report Containing Discussion of Various Types of Data Available at Each Well (Continued)

Well	Unit[1]	Waters								Rocks					
		Solutes	Eh	TOC	PMC	^{3}H	δD	δ^{18}O	A.R.	Mnrlgy	$^{87/86}$Sr	δ^{13}C	δ^{18}O	δD	Δ Head[2]
H-10	Mag	4													+
H-10	Cul	4								3					
H-10	R/S	4													
H-14	49r														(-)
H-14	Mag														+
H-14	Cul		6	6											
H-15	Cul		6	6											
H-16	49r														(-)
H-16	Mag														+
H-16	R/S														(+)
H-17	Cul		6												
H-18	Cul		6												
P-14	Cul	2,4	6	6			5	5							
P-14	R/S	4					5	5							
P-15	Cul	4					5	5							
P-15	R/S	4					5	5							
P-17	Cul	2,4	6	6			5	5							
P-17	R/S	4					5	5							
WIPP-12	Cul									3					
WIPP-13	Mag											5			
WIPP-13	Tam											5			
WIPP-13	Cul	2										5			

Table 1-1. Chapters in This Report Containing Discussion of Various Types of Data Available at Each Well (Continued)

Well	Unit[1]	Waters								Rocks					
		Solutes	Eh	TOC	PMC	^{3}H	δD	δ^{18}O	A.R.	Mnrlgy	$^{87/86}$Sr	δ^{13}C	δ^{18}O	δD	Δ Head[2]
WIPP-14	DL										5			5	
WIPP-19	DL										5			5	
WIPP-19	Cul		6	6						3					
WIPP-25	DL										5				
WIPP-25	49r										5				
WIPP-25	Mag	2,4					5	5	5		5	5	5		0
WIPP-25	Cul	2,4	6	6			5	5	5	3	5	5	5		
WIPP-25	lwr										5				
WIPP-25	R/S	2,4					5	5	5						(-)
WIPP-26	Mag										5				
WIPP-26	Tam										5				
WIPP-26	Cul	2,4	6	6			5	5	5	3	5	5	5		
WIPP-26	R/S	2,4					5	5	5						(-)
WIPP-28	Mag											5	5		+
WIPP-28	Cul	2,4					5	5	5			5	5		
WIPP-28	R/S	2,4					5	5	5						0
WIPP-30	Mag	4					5	5				5	5		+
WIPP-30	Cul	2,4					5	5	5			5	5		
WIPP-30	R/S	2,4					5	5	5						-
WIPP-33	49r										5			5	
WIPP-33	Mag										5	5	5		
WIPP-33	Cul										5				
WIPP-33	lwr										5				
WIPP-34	49r										5			5	
WIPP-34	Mag										5			5	
WIPP-34	lwr										5			5	

Table 1-1. Chapters in This Report Containing Discussion of Various Types of Data Available at Each Well (Continued)

Well	Unit[1]	Waters								Rocks					
		Solutes	Eh	TOC	PMC	^{3}H	δD	δ^{18}O	A.R.	Mnrlgy	$^{87/86}$Sr	δ^{13}C	δ^{18}O	δD	Δ Head[2]
Zone D:															
WIPP-27	Mag	2,4					5	5	5						+
WIPP-27	Cul	2,4					5	5	5			5	5		
WIPP-27	R/S	4					5	5							
WIPP-29	Cul	2,4			6		5	5	5	3		5			
WIPP-29	R/S	2,4					5	5	5						-
S.Spring	Tam	4					5	5							

1. Unit abbreviations:
   - DL: Dewey Lake Red Beds
   - 49r: Rustler Fm., Forty-niner member
   - Mag: Rustler Fm., Magenta dolomite member
   - Tam: Rustler Fm., Tamarisk member
   - Cul: Rustler Fm., Culebra dolomite member
   - lwr: Rustler Fm., lower member
   - BC: Bell Canyon Fm.
2. Comparison of hydraulic heads for nearby units.
   - For Mag and R/S:
     - "+": unit's head is higher than that of Culebra; potential for flow into Culebra.
     - "-": unit's head is lower than that of Culebra; potential for flow from Culebra.
   - For 49r:
     - "-": unit's head is lower than that of Magenta; potential for flow from Magenta into Forty-niner.
   - For all:
     - "0": approximately equivalent heads in units being compared.
     - "()": potential flow direction is based on reported lower or upper limit for head of one of the units (see Beauheim, 1987).
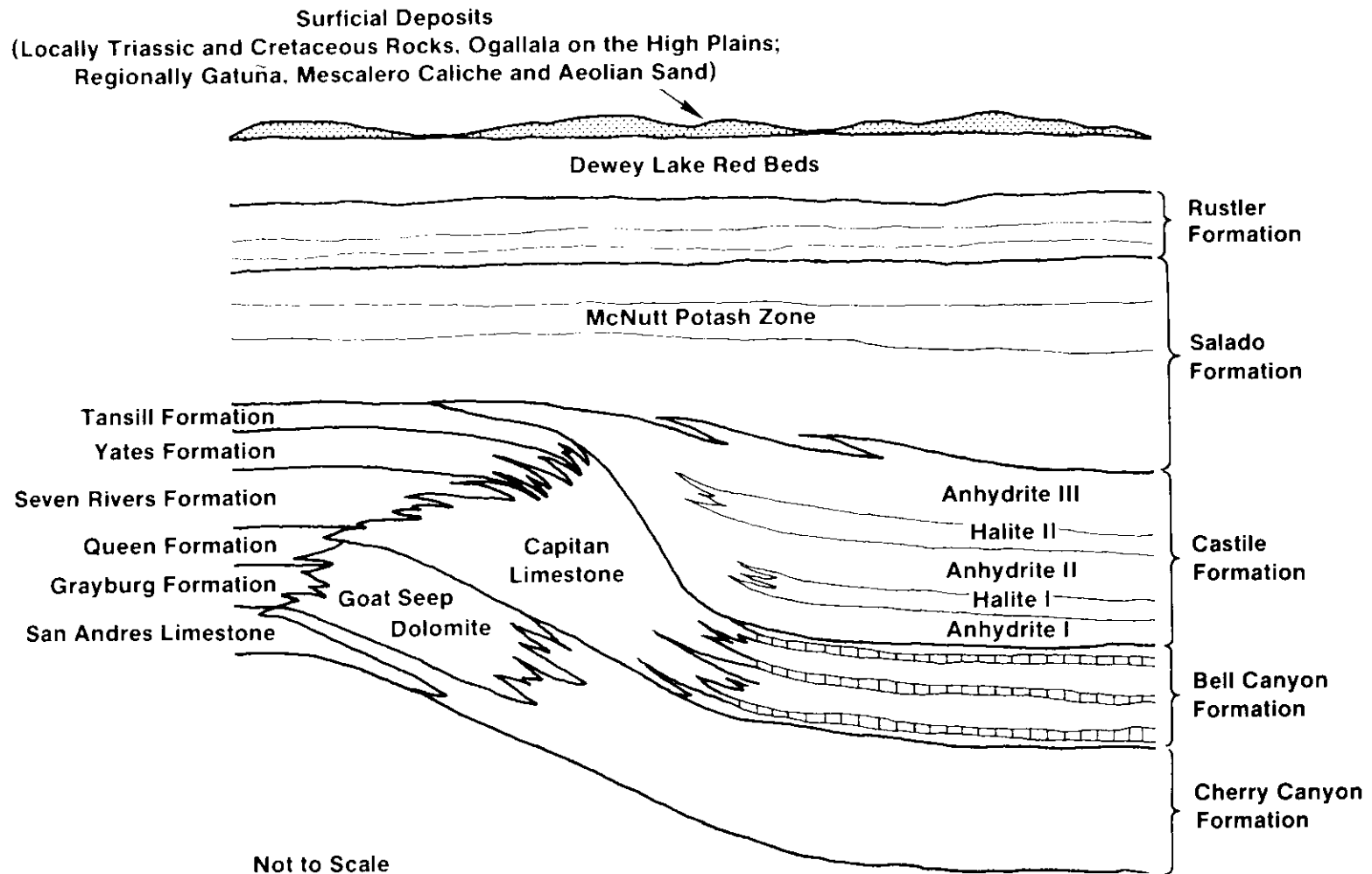
Figure 1-3. Generalized stratigraphy of Guadalupian (Permian) and younger rocks in the Delaware Basin.
A. Idealized north-south section, looking east, at the northern apex of the Capitan Limestone, near the Eddy-Lea County line (from Lambert, 1983).

System	Series	Group	Formation	Member
Recent	Recent		Surficial Deposits	
Quater-nary	Pleisto-cene		Mescalero Caliche	
			Gatuña	
Triassic		Dockum	Undivided	
Permian	Ochoan		Dewey Lake Red Beds	
			Rustler	Forty-niner
				Magenta Dolomite
				Tamarisk
				Culebra Dolomite
				lower
			Salado	
			Castile	
	Guadalupian	Delaware Mountain	Bell Canyon	
			Cherry Canyon	
			Brushy Canyon	

TRI-6330-89-2

Figure 1-3. B. Stratigraphic column of Guadalupian and younger rocks, exclusive of the Capitan complex, including members of the Rustler Formation (from Lappin, 1988).

Table 1-2. Chemical Formulae[1] of Minerals Mentioned in This Chapter

Mineral	Formula
Amesite	$(Mg_4Al_2)(Si_2Al_2)O_{10}(OH)_8$
Anhydrite	$CaSO_4$
Calcite	$CaCO_3$
Carnallite	$KMgCl_3 \cdot 6H_2O$
Chlorite	$(Mg,Al,Fe)_{12}(Si,Al)_8O_{20}(OH)_{16}$
Corrensite	mixed-layer chlorite/smectite
Dolomite	$CaMg(CO_3)_2$
Feldspar	$(K,Na,Ca)(Si,Al)_4O_8$
Glauberite	$Na_2Ca(SO_4)_2$
Gypsum	$CaSO_4 \cdot 2H_2O$
Halite	$NaCl$
Illite	$K_{1-1.5}Al_4[Si_{7-6.5}Al_{1-1.5}O_{20}](OH)_4$
Kainite	$KMgClSO_4 \cdot 3H_2O$
Kieserite	$MgSO_4 \cdot H_2O$
Langbeinite	$K_2Mg_2(SO_4)_3$
Magnesite	$MgCO_3$
Polyhalite	$K_2Ca_2Mg(SO_4)_4 \cdot 2H_2O$
Pyrite	FeS_2
Quartz	SiO_2
Serpentine	$Mg_3Si_2O_5(OH)_4$
Smectite	$(Ca/2,Na)_{0.7}(Al,Mg,Fe)_4(Si,Al)_8O_{20}(OH)_4 \cdot nH_2O$
Sylvite	KCl

1. Formulae are taken from Fleischer (1987) and Deer, Howie, and Zussman (1962).

local occurrences of economically important hydrocarbons and sporadically distributed oilfield-type brines, and forms the substrate for later evaporite deposition. The Capitan Limestone has a locally developed cavernous porosity displaying the classic features of limestone karst and includes Carlsbad Caverns.

The sandstones and shales of the Bell Canyon Formation grade upward into the alternating sequence of sulfate and carbonate laminations characteristic of the Castile Formation. The thick Castile sequences of sulfate/carbonate are interrupted two (and locally three) times by comparably thick sequences of bedded rock salt containing glauberite as an accessory mineral. The Salado Formation overlying the Castile consists dominantly of halite, inter- rupted at various intervals of meters to tens of meters by beds of anhydrite, polyhalite, mudstone, and local potash mineralization (sylvite or langbeinite, with or without accessory carnallite, kieserite, kainite, and glauberite, all in a halite matrix) of economic importance. The nonhalitic units, on the order of 0.1 to 1 m thick, have been numbered (in some cases named) for convenience as "marker" beds, where uniquely identifiable, to facilitate cross- basinal stratigraphic correlation. The WIPP mined facility is being emplaced just above Marker Bed 139 in the Salado, at an approximate depth of 660 m. Radiometric dates on sylvites (Register and Brookins, 1980) and polyhalites (Brookins et al., 1980) give generally concordant post-Permian ages of crystallization and/or recrystallization of 214 ± 15 Ma and 195-205 Ma, respectively. Clay minerals from the WIPP Facility in the Salado preserve a possibly detrital geochemical signature, unaltered by deposition and diagenesis, and having a radiometric age of 428 ± 7 Ma (Brookins and Lambert, 1987; 1988).

The Rustler Formation, overlying the Salado, contains five members according to the regional stratigraphic nomenclature, in ascending stratigraphic sequence: (1) a lower member (unnamed) consisting of siltstone/mudstone, anhydrite locally altered to gypsum, and containing halite under most of the WIPP Site; (2) the relatively permeable Culebra dolomite member, containing dominantly dolomite with subordinate anhydrite and/or gypsum; (3) the Tamarisk member, dominantly anhydrite/gypsum, with subordinate

fine-grained clastics, containing halite to the east of the WIPP Site; (4) the Magenta member, another dolomite/sulfate unit containing sporadic occurrences of groundwater near the WIPP Site; and (5) the Forty-niner member, similar in lithology to the other nondolomitic units, but containing halite only in the easternmost part of the study area. The Culebra member is the first major water-bearing unit above the WIPP Facility; for this reason, the hydrochemistry and hydrology of Culebra groundwater in the study area shown in Figures 1-1 and 1-2 is the primary focus of this work.

The Dewey Lake Red Beds are the uppermost Permian unit, consisting of siltstones and claystones locally transected by concordant and discordant fractures that are either unaltered or contain gypsum (selenite and satin spar). The Dewey Lake contains sporadic occurrences of groundwater, mostly in the area south of the WIPP Site. The Triassic Dockum Group (undivided) rests on the Dewey Lake in the east half of the site and thickens eastward.

Locally throughout the area sands, gravels, and boulder conglomerates of the Gatuña Formation occur as channel and alluvial pond deposits as part of a high-energy stream system that dissected the southeastern New Mexico landscape in the middle Pleistocene. One such channel was Nash Draw, a broad, shallow solution valley west of the WIPP Site, where outcrops of the Rustler Formation have been eroded into shallow karstic landforms typical of subaerially exposed gypsum terrane. The pedogenic Mescalero caliche commonly is developed on top of the Gatuña where it occurs, and on many other rock types as well. Late Pleistocene spring deposits, dominantly of gypsite, occur just inside the eastern scarp of Nash Draw, and are thought to represent remobilization of sulfates from the Dewey Lake Red Beds and perhaps part of the upper Rustler Formation by groundwaters moving westward into Nash Draw during the late Pleistocene.

1.2 HYDROLOGIC SETTING OF CULEBRA AND RELATED ROCKS

1.2.1 Introduction

The hydrologic system in the Rustler Formation has been the subject of intense study since 1976. The results of these studies to date are summarized by Lappin (1988) and briefly reviewed here. Recent findings concerning physical hydrology within the Rustler have yielded various interpretations; consistency between interpretations based on physical hydrology and those based on geochemical and isotopic observations is a significant topic of discussion in this work.

The most important constraints on numerical models for calculating the modern or present-day flow velocities and directions in a groundwater system are the heads and transmissivities in various parts of the system. These parameters are inferred from other observations. The basic data describing the hydrologic properties of the Culebra over the study area consist of water-level measurements and observations of drawdown and/or recovery during hydraulic tests. Equivalent freshwater heads are derived from pressure data (water-level measurements) and a fluid density at each point. The time-dependent drawdown function obtained in response to pumping is then numerically simulated by varying the transmissivity until an optimized match between calculated and observed drawdown function is obtained. Assuming vertical homogeneity across the tested interval, this gives the best available estimate of transmissivity. The hydrologic testing that yielded the head and transmissivity data base is summarized by Lappin (1988).

1.2.2 Culebra Dolomite

Estimated Culebra transmissivities in the WIPP Site area and within Nash Draw range over approximately six orders of magnitude, from about 2×10^{-9} m^2/s a short distance east of the site to about 10^{-3} m^2/s west of the site, on the east side of Nash Draw (Figure 1-4). Values
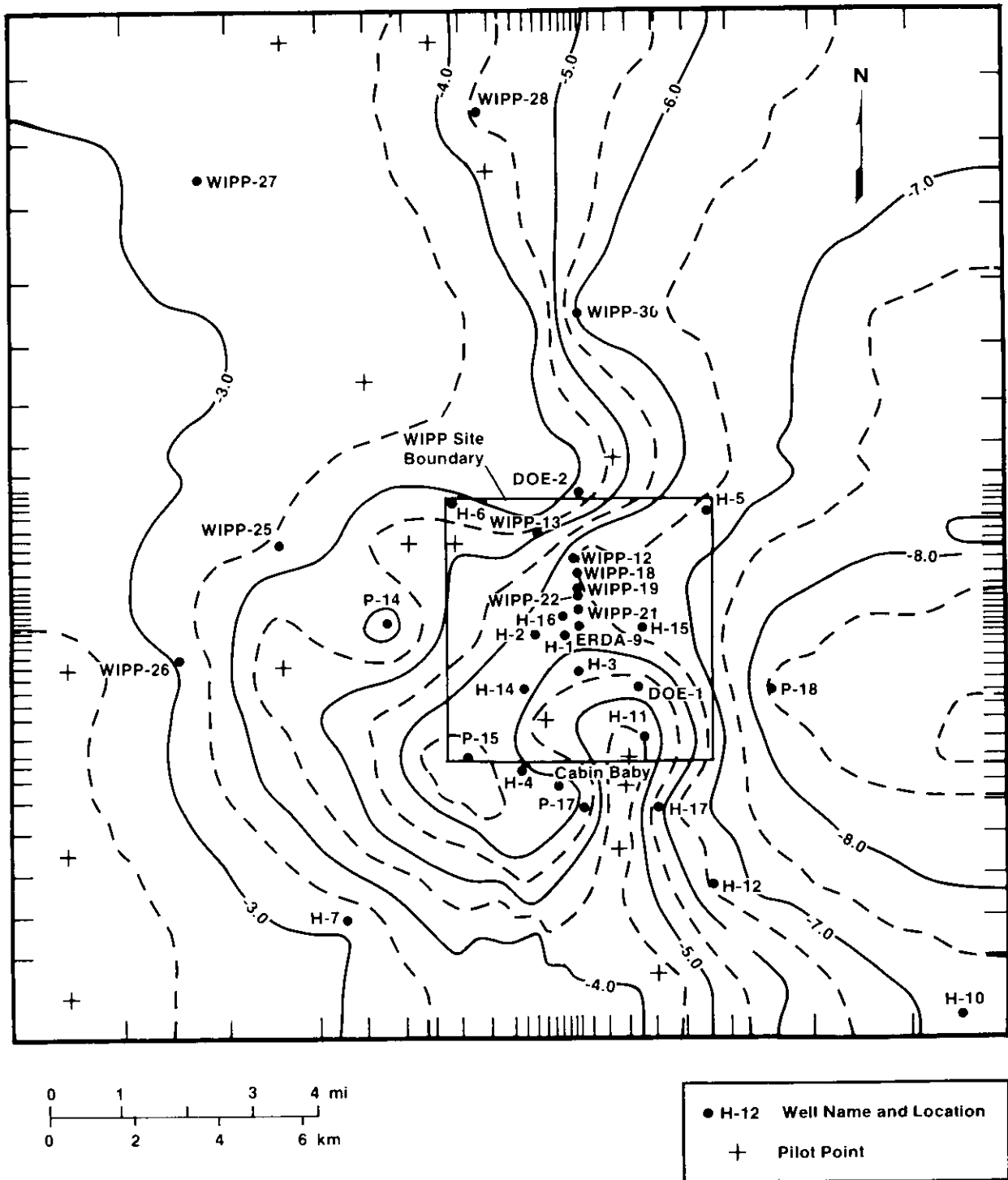
TRI-6330-131-1

Figure 1-4. Logarithms of calculated Culebra transmissivities at and near the WIPP Site (Figure 4.3 of LaVenue et al. [1988]).

shown in Figure 1-4 are $\log_{10}$ of transmissivities in units of m^2/s and are based on a steady-state calibration against the freshwater-equivalent head distribution. Culebra transmissivities in the central portion of the site, including very near the positions of all four WIPP shafts, are less than 10^{-6} m^2/s. LaVenue et al. (1988) estimate that uncertainties in transmissivity measurements are half an order of magnitude or less. They estimate that the uncertainty in calculated freshwater heads at most locations is approximately $\pm$ 2 m.

A continuous but complex zone of variable and higher Culebra transmissivities is present northwest, west, and south of the site; this zone extends into the southeast and northwest portions of the WIPP Site. In spite of the transmissivity determinations at 39 discrete locations in the Culebra, there is no direct field evidence of aqueous mass transport between the relatively high-transmissivity region in the southeast portion of the site (containing the H-4 hydropad and hole DOE-1) and the less saline groundwater system in the halite-free extensively gypsified region of the Rustler further south (containing holes H-7 and H-9). In fact, as discussed in Section 1.4.2, these two regions are geochemically dissimilar. The degree of fracturing appears to have some control over transmissivity in the Culebra, especially where the transmissivity is higher than about 10^{-6} m^2/s. The most fractured portions of the unit almost certainly carry the most groundwater.

The analytical and numerical modeling of Rustler groundwater flow has, over the years, used various assumptions to explain various observations. For example, no hydrologic-modeling studies to date consider possible reactions within the Culebra that might lead to local changes in fluid density or composition, such as halite dissolution from adjacent portions of the Rustler. Assumption of steady-state brine-density distribution (Haug et al., 1987) results in significant problems with model calibration that assumes completely confined flow. Haug et al. (1987) examine the effects of possible steady-state vertical inputs into the Culebra of fluids having different densities, from either the lower member of the Rustler or the Magenta. LaVenue et al. (1988) relax the assumption of long-term steady-state fluid compositions, but do assume that the fluid density distribution

is fixed on the time scale of local fluid-pressure changes in response to site characterization and shaft sinking (as long as 100 years). They also assume that the Culebra is completely confined on this same time scale.

The numerical modeling of the Culebra groundwater system using the measured formation pressures, a function to estimate the distribution of fluid densities, and a transmissivity distribution modified from an original kriged estimate, results in the instantaneous (present-day) flow directions and Darcy velocities within the Culebra shown in Figure 1-5. The hydrologic flow is calculated assuming the transmissivity distribution shown in Figure 1-4 and the freshwater-equivalent head distribution. Present-day flow within the Culebra at and near the WIPP Site, ignoring possible effects of both fractures and anisotropy, appears to be largely north-to-south, except in relatively low-transmissivity areas directly affected by either the high-transmissivity zone in the southeastern portion of the WIPP Site or by Nash Draw west of the WIPP Site. Calculated Darcy velocities range over six orders of magnitude, from 10^{-12} m/s (m^3/m^2s) east of the WIPP Site to as high as 10^{-6} m/s in central Nash Draw.

Darcy velocities do not include consideration of effective porosity and therefore do not represent actual groundwater particle velocities, nor can groundwater travel times be calculated directly from them unless effective in situ porosity values are known or assumed. Particle flowpaths and flowtimes within Nash Draw calculated by LaVenue et al. (1988) assuming steady state, the transmissivity and head distributions used to derive Figure 1-5, and a uniform effective in situ porosity of 16% are shown in Figure 1-6. They range from 450 years along a 25.1-km path in the west (particle A) to 2800 years along a 26.3-km path in the eastern part of Nash Draw (particle C). However, changes in the Nash Draw shallow groundwater system since the beginning of potash mining about 50 years ago (Hunter, 1985) make the steady-state assumption unrealistic in Nash Draw on even this short time scale.

Darcy-Velocity Vector Scale

→────────→	1×10^{-6} m/s
────────→	1×10^{-7} m/s
──→	1×10^{-8} m/s
─→	1×10^{-9} m/s

```
0    1    2    3    4 mi
0    2    4    6 km
```
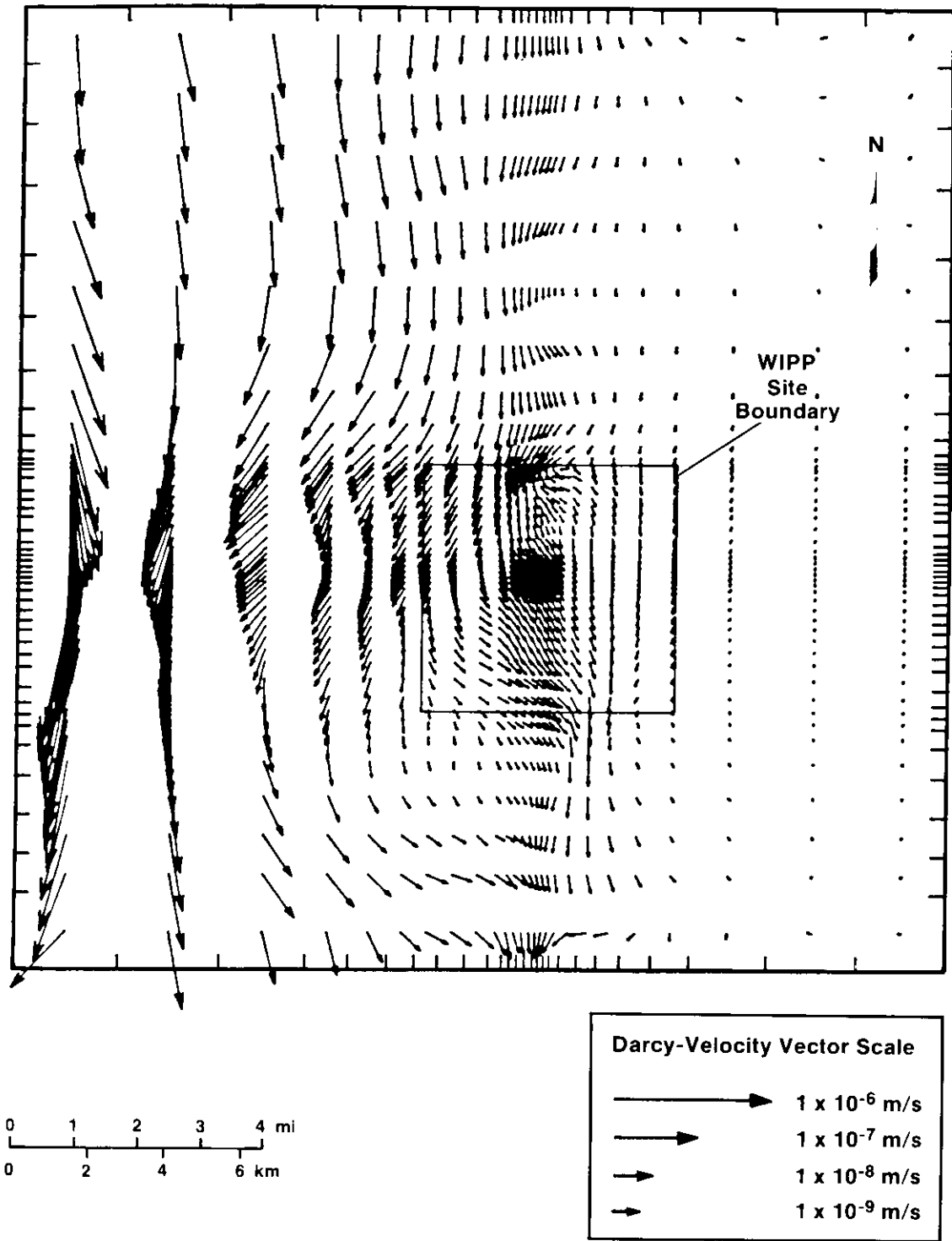
TRI-6342-228-1

Figure 1-5. Calculated Darcy-velocity vectors in the Culebra dolomite (Figure 4.5B of LaVenue et al. [1988]).
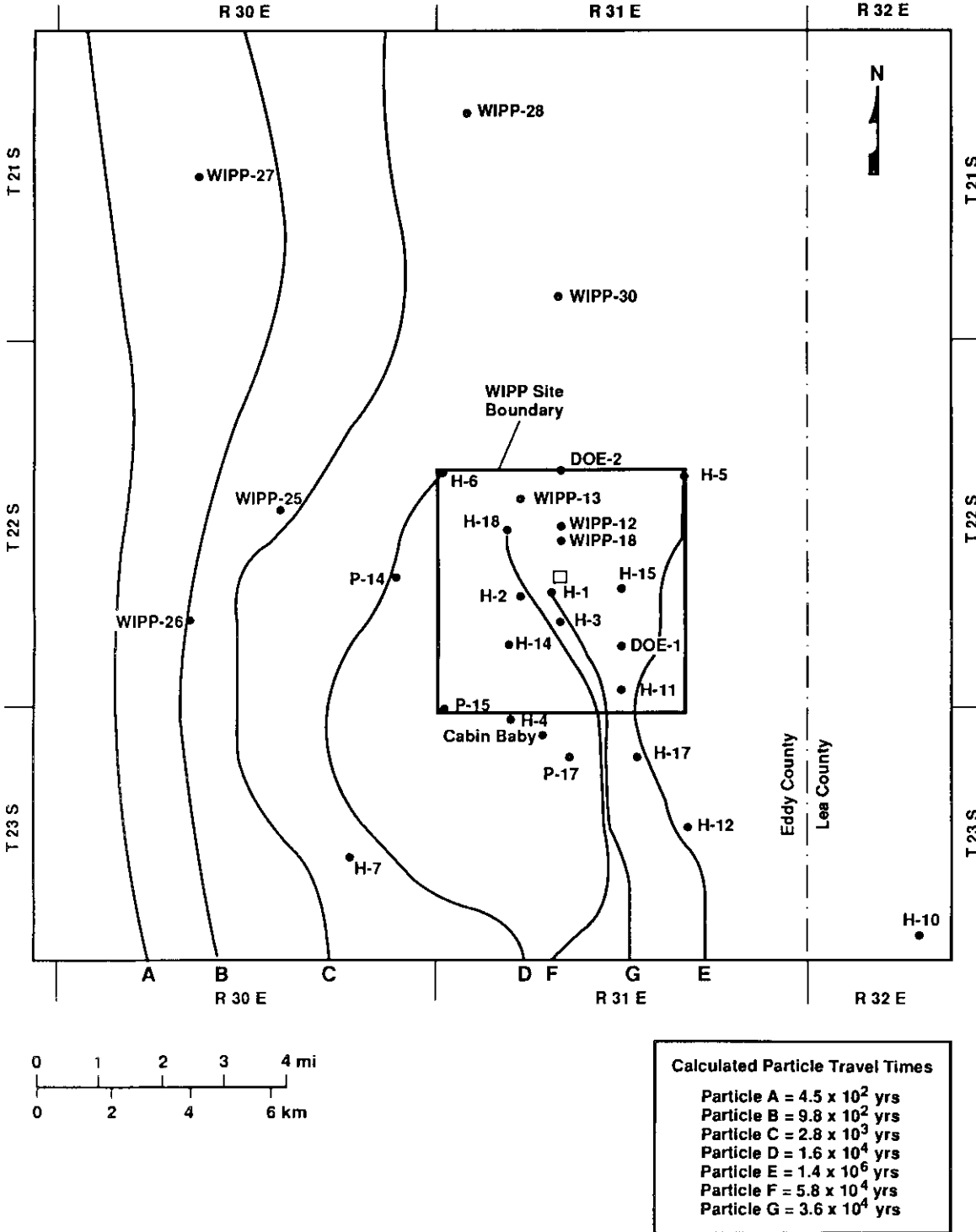
Figure 1-6. Calculated flowpaths and flow times within the Culebra dolomite (Figure 4.17 of LaVenue et al. [1988]).

LaVenue et al. (1988) calculated the particle travel time from north to south along a 13.7-km path in the eastern part of the WIPP Site (particle E) to be more than one million years. Travel time from directly above the center of the waste-emplacement panels to the southern boundary of the WIPP Site (along a 4-km segment of path G in Figure 1-6) is about 13,000 years. These results, however, cannot be used to quantitatively predict the behavior of the groundwater over the next 10,000 to one million years given the probable non-steady-state character of the Culebra hydrology, as discussed in Section 1.5.2. The amount of possible vertical flow into and out of the Culebra near site-center remains indeterminate and cannot be directly measured in the field (see Figure 1-7). At several well locations, the relationships between the heads in the Culebra and adjacent units indicate the potential for vertical flow into the Culebra (see Table 1-1). At H-16, H-3, H-2, H-1, H-14, and DOE-1, the head in the Magenta is higher than that of the Culebra. At H-2 and H-16, the measured head in the Rustler/Salado contact zone is higher than that of the Culebra. The amount of flow, however, may be negligible, making the assumption of confined transient flow within the Culebra adequate for modeling purposes, at least for short-term stresses associated with WIPP shafts and well tests. This assumption may or may not be valid for all modeling aspects over a 10,000-year time frame. In Nash Draw, for example, the development of near-surface gypsum karst has certainly allowed the Culebra to be hydraulically connected to various other Rustler horizons, including the Magenta.

At two localities near the site (holes H-3 and H-14), the Magenta head is greater than the head in claystone in the overlying Forty-niner member; therefore, any modern fluid flow between these two members at these two localities is upward, not downward. The head relationships between the Forty-niner and the Magenta at H-16 are probably similar (Beauheim, 1987). This precludes recharge of the Magenta and underlying units by direct downward infiltration from the surface at those localities. It has not been possible to measure hydraulic conductivities within the upper part of the unnamed lower member of the Rustler in borehole testing from the surface; thus, the degree of upward flow from the Rustler/Salado contact zone near the site-center (where the head relationships
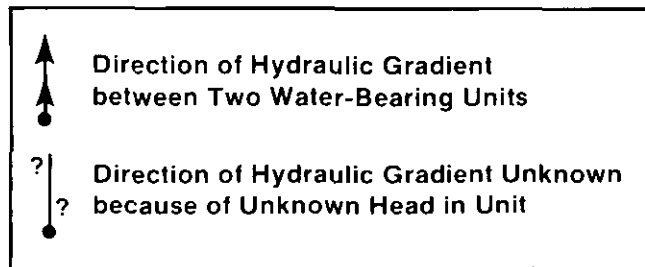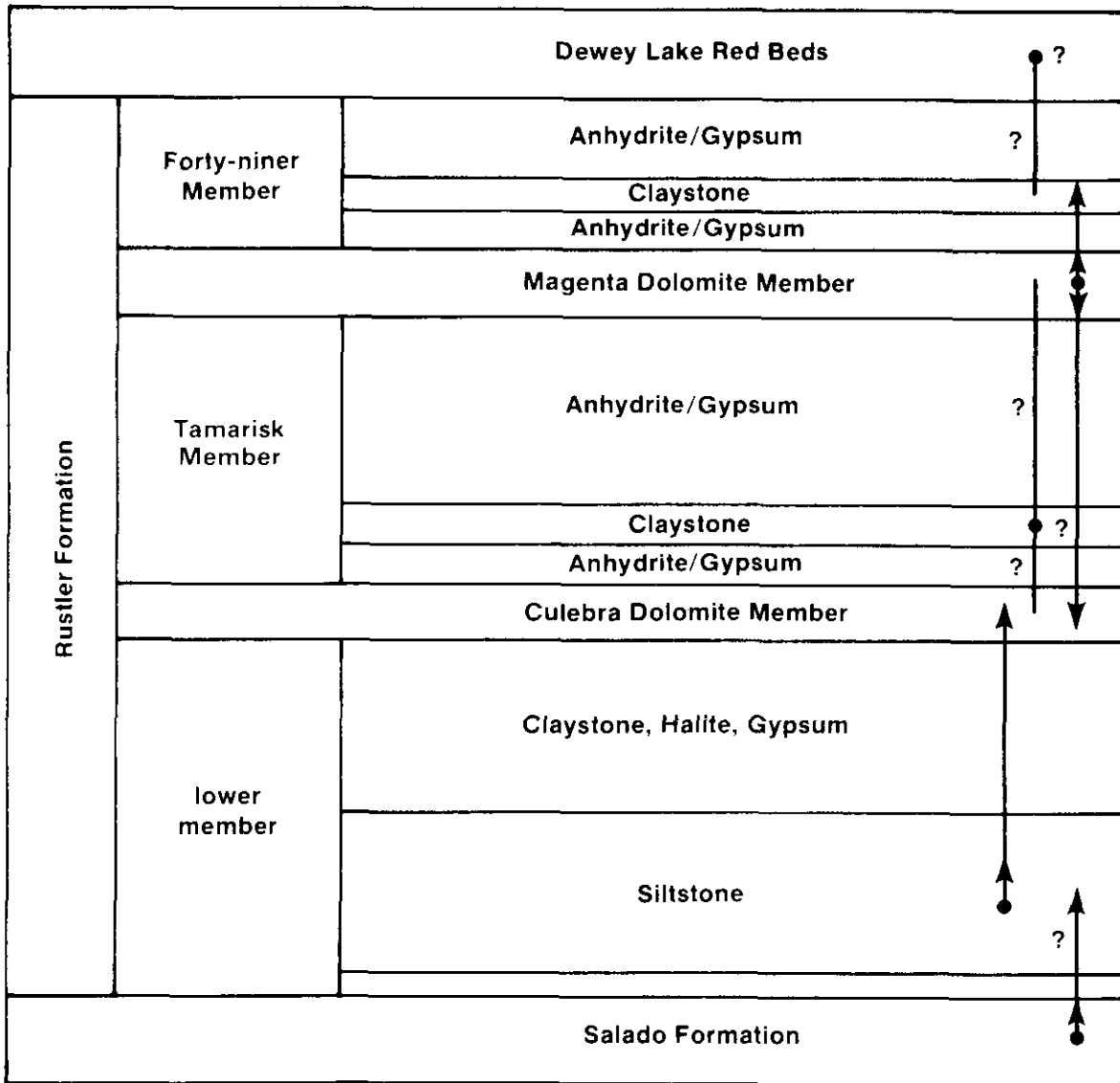
Figure 1-7. Generalized head relations among units in the Rustler Formation and between the Rustler, Dewey Lake Red Beds, and Salado at the WIPP Site (Figure 6-3 of Beauheim [1987]).

favor such a flow direction) cannot be determined. Horizontal hydraulic conductivities within the lower member claystone and siltstone range from 10^{-13} to 10^{-14} m/s. The extremely low hydraulic conductivity of the Tamarisk and relatively high transmissivity of the Culebra suggest that transient confined flow within the Culebra prevails at and near the WIPP Site.

Flow velocities calculated from a given set of heads and a given transmissivity distribution are interpretable as only a "snapshot" of instantaneous or modern behavior, unless the assumption of a steady state can be defended and the distribution of effective porosity is known. Physical measurements alone indicate only the present directions of potential fluid flow within and across the boundaries of the Rustler Formation. These inferences about flow direction and velocity may not be applicable to directions and velocities during the past 10,000 years, or during in the next 10,000 years, the interval of interest to regulatory agencies governing radioactive-waste repositories. Consequently, climatic variations and their influence on groundwater flow will be included as a factor affecting the uncertainty in the hydrologic modeling for performance assessment of the WIPP.

1.2.3 Related Rocks

Data for other hydrologic units of interest, including the Magenta, Dewey Lake, Triassic, and "brine aquifer" near the Rustler/Salado contact zone, are much less abundant than for the Culebra, although some of them have been used in various model calculations of hypothetical flow crossing bedding planes into or out of the Culebra. Some testing at selected points has been carried out in other horizons of the Rustler, including the Forty-niner, Tamarisk, and lower members of the Rustler (Lappin, 1988). Most of the data from non-Culebra units overlying the Salado in the study are reported by Mercer (1983) and Beauheim (1987).

1.3 SOURCES AND QUALITY OF GEOCHEMICAL DATA

1.3.1 Major and Minor Solute Data

Analyses of major and minor solutes from water samples collected by several different agencies and analyzed in different laboratories from 1976 to 1987 were considered in this work. The sources of data include the US Geological Survey (USGS) (Mercer, 1983; Mercer and Orr, 1979; Bodine et al., Chapter 4), the International Technologies (IT) Corporation (Uhland and Randall, 1986; Uhland et al., 1987; Randall et al., 1988), and Sandia National Laboratories (Robinson, 1988). In many cases, large discrepancies exist in the concentrations of major and minor solutes reported for the same location by different agencies. Much of the variation can be attributed to differences in sampling methods, to differences in analytical techniques, or to changes in the groundwater chemistry due to contamination. As discussed below, some of the inconsistencies among conceptual models proposed for the hydrochemical system at the WIPP can be attributed to discrepancies among the data sets. A list of wells from which water analyses were obtained is found in Table 1-1. Additional details concerning the solutes analyzed at each well, the dates of sample collection, and the methods of chemical analyses are found in Chapters 2, 4, and 6 and in the references cited in these chapters.

Siegel et al. (see Table 2-2) tabulate the values used for their calculations dealing with the concentrations of major and minor elements for waters in the Rustler Formation. Data from Table 2-2 were used in the saturation index calculations, factor analyses, and element ratio contours discussed below. Robinson (1988), Lambert and Harvey (1987), and Siegel et al. (Chapter 2) describe the different data sets examined and the development of a critical evaluation procedure to determine the criteria for acceptable values.

Bodine et al. (Chapter 4) used the SNORM computer code (Bodine and Jones, 1986) to evaluate data for their hydrochemical study. Their final data base for the Rustler Formation includes 161 chemical analyses from 70 sites representing 107 horizon-site

sampling points (see Table 1-1). The authors compiled data for the calculations from a variety of sources, including the data compiled in Robinson (1988), analyses reported in previous WIPP Site characterization and USGS Technical File reports, and new chemical analyses by USGS staff. In several cases, data from samples rejected by Robinson (1988) or Lambert and Harvey (1987) were accepted by Bodine et al. for use in calculating salt norms.

1.3.2 Evaluation of Oxidation-Reduction Potential and Occurrence of Organic Constituents in the Culebra

A data set from the WIPP Water Quality Sampling Program (WQSP) was independently evaluated by the IT Corporation and used in the calculations of Eh described below and in Chapter 6. Analyses of concentrations of members of four oxidation-reduction ("redox") couples and platinum electrode potential measurements were obtained from 21 wells in the Culebra during the period from 1985 to 1987 and used to calculate apparent Eh values (see Table 1-1). In most cases, the concentration of one of the members of a specific redox couple was below the limit of detection and only an upper or lower bound for the Eh could be calculated. Robinson (Appendix 6A) independently evaluated these redox data and compared them to a larger data set collected between 1985 and 1989.

Final groundwater samples from 21 Culebra wells listed in Table 1-1 were analyzed for total organic carbon (TOC) in acidified solutions passed through a 0.45 micron filter. Details of the sample collection and analytical techniques are found in Chapter 6.

1.3.3 Mineralogical Data

Mineralogical data were obtained from 12 cores from three east-west traverses in the Culebra member. Over 100 samples were analyzed by optical microscopy, quantitative x-ray diffraction (XRD), and x-ray fluorescence. Core from one borehole (WIPP-12) was examined to obtain a representation of the textural variations in the Culebra, while core from another (WIPP-19) was examined both texturally and mineralogically to obtain some

degree of representation of the entire Rustler near the center of the WIPP Site. Sample locations are listed in Table 1-1 and analysis techniques are summarized in Chapter 3. As discussed in more detail in Chapter 3, the samples examined in this study were from intact core that may not be representative of the principal water-bearing zones. The rock most recently in contact with Culebra groundwater is commonly a small fraction of the dolomite member and is likely to be reduced to rubble by partial dissolution, and hence be poorly recovered from the borehole.

1.3.4 Isotopic Data

Several isotopic studies have been conducted on rocks and waters from the Rustler Formation and related units. Lists of sample locations for each isotope are found in Table 1-1. Data pairs for δD-$\delta^{18}O$ are available for water samples from 70 localities: six from the Magenta, 21 from the Culebra, 17 from the Rustler/Salado contact zone, three from the Dewey Lake, four from the confined portion of the Capitan limestone, 12 from the vadose Capitan, one from the Triassic, one from alluvium, and five from the surface. The total number of replicate data-pairs, whether they represent replicate samplings at different times or replicate analyses of the same sample, was 86. Ten of these data pairs are for samples suspected to be nonrepresentative. A description of the samples, analytical methods, and criteria for judging sample quality is given in detail by Lambert and Harvey (1987). Carbonates from the Magenta (five localities) and Culebra (nine localities) were analyzed for their $\delta^{13}C$ and $\delta^{18}O$ values in a total of 43 replicates (Lambert, 1987; Lambert and Harvey, 1987). Values for δD of the water of crystallization in gypsums from selenite veins in the Dewey Lake and veins and alabaster from the Rustler have been measured at 11 horizon-sites representing five different boreholes (20 total replicates). Values for $\delta^{13}C$ and ^{14}C (percent-modern-carbon) have been obtained from waters from 16 horizon-sites representing 12 different wells (21 replicates); tritium measurements are available for seven wells (eight replicates). These are described in detail by Lambert (1987). Total uranium concentrations and uranium-isotope activity ratios are available for waters from five Rustler/Salado contacts, nine Culebra locations, two Magenta locations, one potash mine, one rainfall, and one surface spring locality (Lambert and Carter, 1987). Finally, 38

gypsums and anhydrites and 29 carbonates from Dewey Lake veins, Rustler veins and beds, Salado and Castile beds, caliche, and spring deposits have been analyzed for their $^{87}Sr/^{86}Sr$ ratios (Brookins and Lambert, 1988).

Lambert and Harvey (1987) proposed that the same criteria for evaluating the validity of a water sample used in determining a representative solute composition were also applicable to stable-isotope studies. The same criteria described by Robinson (1988) for judging the representativeness of the major solute composition of a water sample, however, are not applicable to certain trace isotope studies, such as radiocarbon. Many of the water samples used in the radiocarbon studies reported by Lambert (1987) and summarized here were collected according to the same criteria for major solutes. However, despite evaluation by such criteria, 12 of the 16 radiocarbon samples were found to be mixtures of native dissolved carbon and contaminant modern carbon introduced during the development of the sampling boreholes.

Other trace isotopes in groundwaters, such as uranium, have required still different sampling criteria. Barr et al. (1979) reported the correlative changes in total dissolved uranium and $^{234}U/^{238}U$ activity ratio with total iron. Lambert and Carter (1984) illustrated the effects of introduced contaminants on the uranium-isotope composition of water from a flowing well. It is tentatively concluded that preferred sampling criteria for $^{234}U/^{238}U$ studies are similar to those for metallic trace elements. The transient changes in such elements (e.g., iron) during a sampling period are discussed by Robinson (1988).

1.4 RESULTS OF GEOCHEMICAL STUDIES

1.4.1 Major/Minor Element Ratios and Correlations

In simple hydrologic and hydrochemical systems, spatial trends in element concentrations and ratios can be used to suggest flow directions and to delineate potential sites of recharge or interaquifer leakage. Average concentrations of major and minor elements in Culebra

waters were calculated from data sets obtained from the Sandia National Laboratories (SNL), IT Corporation, USGS, and New Mexico Environmental Evaluation Group (EEG) sampling and analysis programs. These average values are given in Table 2-2. Figure 1-8 shows contours of sodium concentration over the study area. Actual values for each well are also given. Contour placement is controlled by several factors, including the selected contour interval, smoothing factors, and radius of influence of the data points. The location of each contour is influenced by several data points; therefore, there may be discrepancies between the placement of contour lines and the concentrations at some well locations. The contours for sodium are similar to those for chloride, total dissolved solids (TDS) and fluid density.

The spatial trends in interelement correlations were examined by contouring ratios of Br/Cl, Na/Cl, Na/K, Sr/Ca, and other minor/major solute ratios. Results of these calculations are given in Chapter 2. The important features that emerge from these plots are given below:

- The Na/Cl molar ratio in the southern portion of the site is higher than would be produced by simple dissolution of halite, suggesting the potential contribution by dissolution of Na-silicates in this area.

- The K/Na weight ratios, Mg/Ca molar ratios, and Na and Sr concentrations are anomalously high at WIPP-27 and WIPP-29, suggesting that contamination by potash refining operations is important at these locations. Contours for the K/Na weight ratio are shown in Figure 1-9. Names for the wells indicated in Figure 1-9 are given in Figure 1-8.

- Element ratios and concentrations of several elements are anomalous at P-14 when compared to water compositions at the surrounding wells. Concentrations of Ca, Sr, and I are anomalously high, and the concentration of SO_4 is anomalously low at this site.

● WIPP-28
15,000

● WIPP-27

WIPP-30
8600

N

H-6
18,000

DOE-2
18,000

WIPP-25
3250

H-5
63,000

WIPP-13
19,000

H-3
18,000

WIPP-26
3500

P-14
4100

DOE-1
46,000

● WIPP-29

WIPP Site
Boundary

50,000

H-4
6000

H-11
39,000

P-17
28,000

H-12
● 50,000

H-7
210

40,000

30,000

20,000

10,000

H-9 ●
150

● Engle Well
190

0   1   2   3   4 mi

0   2   4   6 km

H-8
54
●
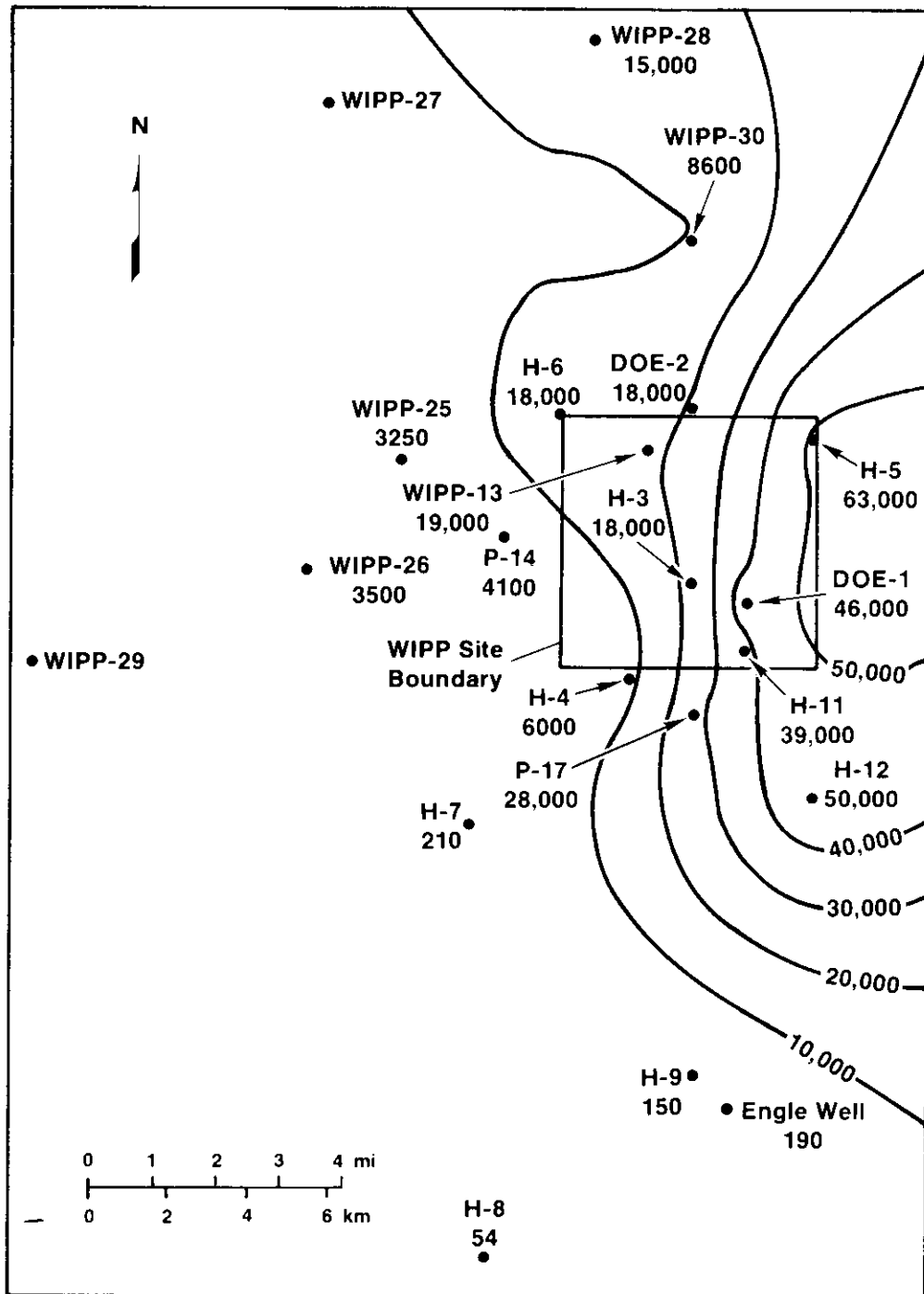
TRI-6341-27-0

Figure 1-8. Contours of sodium concentration (mg/L) in study area. The WIPP Site boundary is indicated for reference (from Siegel et al., Chapter 2).
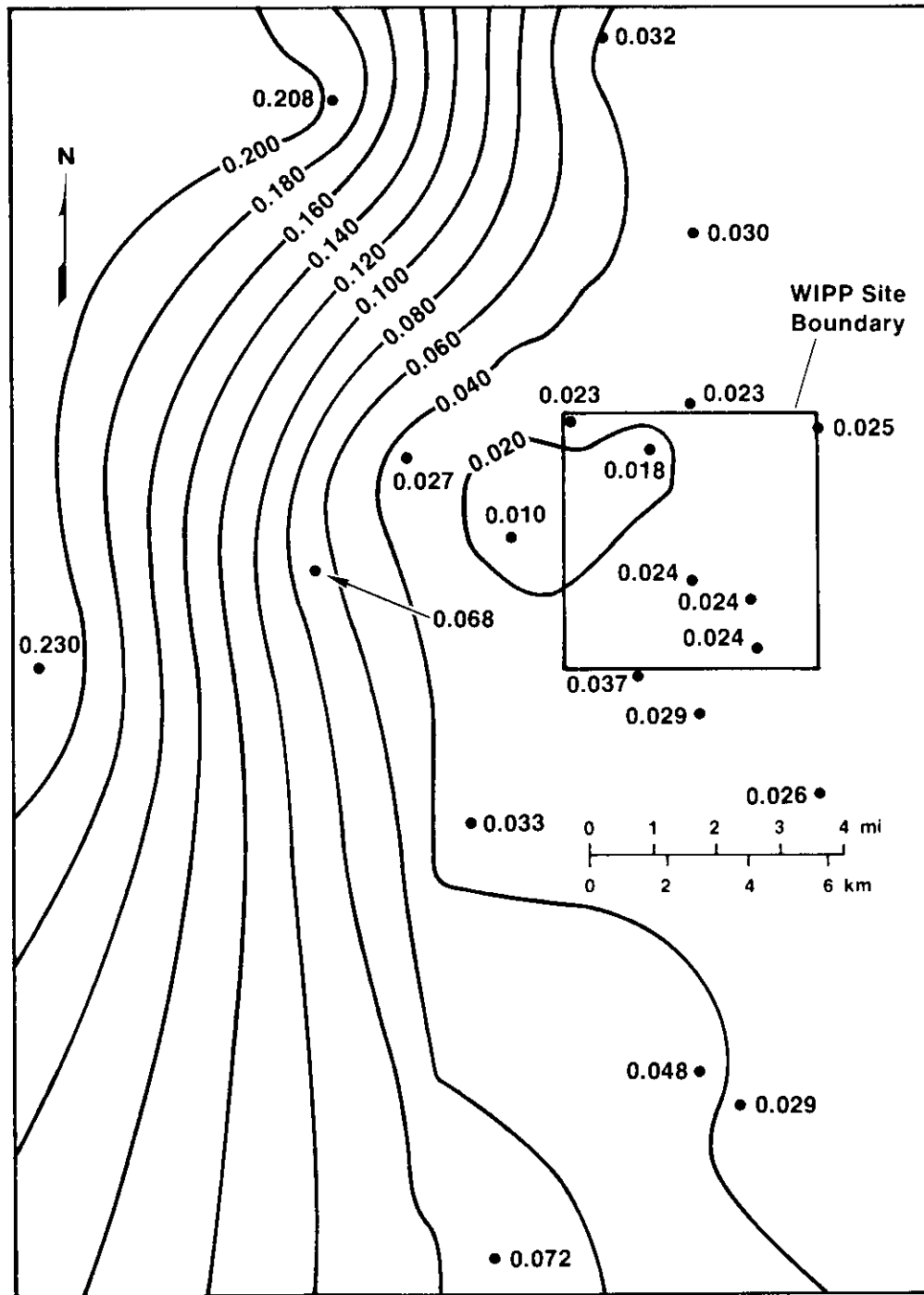
Figure 1-9. Contours of ratios of K/Na concentrations in study area (from Siegel et al.,
Chapter 2).

- The Cl/Br ratio is highest in Nash Draw, intermediate through the center of the WIPP Site, and lowest in P-14 and H-4.

1.4.2 Definition of Hydrochemical Facies of Culebra Groundwater Based on Relative Proportions of Major Solutes

Based on the major solute compositions presented in Table 2-2, four hydrochemical facies are delineated in Figures 1-10, 1-11, 1-12, and 1-13. Compositions of waters at locations indicated by solid circles in Figure 1-10 are described in Figure 1-13. Compositions of several other wells (see Chapter 4) indicated by open circles were not included in the original data set used to define the facies, but their compositions are consistent with the facies borders. The facies borders indicated in Figure 1-13 are located by reference to the wells, whereas the boundaries of the halite dissolution zones are located by reference to control points (Snyder, 1985) plotted by Lappin (1988, Figure 4.1.2).

Zone A contains a saline (about 3.0 molal) NaCl brine with a Mg/Ca molar ratio between 1.2 and 2.0. This water is found in the eastern third of the site; the zone is roughly coincident with the region of low transmissivity. On the western side of the zone, halite in the Rustler has been found only in the unnamed lower member; in the eastern portion of the zone, halite has been observed throughout the Rustler (see Figure 1-13).

Zone B contains a dilute $CaSO_4$-rich water (ionic strength <0.1 m) in the southern part of the site. Mg/Ca molar ratios are uniformly low (0.4-0.5). This zone is coincident with a high-transmissivity region; halite is not found in the Rustler in this zone.

Zone C contains waters of variable composition with low-to-moderate ionic strength (0.3 to 1.6 m) in the western part of the WIPP Site and the eastern side of Nash Draw. Mg/Ca molar ratios range from 0.5 to 1.2. This zone is coincident with a region of variable transmissivity. In the eastern part of this zone, halite is present in the lower member of the Rustler; on the western side of the zone, halite is not observed in the formation. The most
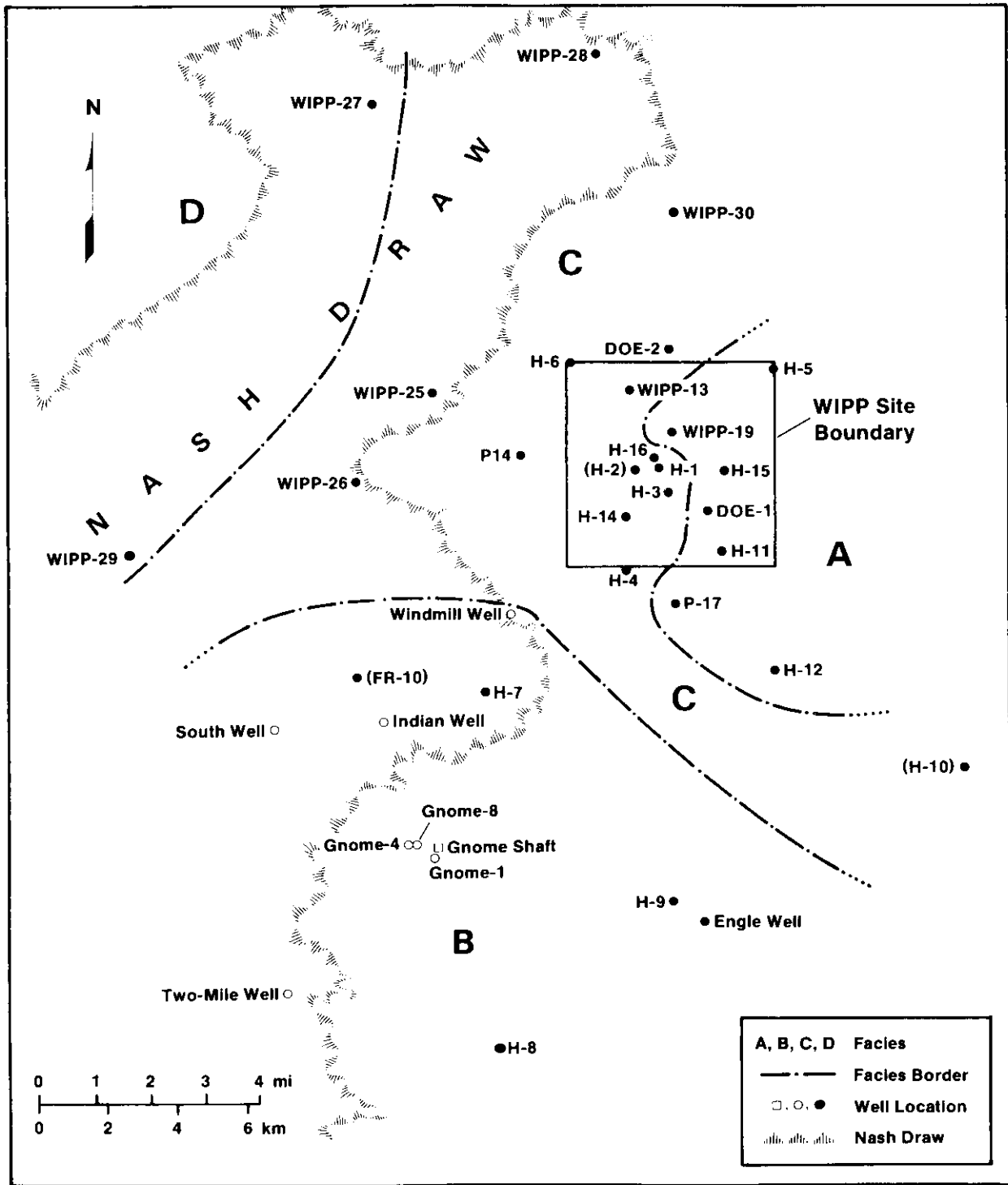
TRI-6331-78-1

Figure 1-10. Hydrochemical facies of the Culebra dolomite (from Siegel et al., Chapter 2).
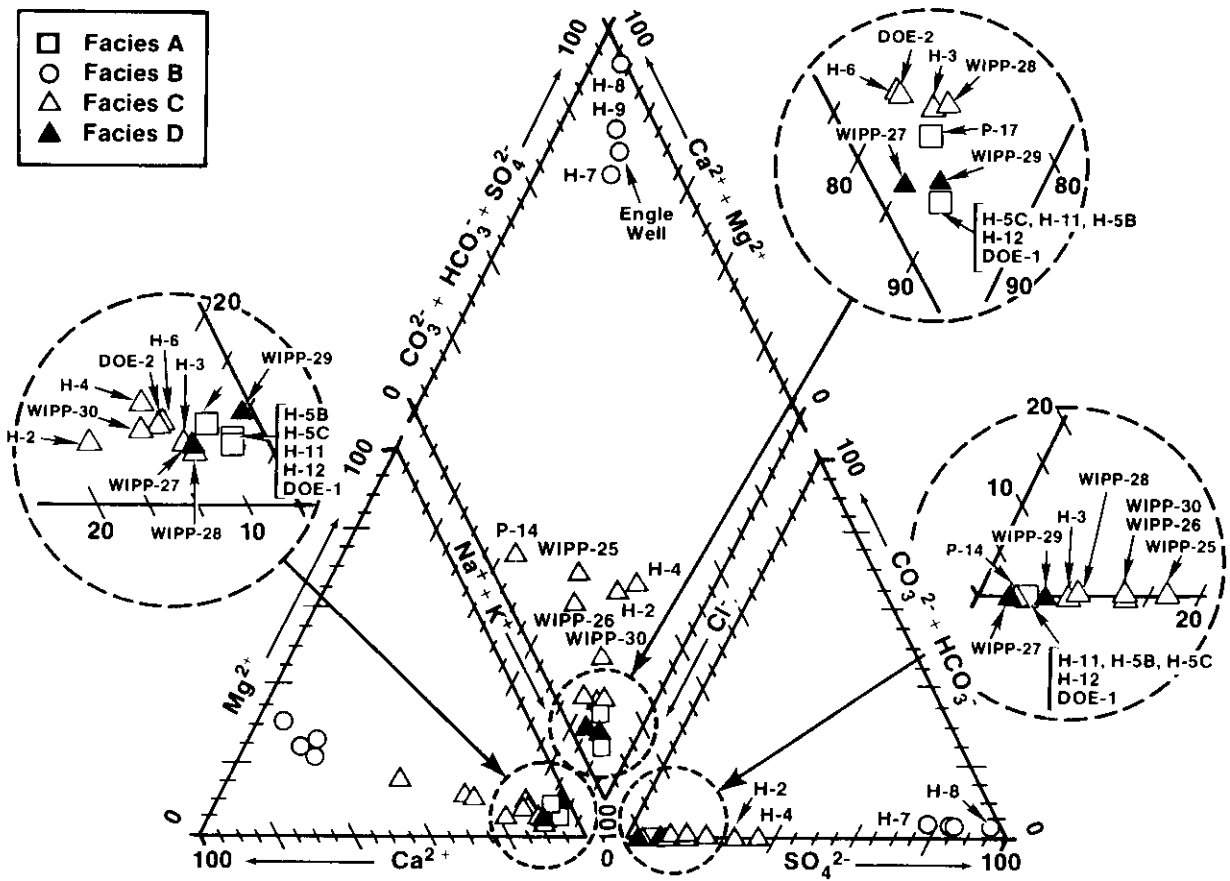
Figure 1-11. Trilinear diagram for Culebra groundwaters (from Siegel et al., Chapter 2).

TRI-6330-35-1
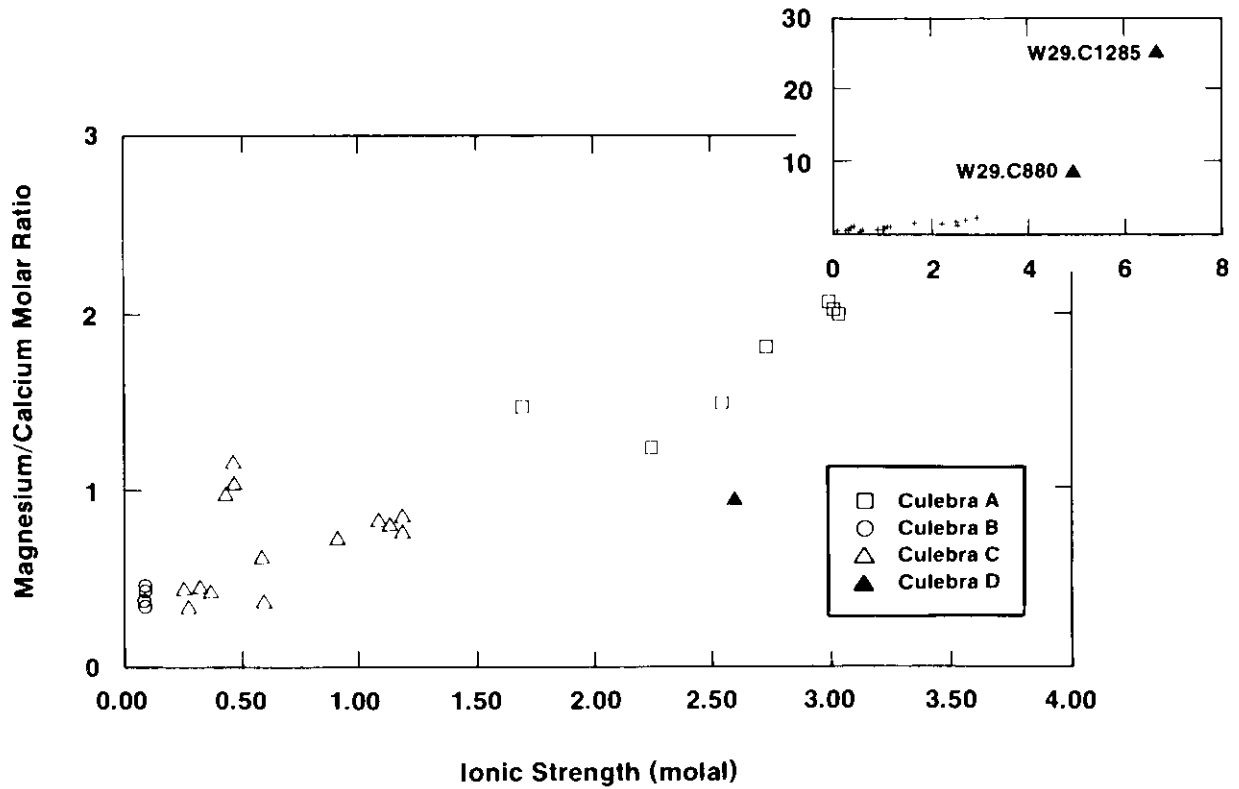
Figure 1-12. Relationship between Mg/Ca molar ratio and ionic strength (molal) for Culebra groundwater samples in different hydrochemical facies (from Siegel et al., Chapter 2).
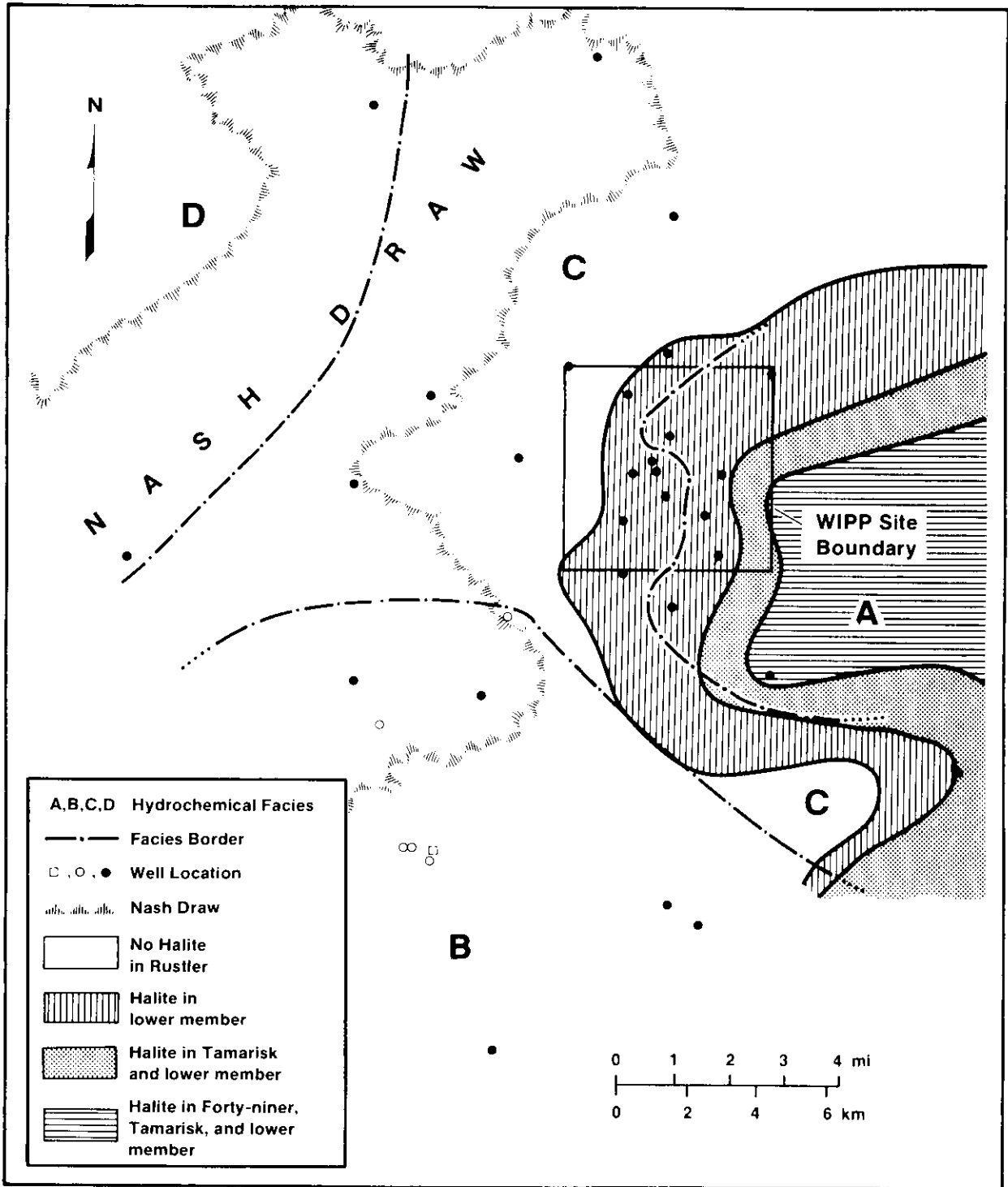
TRI-6344-97-0

Figure 1-13. Relationship between occurrence of halite in the Rustler and hydrochemical facies of the Culebra dolomite.

saline (NaCl-rich) water is found in the eastern edge of the zone, close to core locations where halite is observed in the Tamarisk Member.

Zone D, a fourth zone comprising wells WIPP-27 and WIPP-29, can be defined based on inferred contamination related to potash refining operations in the area. Waters from these wells have anomalously high salinities (3-6 m) and K/Na weight ratios (0.22) compared to other wells at the site (0.01-0.09). At WIPP-29, the composition of the Culebra water has changed over the course of a 7-year monitoring period. The Mg/Ca molar ratio at WIPP-29 is anomalously high, ranging from 10 to 30 during the monitoring period.

The chemical characteristics of each of the facies are described by the Piper (trilinear) diagram shown in Figure 1-11. This plot summarizes relationships between the major solutes in the $Na-K-Mg-Ca-Cl-SO_4-CO_3$ system. The diagram shows the relative proportions of the ions on an equivalents/liter basis. Relative proportions of cations and anions are displayed separately in the triangular plots in the bottom half of the figure. In the rhombus in the upper portion of the diagram, the ratio of divalent to monovalent cations and the ratio of chloride to sulfate + carbonate + bicarbonate are shown.

Compositions of Culebra waters from Zone A have nearly identical ionic proportions and plot on the same location in the graph near the Na-Cl corner. They are distinguished from waters in Zone C by their higher Mg/Ca ratio and ionic strengths (see Figure 1-12). Dilute groundwater from Zone B plot near the $Ca-SO_4$ corner and water from Zone C cover a wide area in the plot. Waters from Zone D have similar ionic proportions to those of Zone A and are distinguished primarily on the basis of salinity and K/Na ratio, parameters that are not shown in Figure 1-11.

1.4.3 Principal Component Analysis of Rustler Groundwater Compositions

In the previous section, hydrochemical facies for Culebra groundwaters were defined using the relative proportions of the concentrations of seven major solutes. These solute ratios

can be represented by a trilinear plot as shown in Figure 1-11. To show relationships among the 17 independent chemical variables presented in Table 2-2, the method of principal component analysis (PCA) was used. This method summarizes the relationships among the variables and shows how these relationships differ for each water composition.

The principal components or factors identified from PCA can be thought of as hypothetical compositional end members (Q-mode PCA) or can be used to express the relationships among the compositions in terms of a small number of independent underlying correlations (R-mode PCA). This information can be used to refine the definition of hydro-chemical facies and to suggest the nature of chemical reactions that control groundwater composition.

In R-mode PCA, several kinds of correlations are possible. For example, two cations that are dissolved from the source mineral will be positively correlated, whereas elements whose concentrations are inversely related by a solubility product will be negatively corre-lated. Appendix 2B explains the basic concepts and vocabulary of PCA. The origins of the factor-loading matrices and factor-score matrices, the significance of factor rotations, examples of interelement correlations and their possible geochemical interpretations, and the need for data transformations are explained. Section 2.3.3 describes the application of this technique to waters from the Culebra dolomite and related rock units. The following section is a summary of that work.

Two data sets were used in the analysis. Population 1 included data for Ca, Mg, K, Na, Cl, SO_4, B, Li, SiO_2, Br, Sr, alkalinity, and pH from 22 samples from the Culebra. Population 2 included data from wells for which analyses of the above elements plus Fe, Mn, F, and I were available (20 samples from the Culebra, Magenta, Dewey Lake, and Bell Canyon units). In most respects, the results for the two populations were similar.

1.4.3.1 Unrotated Principal Components

R-mode PCA was carried out using the PCA programs in SAS (Statistical Analysis System Institute, 1982). Three principal components (factors) account for approximately 96% of the total variance of population 1 and are shown in Figure 1-14. Factor loadings are listed in Table 2-7. Factor 1 accounts for approximately 67% of the total variance of the data set. It is characterized by high positive correlations (loadings) for all of the variables except pH, bicarbonate alkalinity, and silica. The factor accounts for most of the variance of sodium and chloride, and it is likely that this factor represents addition of solutes by dissolution of evaporite minerals. For this reason, the factor is referred to as the "salinity factor" in this report.

Factor 2 accounts for approximately 18% of the variance of the data set. It is characterized by large loadings for pH, bicarbonate alkalinity, and silica and boron concentrations. This combination of elements may reflect sorption and silicate and carbonate diagenesis. It is referred to as the "silicate/bicarbonate factor" in this report.

Factor 3 accounts for approximately 11% of the total variance and exhibits high positive loadings for calcium and strontium and a high negative loading for sulfate. This element association probably reflects dissolution/precipitation of gypsum and is referred to as the "sulfate factor" in this report.

1.4.3.2 Rotated Principal Components

As discussed in Appendix 2B, several alternative orientations of the principal component axes may be equally efficient in describing the variance in the data set. The unrotated principal components described in the previous section were compared to those obtained from varimax, equamax, and quartimax rotational schemes to determine if any element associations were common. It was found that the factor-loading matrices from all rotational schemes contained the same key element associations described above for the unrotated components. The loading matrices differed primarily in the relative loadings of
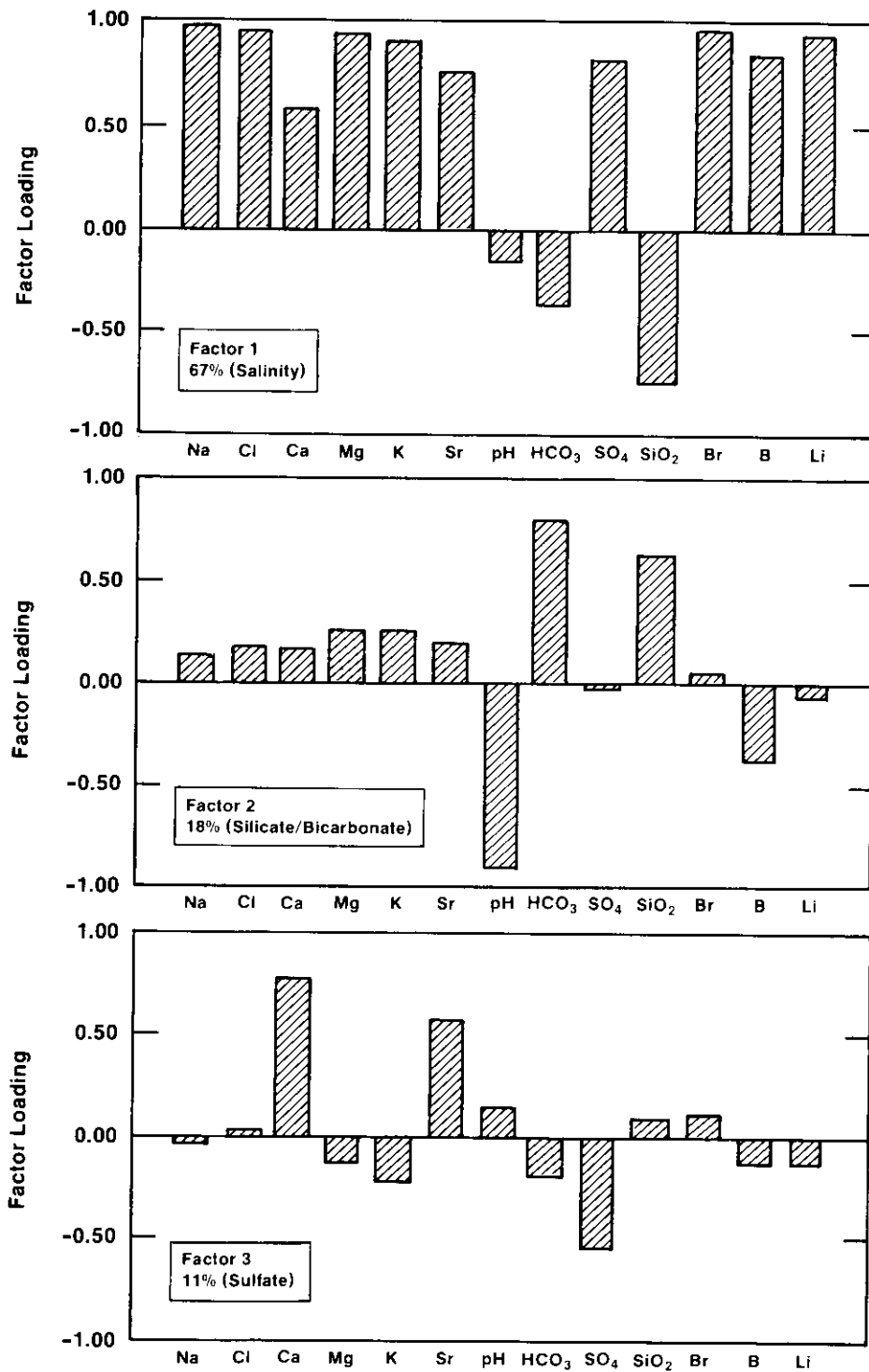
TRI-6344-113-0

Figure 1-14. Unrotated R-mode factor loadings for factors 1, 2, and 3 for Culebra groundwaters (population 1).

other elements and the variance explained by the salinity, silicate/bicarbonate, and sulfate factors.

The compositions of the samples in terms of the factors are described by the factor scores. Relationships between varimax factor scores for the salinity and sulfate factors are plotted in Figure 1-15, which also indicates hydrochemical facies of each well. Factor scores are listed in Table 2C-2. Figure 1-15 shows that the first two principal components can be used to delineate the same groups of wells identified in Figures 1-10 through 1-12. Thus, the definition of hydrochemical facies based on the proportions of major solutes is supported by correlations among the major and minor elements examined in this study.

1.4.3.3 R-mode Factors Obtained after Partialling Out Total Dissolved Solids

The three major factors obtained from the R-mode analysis described above are strongly affected by halite dissolution. Solutes are added directly from the halite, or indirectly because the solubilities of sulfate and carbonate phases increase as the ionic strength increases (see Section 1.4.5). A second R-mode PCA examined interelement correlations independent of the effects of halite dissolution. In this analysis, the principal components of the partial correlation matrix with respect to TDS concentration were extracted. A more detailed description of the procedure is in Appendix 2B.

Five factors accounted for 99% of the variance that remains after the TDS were partialled out. In Figure 1-16, the variables with the highest loadings for each factor are identified. Factor loadings are plotted only for elements that have important geochemical significance or that strongly influence the orientation of the factors (loading >0.23). The complete factor-loading matrix is found in Table 2-8. Factor 1B is dominated by the negative correlation of Ca and Sr with sulfate and is suggestive of dissolution/coprecipitation of Sr and Ca in a sulfate phase such as gypsum or anhydrite. It accounts for 67% of the total variance of Ca, 35% of the total variance of Sr, and 24% of the total variance of sulfate. This factor is similar to the sulfate factor (3) described previously. Factors 2B, 4B, and 5B are similar to the silicate factor (2) described previously and contain all or portions of two negatively
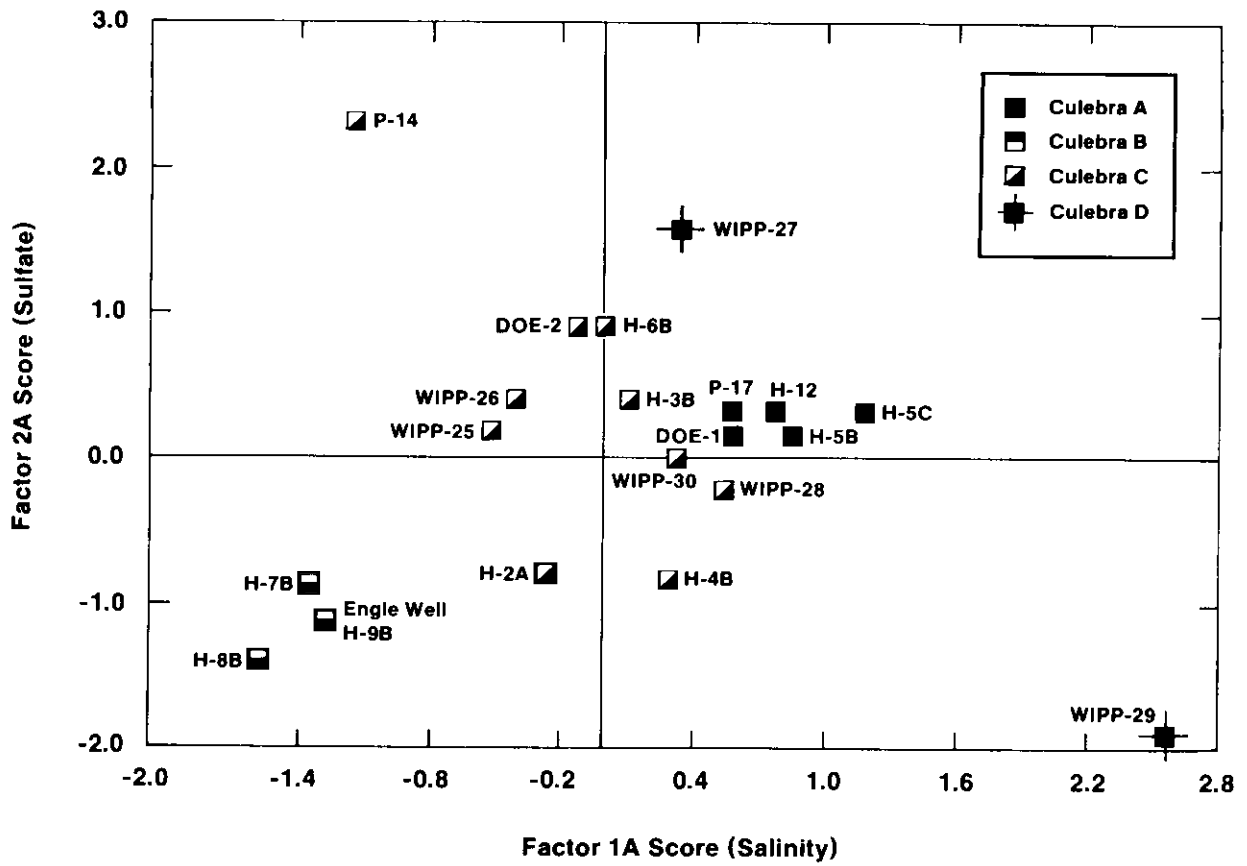
Figure 1-15. Relationship between varimax R-mode factor scores for factors 1A and 2A for Culebra groundwaters (population 1).
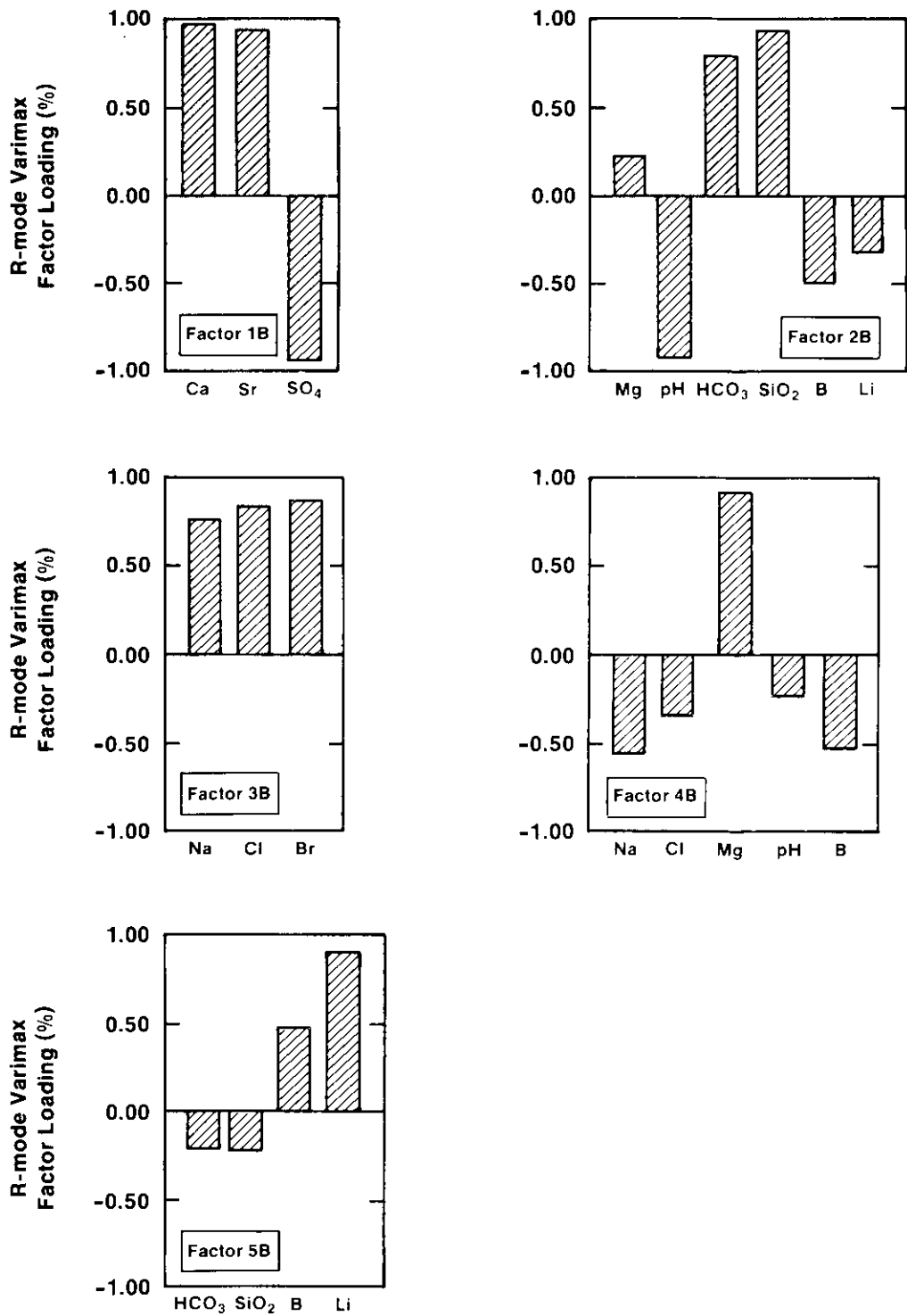
TRI-6344-112-0

Figure 1-16. Varimax R-mode factor loadings of key elements for factors 1B, 2B, 3B, 4B, and 5B obtained from partial-correlation matrix with respect to TDS for Culebra groundwaters (population 1).

correlated groups of variables. One group involves the correlation of Mg, K, bicarbonate alkalinity, and silica; the other group contains pH, B, and Li. This pattern of element associations may be due to a combination of processes including sorption, ion exchange, carbonate diagenesis and silicate diagenesis and is discussed in more detail in Section 2.4.3.

In another factor extracted from population 2, variance in Mg was associated with a large amount of the variance of F and SO_4. As discussed in Chapter 2, this factor may indicate the presence of sellaite (MgF_2) contained in anhydrite. Descriptions of the other factors and representation of the compositions of the water samples in terms of the factors are also in Chapter 2.

The correlations of the major elements described by the PCAs confirm the definition of hydrochemical facies described in previous sections. The correlations of the minor elements, as revealed by the PCA, provide insight into the identity of the minerals that control the concentrations of Sr, F, Si, B, and Li. The calculations suggest that Sr is present in sulfates, that F is present as MgF_2 in anhydrite, and that concentrations of Si, B, and Li are affected by reactions involving clay minerals.

1.4.4 Classification of Rustler Groundwaters by Normative Salt Assemblages

Bodine et al. (Chapter 4) suggest that recasting the chemical composition of a water into a "salt norm" is a useful diagnostic tool for inferring possible origins of the water's solutes. The normative salt assemblage (or "salt norm") is the quantitative equilibrium assemblage of salts that would precipitate from a natural water if it were evaporated to dryness under ideal equilibrium conditions at 25°C and atmospheric pressure. The normative assemblage yields a diagnostic chemical-mineralogical characterization of the water that indicates the nature of possible water/rock interactions in subsurface environments and may contribute in determining the water chemistry's evolutionary path.

The SNORM computer code (Bodine and Jones, 1986) calculates salt norms based on the Gibbs Phase Rule, free energy data, and observed low-temperature mineral associations. Bodine et al. (Chapter 4) applied SNORM to the data set described above that was obtained from their independent evaluation of water chemistry data from the Rustler Formation. Based on these calculations, they identify four end-member norms in brines collected from the WIPP Site:

- Type 1 brines contain normative alkaline-earth chloride salts and low Cl/Br (<300) ratios; these are termed "primitive-diagenetic" norms and may result when connate waters are involved in dolomitization

- Type 2 dilute solutions contain normative alkali-bearing carbonates that suggest dissolution of detrital silicates through carbonic acid hydrolysis in a weathering/recharge zone

- Type 3 dilute sulfate-rich solutions are produced when surface-derived (fresh) waters dissolve anhydrite or gypsum and little else

- Type 4 saline halite-rich brines are produced when surface-derived (fresh) waters dissolve anhydrite or gypsum and halite in the Rustler and upper Salado.

In Chapter 4, Bodine et al. show that the compositions of most waters in the Rustler Formation can be produced by mixing of the above four end-member brines, types 1 and 4 being the most common. The fluid produced by the dehydration of gypsum may also be a component of some well waters. Note, however, that most waters of the four types considered by Bodine et al. for which $\delta^{18}O$ and δD values are available have diagnostically meteoric stable-isotope characteristics (Lambert and Harvey, 1987; Lambert, Chapter 5).

In the Culebra member, water (which may or may not be representative of fluid native to the formation) sampled from P-18 contains the highest proportion of primitive-diagenetic brine. In the Rustler/Salado contact zone, wells in the center of the WIPP Site (H-5 and

H-6) contain the highest proportions of the "primitive"-norm-type fluids. Water from WIPP-15 in the Gatuña Formation is dominantly type 2; dissolution of an anhydrite-rich rock by this water would produce waters like H-7 or H-1, which have strong type 3 signatures. Examples of waters with a significant component of type 4 water include H-5 and DOE-1. According to Bodine et al. in Chapter 4, in both the Culebra and the Rustler/Salado contact zones, the relative proportion of recharge water to primitive-diagenetic water increases to the north, west, and south of the WIPP Site.

1.4.5 Calculations of Mineral Saturation Indices for Culebra Waters

Mineral saturation indices may provide insight into the nature of chemical processes that control solute concentrations in groundwaters. Saturation indices in Culebra waters have been calculated for minerals commonly observed in the Ochoan Series (see Table 1-3). The computer code PHRQPITZ (Plummer et al., 1988), which uses the Pitzer model for ion-interactions, was utilized for these calculations. All water samples are saturated with respect to gypsum, undersaturated with respect to halite, and with the exception of WIPP-29 in Zone D, all samples are undersaturated with respect to anhydrite. Dolomite and calcite saturation indices are variable, indicating both undersaturation and supersaturation with respect to the carbonates. The relationships between saturation indices and ionic strength for several minerals are shown in Figures 1-17, 1-18, and 1-19.

As discussed by Siegel et al. in Chapter 2, the relationships among the saturation indices, pH, and calculated pCO_2 suggest that the loss of CO_2 gas from the water during sample collection may be responsible for part of the apparent supersaturation of the carbonates. Other potential sources of error in the calculations of carbonate equilibria include uncertainties in the pH measurements due to the use of an activity scale inappropriate for saline Na-Cl brines, errors in laboratory measurements of major solute compositions, and the choice of an inappropriate value for the Gibbs free energy of formation for dolomite to calculate the saturation indices.

Table 1-3. Saturation Indices for Common Evaporite Minerals Calculated by PHRQPITZ

Well	Date	Lab	Ionic Strength (molal)	pH	a_{H_2O}	Charge[1] Balance Error	Saturation Indices[2] Anh	Cal	Dol	Gyp	Hal	Mag	log pCO_2
Culebra:													
DOE-1	4/85	UNC	2.53	7.10	0.923	9.05E-03	-0.12	-0.34	-0.13	0.03	-1.26	-0.62	-2.60
DOE-2	3/85	UNC	1.19	7.00	0.968	-6.52E-02	-0.18	-0.21	-0.14	0.01	-2.03	-0.77	-2.33
ENGLE	3/85	UNC	0.09	7.40	0.999	1.00E-03	-0.22	0.22	0.38	0.00	-6.02	-0.68	-2.44
H-2A	4/86	UNC	0.27	8.00	0.994	-4.33E-03	-0.25	0.45	0.78	-0.04	-3.49	-0.52	-3.38
H-3B3	2/85	UNC	1.08	7.40	0.971	-2.53E-03	-0.20	-0.08	0.12	0.00	-2.11	-0.65	-2.86
H-3B3	6/84	UNC	1.08	7.40	0.972	-2.56E-02	-0.15	-0.02	0.23	0.04	-2.13	-0.59	-2.83
H-4B	5/81	UNC	0.455	8.00	0.991	-1.49E-02	-0.17	0.36	1.07	0.04	-3.13	-0.13	-3.35
H-4B	7/85	UNC	0.42	7.70	0.991	4.14E-03	-0.20	0.07	0.46	0.01	-3.17	-0.45	-3.04
H-4C	8/84	UNC	0.45	7.80	0.991	4.82E-03	-0.20	0.19	0.77	0.01	-3.12	-0.26	-3.11
H-5B	6/81	UNC	2.993	7.90	0.906	-1.18E-01	-0.10	0.71	2.12	0.04	-1.08	0.57	-3.21
H-5B	8/85	UNC	2.97	7.40	0.908	8.46E-02	-0.11	-0.02	0.68	0.03	-1.09	-0.15	-2.86
H-5C	10/81	UNC	3.002	7.90	0.906	-1.20E-01	-0.08	0.75	2.20	0.05	-1.08	0.61	-3.17
H-6B	5/81	UNC	1.178	7.00	0.969	2.24E-04	-0.15	-0.04	0.16	0.05	-2.05	-0.64	-2.16
H-6B	9/85	UNC	1.13	6.90	0.970	-1.28E-02	-0.20	-0.16	-0.07	-0.01	-2.08	-0.75	-2.07
H-7B1	3/86	UNC	0.089	7.20	0.999	-4.09E-04	-0.23	0.07	0.01	-0.01	-5.86	-0.90	-2.20
H-8B	1/86	UNC	0.083	7.60	0.999	-1.97E-04	-0.23	0.33	0.66	-0.01	-7.45	-0.52	-2.70
H-9B	11/85	UNC	0.087	7.40	0.999	3.70E-04	-0.22	0.24	0.37	0.00	-6.23	-0.71	-2.43

Table 1-3. Saturation Indices for Common Evaporite Minerals Calculated by PHRQPITZ (Continued)

Well	Date	Lab	Ionic Strength (molal)	pH	$^a H_2O$	Charge[1] Balance Error	Saturation Indices[2]						log pCO$_2$
							Anh	Cal	Dol	Gyp	Hal	Mag	
H-11B3	6/85	UNC	2.23	7.20	0.934	-3.60E-02	-0.13	-0.17	0.12	0.03	-1.39	-0.54	-2.63
H-12	8/85	UNC	2.72	7.20	0.916	4.42E-02	-0.12	-0.15	0.34	0.02	-1.18	-0.35	-2.61
P-14	2/86	UNC	0.582	6.80	0.988	-9.06E-03	-0.15	0.14	0.18	0.05	-3.01	-0.81	-1.81
P-17	3/86	UNC	1.67	7.50	0.953	-3.61E-02	-0.18	0.10	0.73	0.00	-1.70	-0.22	-2.90
WIPP-25	8/80	UNC	0.26	6.90	0.995	3.21E-03	-0.24	0.03	0.04	-0.03	-3.56	-0.84	-1.69
WIPP-26	8/80	UNC	0.329	6.90	0.993	-5.12E-03	-0.18	-0.04	-0.10	0.03	-3.36	-0.91	-1.86
WIPP-26	8/80	G	0.330	6.90	0.993	-3.71E-02	-0.23	0.09	0.14	-0.02	-3.32	-0.79	-1.84
WIPP-26	11/85	UNC	0.371	7.10	0.992	-9.29E-03	-0.20	0.10	0.18	0.02	-3.22	-0.77	-2.14
WIPP-27	9/80	UNC	2.573	6.30	0.922	-7.62E-02	-0.12	-0.38	-0.40	0.03	-1.29	-0.87	-1.33
WIPP-28	9/80	UNC	0.903	6.50	0.976	-2.42E-02	-0.26	0.16	0.53	-0.07	-2.27	-0.48	-0.76
WIPP-29	8/80	UNC	4.908	6.10	0.840	-2.06E-01	0.02	-0.72	0.01	0.09	-0.61	-0.21	-0.87
WIPP-29	8/80	G	4.472	6.10	0.853	-2.74E-01	-0.15	-0.45	0.61	-0.07	-0.64	0.21	-1.10
WIPP-29	12/85	UNC	6.57	5.90	0.773	-2.07D-01	-0.01	-1.25	-0.56	-0.01	-0.20	-0.16	-0.75
WIPP-30	9/80	UNC	0.582	8.80	0.986	-2.50E-02	-0.18	1.12	2.37	0.02	-2.73	0.41	-4.41

Table 1-3. Saturation Indices for Common Evaporite Minerals Calculated by PHRQPITZ (Continued)

Well	Date	Lab	Ionic Strength (molal)	pH	a_{H_2O}	Charge[1] Balance Error	Anh	Cal	Dol	Gyp	Hal	Mag	log pCO_2
Magenta:													
H-3B1	7/85	UNC	0.20	8.00	0.997	-2.79E-03	-0.16	0.52	1.02	0.06	-4.04	-0.34	-3.47
Dewey Lake:													
TWIN-P	1/86	UNC	0.011	7.70	0.999	4.89E-04	-1.88	0.37	0.67	-1.66	-7.52	-0.54	-2.39
Bell Canyon:													
DOE-2	7/85	UNC	2.95	6.60	0.907	8.68E-03	-0.13	-0.17	-0.40	0.00	-1.09	-1.07	-1.96

1. Charge balance error (CBE in equivalents per kilogram of water) is calculated as: CBE (eq/kg H_2O) = Σ cations (eq/kg H_2O) - Σ anions (eq/kg H_2O)
2. Mineral names: Anh = anhydrite; Cal = calicite; Dol = dolomite; Gyp = gypsum; Hal = halite; Mag = magnesite.
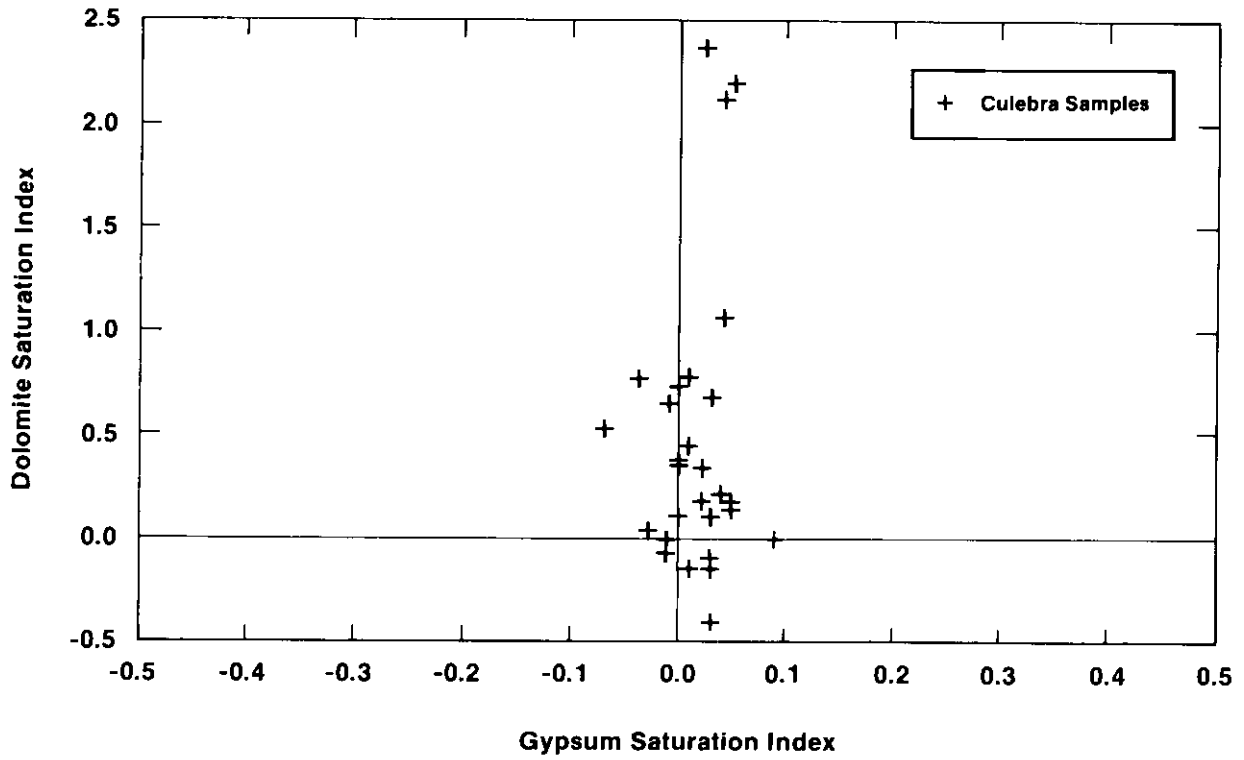
Figure 1-17. Relationship between gypsum and dolomite saturation indices in Culebra groundwater samples (from Siegel et al., Chapter 2).
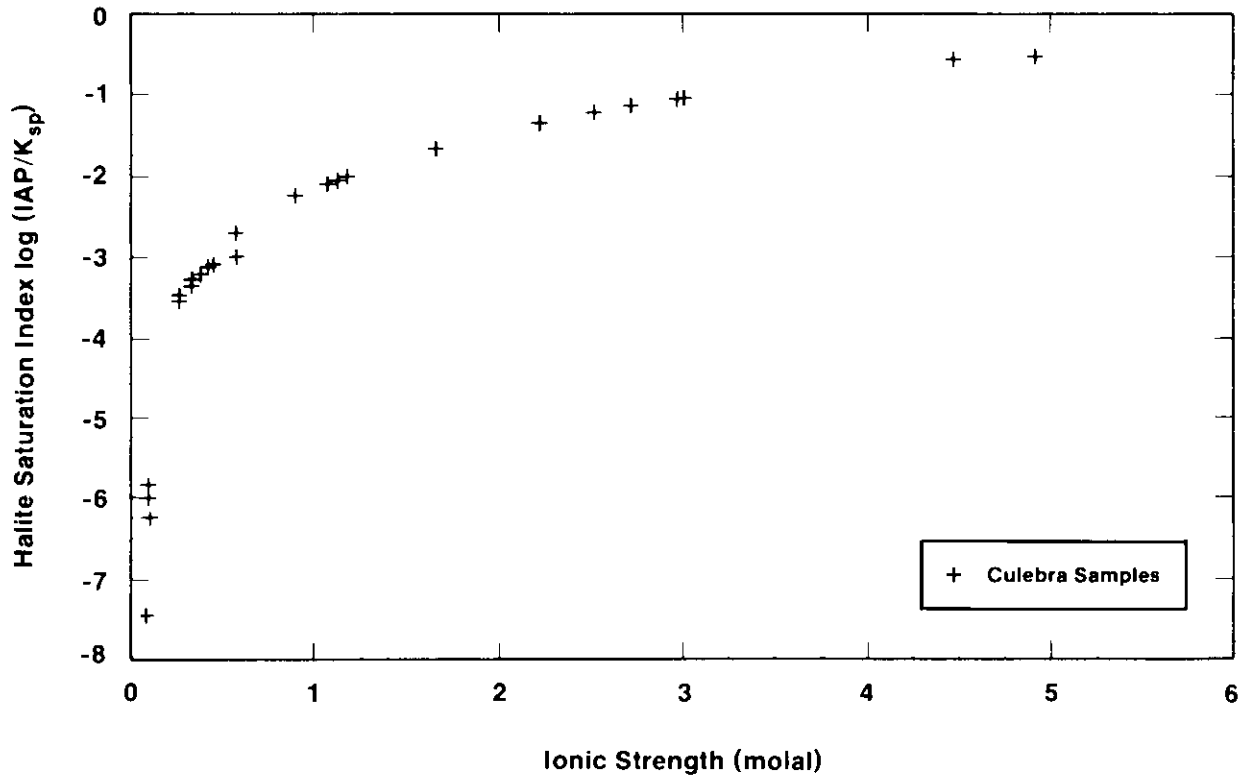
TRI-6344-102-0

Figure 1-18. Relationship between halite saturation indices and ionic strengths of Culebra
groundwater samples (from Siegel et al., Chapter 2).
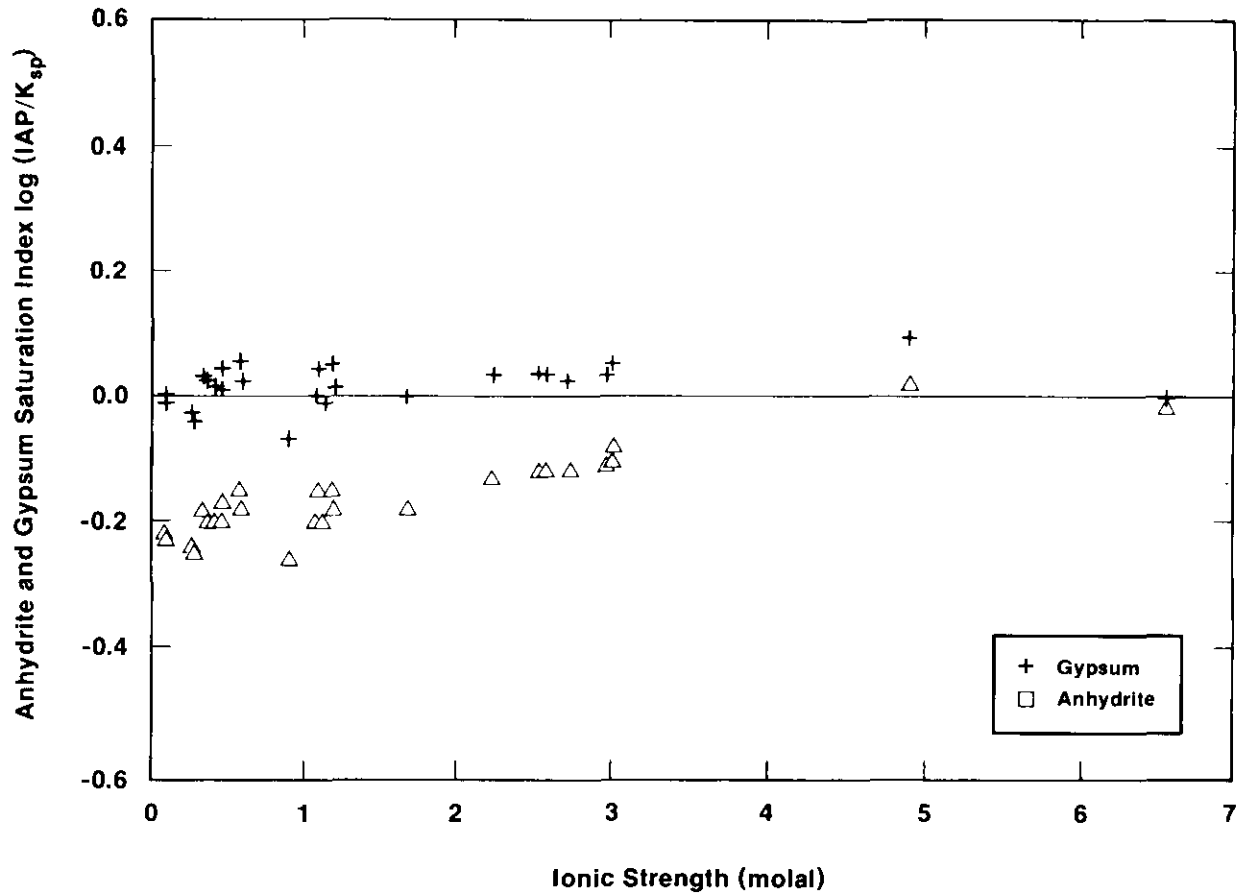
TRI-6344-96-0

Figure 1-19. Relationship between anhydrite and gypsum saturation indices (states) and ionic strengths of Culebra groundwater samples (from Siegel et al., Chapter 2).

The degree of carbonate mineral saturation independent of the effects due to CO_2 outgassing can be determined by examining the value of the saturation index (SI) expression:

$$2\,SI_{calcite} - SI_{dolomite}\,.$$

The value of this expression is independent of the uncertainty in the carbonate ion activity and equals zero when the solution is saturated with respect to both calcite and dolomite.

Figure 1-20 shows that the value of the saturation index expression for the Culebra waters decreases as a function of ionic strength. This means that once the effects of the CO_2 outgassing are corrected for, many of these waters are either supersaturated with respect to dolomite and/or undersaturated with respect to calcite. The degree of disequilibrium increases with ionic strength.

1.4.6 Partial Equilibrium Model for Major Solutes

In Chapter 2, Siegel et al. suggest that the solute relationships described in the preceding sections might be indicative of a partial equilibrium system. In a partial equilibrium system, solution/mineral equilibria shift nearly reversibly in response to an irreversible process (Helgeson, 1968; Plummer, 1984). Increase of salinity in Culebra waters due to dissolution of evaporite salts in adjacent rock units is an irreversible chemical reaction process affecting the water chemistry. The increase in salinity changes the apparent solubilities of carbonates and sulfates. As shown in Figure 1-21, the solubilities of dolomite, calcite, and gypsum increase with salinity up to 3 molal ionic strength and then decrease. Thus, even if the saturation indices for these minerals are near zero, the waters may still be capable of dissolving significant amounts of these phases in response to salinity increase.
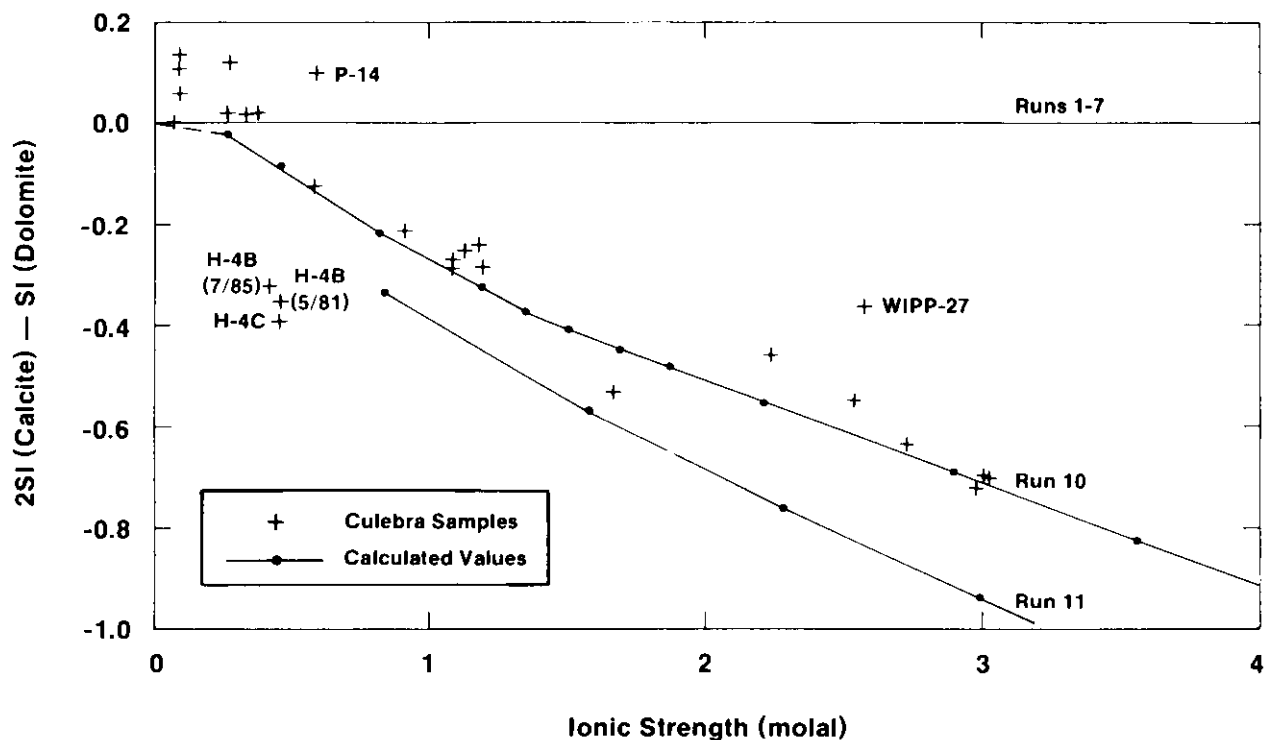
Figure 1-20. Relationship between saturated index expression $(2SI_{calcite} - SI_{dolomite})$ and ionic strengths for Culebra groundwaters. Compositions of hypothetical solutions calculated by reaction-path simulations described in Section 2.4.2.2 are indicated by solid lines (from Siegel et al., Chapter 2).
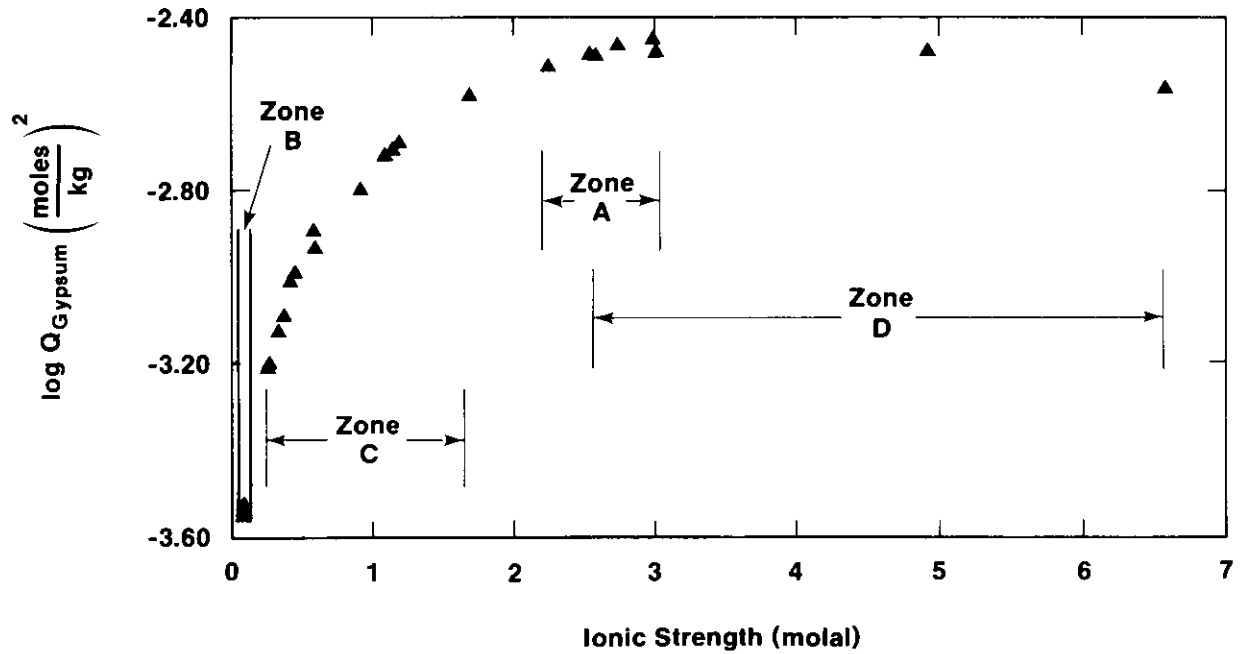
TRI-6344-93-0

Figure 1-21. Relationship between apparent solubility product logQ for gypsum and ionic strength in Culebra water samples. LogQ is calculated from the thermodynamic solubility constant logK and the activity coefficients of the reactants ($logQ = logK - log\gamma_{Ca^{2+}} - log\gamma_{SO_4^2} - 2log\ a_{H_2O}$).

In Section 2.4.2.2, Siegel et al. use the PHRQPITZ code (Plummer et al., 1988) to evaluate a partial equilibrium model for precipitation/dissolution of gypsum, calcite, and dolomite in the Culebra. The PHRQPITZ code was used to calculate the compositions of waters that would be produced by several hypothetical reaction paths. Parametric simulations were carried out to determine the effect of certain assumptions about chemical reaction rates, sources of solutes, and initial conditions on the groundwater compositions. Figures 1-22 and 1-23 compare the changes in concentrations of major solutes along two hypothetical reaction paths with compositions of waters in the Culebra. Both runs assume equilibrium is maintained with respect to calcite and gypsum, while halite plus accessory evaporite salts are added to solution. The solutions are closed with respect to atmospheric CO_2, and initial pCO_2 is 10^{-2} atmosphere. For Figure 1-22, reaction progress is indicated by ionic strength. For Run 1, dolomite saturation is maintained (SI = 0), while pure halite is added to the hypothetical solution. For Run 10, dolomite does not react with solution (variable saturation index), while halite and leonite plus $MgCl_2$ are added. Mg/Ca molar ratios of Culebra groundwaters are plotted for comparison. Values for WIPP-29 are not plotted. For Figure 1-23, reaction progress is indicated by moles of chloride added. Sulfate concentrations of Culebra groundwaters are plotted for comparison.

Run 1 assumes a simple partial equilibrium model in which pure NaCl is added to the solution while the groundwaters are maintained at equilibrium with respect to calcite, dolomite, and gypsum. The concentrations of Ca, Mg, SO_4, and CO_3 change due to the changes in the solubilities of calcite, dolomite, and gypsum described above. The system is closed with respect to CO_2 gas exchange; the initial partial pressure of CO_2 is 10^{-2} atmospheres. As the reaction proceeds, dedolomitization (dissolution of dolomite and precipitation of calcite) and dissolution of gypsum occur. Figures 1-22 and 1-23 show that Run 1 does not reproduce the compositions of Culebra waters. This simple model provides a good fit to many of the observed calcium concentrations; however, concentrations of Mg and SO_4 are considerably below the predicted values.
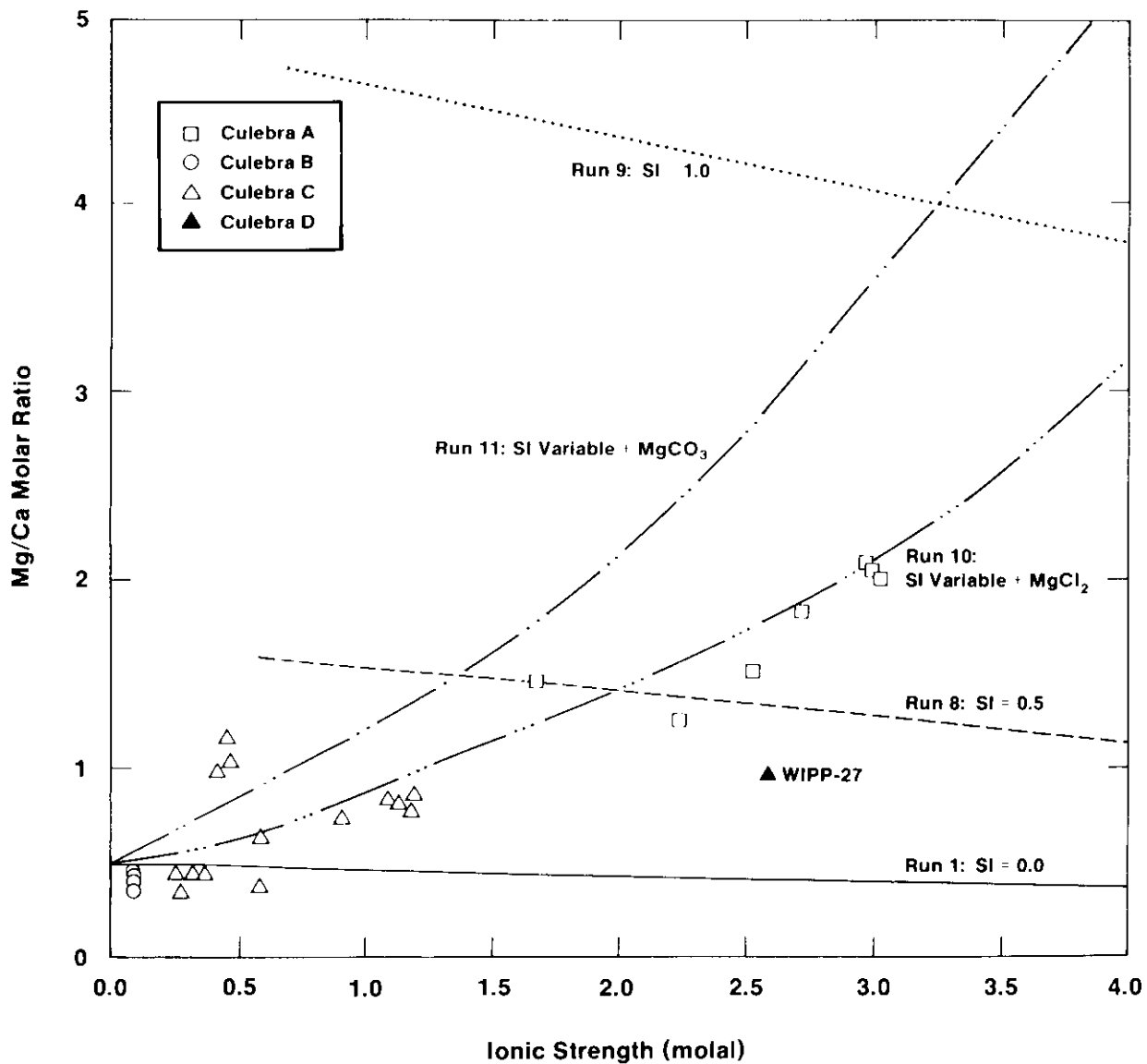
Figure 1-22. Change in Mg/Ca molar ratio as a function of reaction progress, types of added salts, and dolomite saturation index for simulated evolution of Culebra groundwaters.
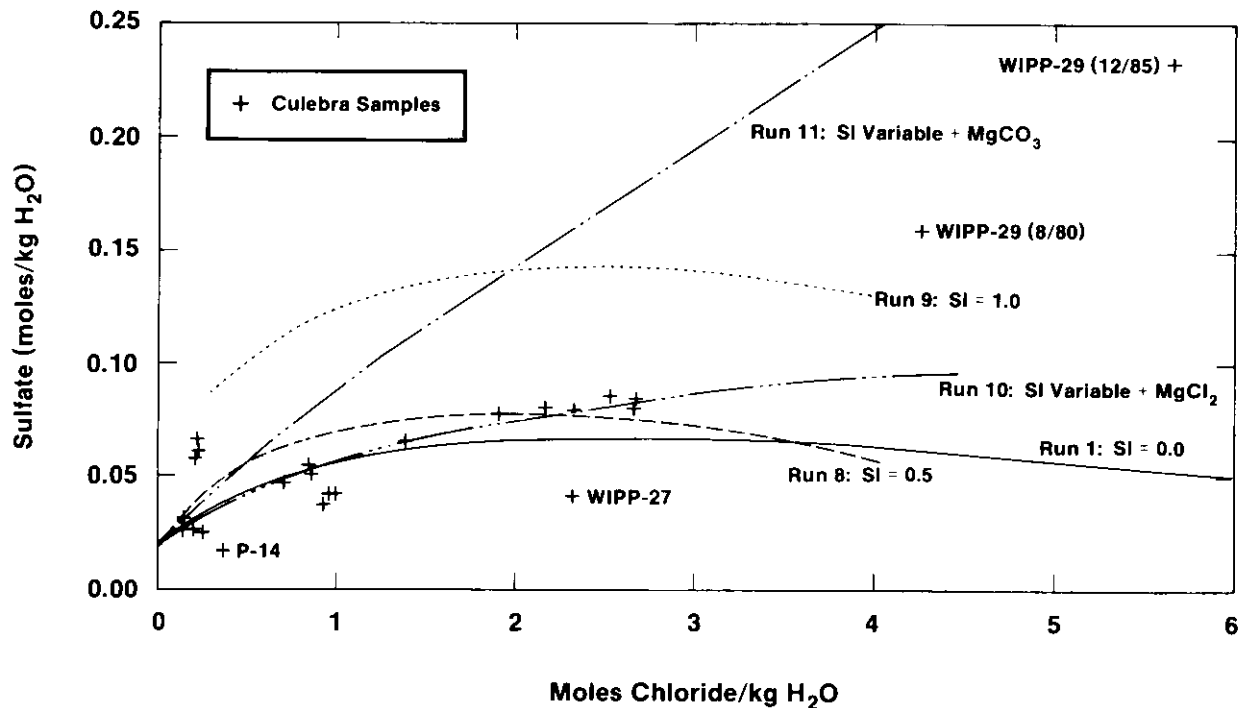
Figure 1-23. Change in sulfate concentration as a function of reaction progress, types of added salts, and dolomite saturation index for simulated evolution of Culebra groundwater compositions.

In Run 10, saturation with dolomite was not maintained. The starting solution was produced by equilibrating distilled water with calcite, dolomite, and gypsum at an initial pCO_2 of 10^{-2} atmosphere. The system was then closed to pCO_2 gas, and addition of Na, Cl, K, Mg, and SO_4 by congruent dissolution of halite and incongruent dissolution of polyhalite and carnallite was simulated. Carnallite dissolves incongruently to form KCl and a solution containing Mg^{2+} and Cl^-. In Run 10, this was simulated by adding $MgCl_2$ to the reaction solution. Incongruent dissolution of polyhalite was simulated by addition of leonite $(K_2Mg(SO_4) \cdot 4H_2O)$. The K/Cl ratio of the Culebra waters was used to estimate a reasonable leonite/halite ratio. The $MgCl_2$/halite ratio was then adjusted to fit the observed Mg/Cl ratio of the Culebra waters. Equilibrium between the waters and gypsum and calcite was maintained; as the reaction proceeded both calcite and gypsum dissolved. The saturation index of dolomite was calculated as the reaction progressed, but dolomite was not allowed to dissolve or precipitate.

Figures 1-22 and 1-23 show that Run 10 reproduces the trends of the Ca, Mg, and SO_2 concentrations in this suite of Culebra groundwaters. The calculated dolomite saturation indices for Run 10 were used to calculate values of the saturation index expression described previously and are plotted in Figure 1-20. The good correspondence between the theoretical and observed solute concentrations in these figures shows that addition of solutes (Mg, SO_4, K, and Cl) to the Culebra from evaporite minerals such as polyhalite and carnallite in a partial equilibrium system is consistent with the observed groundwater compositions if dolomite does not precipitate from supersaturated solutions.

1.4.7 Estimation of Oxidation-Reduction Potentials and Occurrence of Organics in the Culebra Groundwaters

Measurements of redox potentials have been made in Culebra waters using Pt electrodes and N, I, As, and Se redox couple data. Apparent Eh values were calculated from the concentrations of the redox couples using the Nernst equation. Sensitivity calculations showed that the calculated Eh values were fairly insensitive to assumptions about activity/concentration relationships, to reasonable uncertainties in the analytical data, and

to errors introduced by uncertainty in the field pH measurements. However, the total concentrations and concentrations of individual members of the couples were very close to the detection limits of the analytical methods used. This meant that in most cases, the existence of redox equilibria or disequilibria could not be established. Descriptions of the sampling procedure, analytical techniques, and calculations are given in Myers et al. (Chapter 6).

The results of the calculations for the most recent WQSP water samples are summarized in Figure 1-24. Arrows indicate upper or lower limits resulting from one member of the pair being present at levels below the detection limit. In these cases, the analyses were used to set an upper or lower bound on the potential for that couple. Redox potentials could be calculated for four wells and two wells, respectively, from the iodine and nitrogen couples. For most of the other wells, an upper or lower bound could be calculated for these couples. Three wells provided data to calculate potentials for the selenium couple, and data from six wells could be used to calculate potentials for the arsenic couple. Lower redox bounds for three additional wells could be calculated for the arsenic couple.

Although redox equilibrium cannot be established for any of these wells, groups of wells that have similar characteristics can be identified. Samples in the first group include waters from the Engle, H-7B, H-8B, and H-9B wells that show a range of calculated redox potentials all of which are greater than approximately 350 mV. This lower bound is defined by the absence of measurable NH_4^+. Samples from H-7B, H-8B, and H-9B from earlier WQSP rounds, however, had measurable NH_4^+, and thus the lower bound (indicated by the arrows in the figure) may be an artifact of the analytical technique.

Data from a second group consisting of the WIPP-25, WIPP-26, H-12, and P-14 wells may indicate redox disequilibrium. The calculated potentials span wide ranges and in some wells the redox values calculated for the I^-/IO_3^- data lie above upper bounds defined by the nitrogen data or values calculated for the arsenic couple.
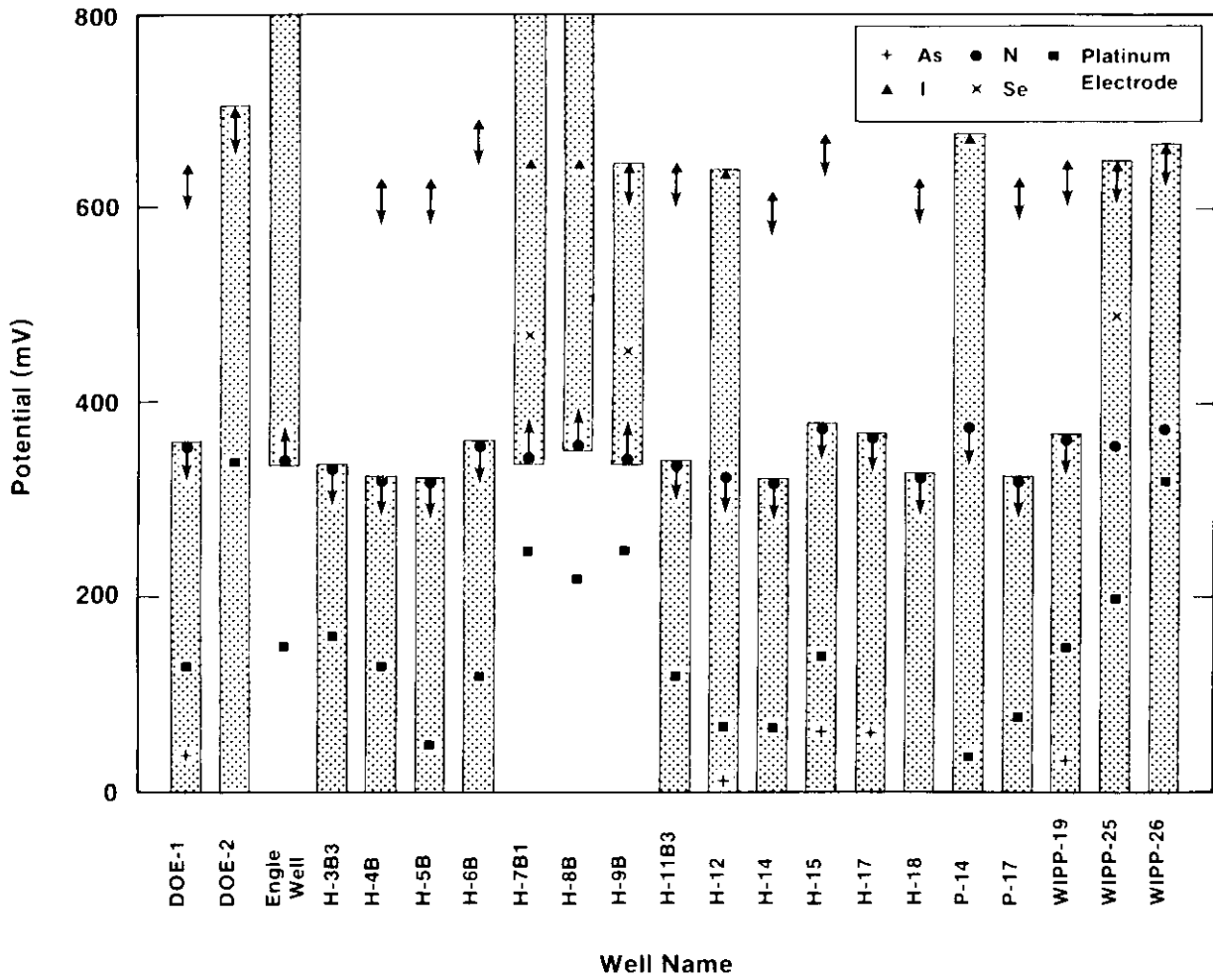
TRI-6341-60-0

Figure 1-24. Comparison of redox potentials calculated for several different redox couples in waters from Culebra wells.

The final group, consisting of the balance of the wells, has calculated redox values below approximately 350 mV. This upper bound is defined only by the absence of measurable nitrate. Waters from these wells are relatively saline and contain low levels of total nitrogen. If the high salt content of the water has prevented detection of the nitrate, then the "upper bound" may be an artifact of the analytical technique.

In Chapter 6, Myers et al. note that the four wells in the southern part of the study area are distinguished from the other wells by their higher redox potential ranges, lower TDS, and lower halite saturation indices. They conclude that these characteristics suggest that either a hydrologic divide separates them from the other more reduced wells of the north, or that a region of recharge in the southern area provides a source of relatively oxic, low-TDS groundwater to the Culebra.

Observations attesting to the presence of reduced species in some Rustler groundwaters (WIPP-25, WIPP-26, WIPP-28, and WIPP-30) were reported by Lambert and Robinson (1984). These included measurable to less-than-measurable but odoriferous concentrations of hydrogen sulfide, iron slimes, rank (but not H_2S) odors, milky-white and black precipitates that developed as water samples stood in bottles under surface conditions, and gaseous effervescence. Some of these observations were only transient over the time of some pump tests. Whether they represent purging of accumulated concentrations of species related to organic chemical reduction or an actual change in redox potential is not known.

There are few data available for oxidation-reduction potentials in the other members of the Rustler Formation. Redox potentials measured by Pt electrodes in wells in Nash Draw were previously shown to be generally higher in the Culebra than at the Rustler/Salado contact (Lambert and Robinson, 1984).

Values of TOC of Culebra samples described by Myers et al. in Chapter 6 range from < 1 to 7 mg/L. This range does not include higher values (14-15 mg/L) that are probably

associated with contamination due to drilling or sampling activities. The amount of organic carbon associated with halides (TOX) (Cl, Br, and Cl) was also analyzed and ranged from <0.1 to 9.7 mg/L; however, an observed correlation between TOX and Cl concentration may indicate significant analytical interference. In Chapter 6, Myers et al. conclude that there was no reason to suspect the occurrence of halogenated organics contaminating the Culebra. Other evidence for organic contamination of water samples drawn from the Culebra is based on radiocarbon data and is discussed by Lambert (1987; Chapter 5).

1.4.8 Isotopic Studies of Rustler Waters

The isotopic geochemistry of Rustler and related groundwaters is discussed in detail by Lambert in Chapter 5, with a summary of the sources of data (oxygen and hydrogen isotopes, carbon isotopes including radiocarbon, tritium, radiochloride, and uranium concentration and $^{234}U/^{238}U$ activity ratios) and their interpretations. This discussion is in turn a summary of that work, which is drawn from several source documents: Lambert (1978), Lambert (1983), Lambert and Harvey (1987), Lambert (1987), and Lambert and Carter (1987).

Confined Rustler groundwaters near the WIPP and in Nash Draw have isotopic compositions very tightly clustered along the worldwide meteoric field in δD-$\delta^{18}O$ space (Figure 1-RU). The tightly clustered Rustler data plotting along the meteoric field (heavy solid lines) at more negative δ-values have isotopic compositions that differ from the field of less confined groundwaters having more positive δ-values. Small (up to -10‰) deviations of δ-values from the meteoric field are not considered significant (line a; cf. Allison et al., 1985). WIPP 29 Culebra and Surprise Spring may have evolved by evaporation from a shallow water table, with a $\delta D/\delta^{18}O$ slope of 2 (lines b; cf. Allison, 1982), from water imported from the Ogallala aquifer for use in nearby potash-refining operations, from modern-type water by oxygen-isotope shift (lines c), but probably not from evaporation of confined Rustler-type water (slope = 5; line d; cf. Craig et al., 1963). Groundwaters whose stable-isotope compositions deviate markedly from that of a characteristically meteoric
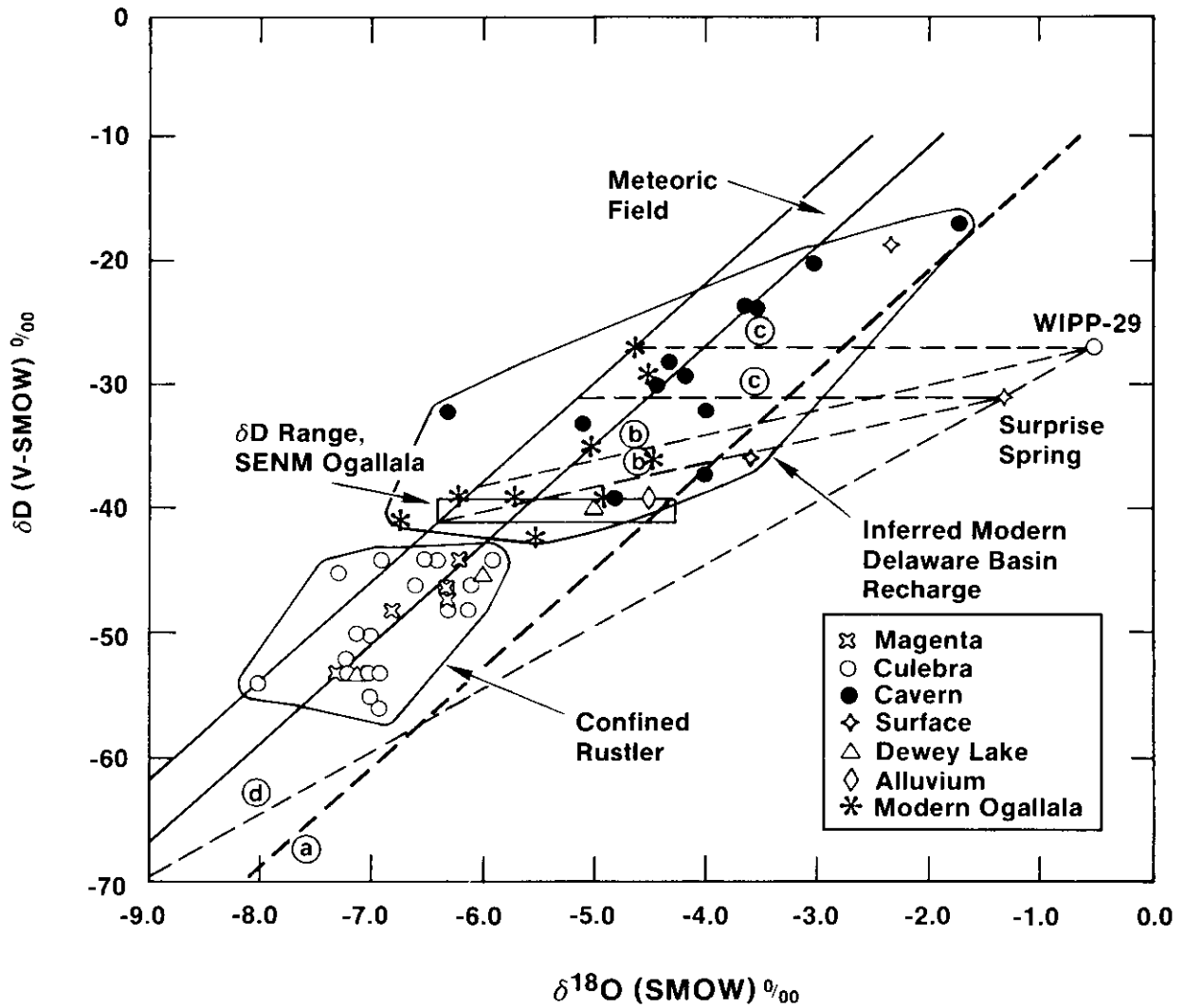
Figure 1-25. Stable-isotope compositions of groundwaters from the Rustler Formation (Figure 5-1, adapted from Lambert and Harvey, 1987).

signature occur at the Rustler/Salado contact in the low-permeability portions of that zone in the central and eastern parts of the WIPP Site (Lambert, Chapter 5) and near the surface in the Culebra and Tamarisk members in the southwest portion of Nash Draw, where hydrologic conditions are not as confining (Figure 1-25). Deviations in waters at the Rustler/Salado contact are attributable to a profound degree of rock/water interaction involving a relatively large rock/water ratio, while the isotopic signatures observed in southwestern Nash Draw can arise from partial evaporation from the vadose zone and the capillary fringe above the water table. Confined meteoric Rustler waters are virtually identical in stable-isotope composition to confined meteoric Capitan waters at the basin margin, indicating recharge of both types of confined waters under similar climatic conditions.

By comparison, vadose Capitan waters from the Carlsbad Caverns system, groundwater from a water table in alluvium, and near-surface accumulations that homogenize seasonal variations in isotopic composition also have meteoric isotopic signatures, but have isotopic compositions more positive in δD-$\delta^{18}O$ space than confined Rustler and Capitan waters (Lambert and Harvey, 1987). The envelopes of δ-values for these two populations of differing hydrologic character do not overlap (Figure 1-25). The data of Nativ and Smith (1987) reveal that in Ogallala groundwaters underlying the high plains to the east, climatically similar to the Delaware Basin, the only groundwaters containing tritium levels indicative of recent (post-1950) meteoric derivation (>10 tritium units [TU]) all have δD values >-42‰ (Figure 1-25), comparable to near-surface unconfined meteoric waters in the Delaware Basin (Figure 1-26). High Plains data for Figure 1-26 are from Nativ and Smith (1987); WIPP data are from Lambert and Harvey (1987) and Lambert (1987). Significantly high tritium concentrations (>10 TU), indicating derivation from a meteoric source since 1950, are restricted largely to groundwaters having δD values more positive than about -42‰. Ogallala waters from nearby southeastern New Mexico have δD values between -39 and -41‰, corresponding with δD values of modern groundwater recharge in the Texas High Plains. Hydrogen-isotope characteristics of groundwaters from the nearby
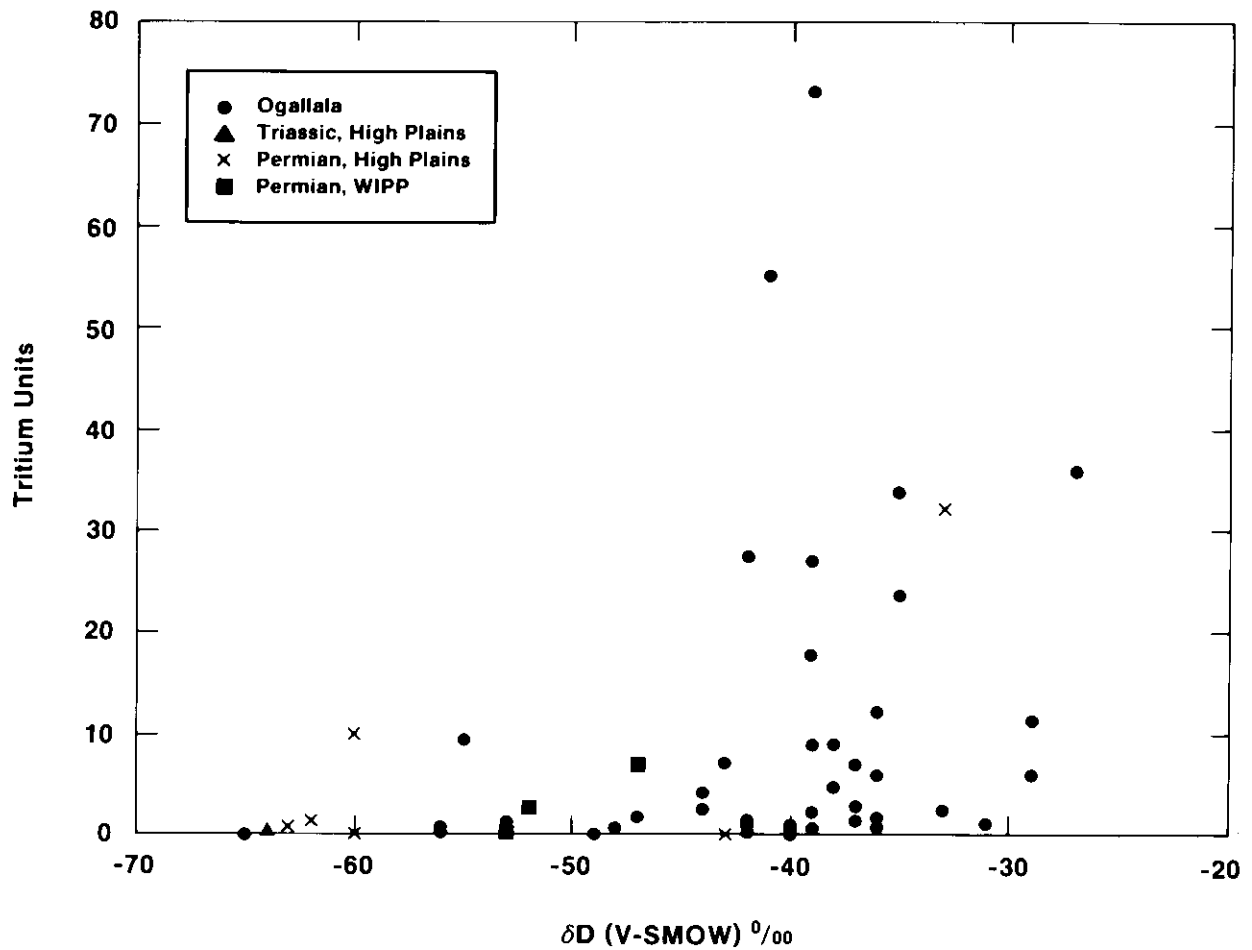
Figure 1-26. Tritium and deuterium concentrations in groundwaters from the Southern High Plains, Texas, and the Delaware Basin, southeastern New Mexico (Figure 5-2, from Lambert and Harvey, 1987).

climatically similar Delaware Basin (WIPP data) are shown for comparison. The isotopic signatures of confined Rustler and Capitan waters are distinct from that of both Ogallala water with discernable modern input and of vadose Capitan and alluvial water. Thus, it is likely that the isotopic compositions of confined Rustler and Capitan groundwaters in the northern Delaware Basin are not characteristic of groundwaters that would be receiving modern meteoric recharge under the present climatic conditions.

Some, but not all, Dewey Lake groundwaters may have a component characteristic of climatic conditions fostering modern surficial recharge (Figure 1-25). Some have stable-isotope compositions comparable to the near-surface occurrences, and some are comparable to confined Rustler groundwaters. Thus, recharge to the Dewey Lake, like recharge to the Ogallala, appears to be variable in both space and time.

Only four out of 16 well-water occurrences gave internally consistent radiocarbon "age" calculations based on the internally consistent interpretive model and assumptions of Evans et al. (1979) for water-bearing carbonate rocks. The model of Evans et al. takes into account dilution of atmospheric carbon by dissolution of carbonate rock, and carbon isotope exchange between water and host rock. The mean of these four is 14,000 years; 95% confidence limits are ± 5,000 years. This is a minimum age estimate. It is not possible to estimate an upper age limit because of the unavoidable possibility of at least small amounts of unmitigable contamination even in these four samples. These tightly clustered ages, given their individual confidence limits, while spread out from north to south across the WIPP Site, do not allow consistent age gradients or travel times to be inferred across the WIPP Site based on differences in radiocarbon ages (Figure 1-27). Ten of the 16 well-water occurrences were complexly contaminated due to unmitigable anthropogenic well-bore effects. The remaining two are ambiguous, but all 16 probably represent three-component mixing, including some contamination. The four dated groundwaters (three Culebra and one Dewey Lake) all have stable-isotope compositions belonging to the more negative population in δD-$\delta^{18}O$ space (Figure 1-25). Thus, it is inferred that Rustler and Dewey Lake groundwaters in this population have a significant component at least
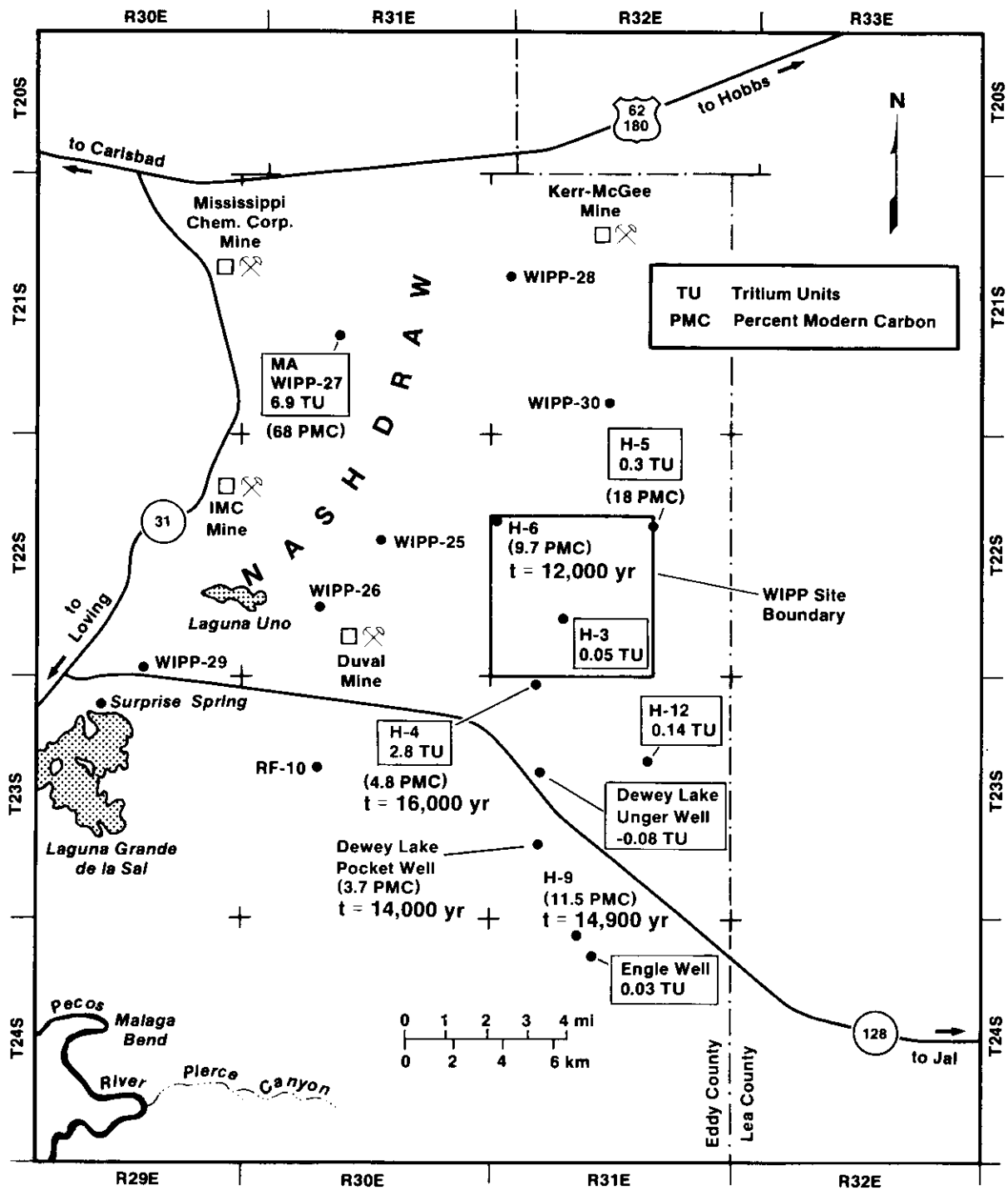
Figure 1-27. Tritium and radiocarbon in Rustler and Dewey Lake groundwaters (Figure 5-11, adapted from Lambert and Harvey, 1987).

12,000 radiocarbon years old. All the tritium measurements from the WIPP area, which are associated with the more negative (confined Rustler) isotopic compositions, are <3 TU, indicating little or no contribution from the atmosphere since 1950. Figure 1-27 shows tritium and radiocarbon in Rustler and Dewey₊Lake groundwaters. Unless otherwise specified as Dewey Lake (DL) or Magenta (MA), measurements in Figure 1-27 (all from Lambert, 1987) apply to water from the Culebra member of the Rustler Formation. The uniformly low (<7 TU) tritium concentrations near the WIPP Site indicate no introduction of an atmospheric component since 1950 (cf. Isaacson et al., 1974). Three Culebra and one Dewey Lake water were amenable to dating by the carbonate-aquifer model of Evans et al. (1979), giving times of isolation from the atmosphere ranging from 12,000 to 16,000 radiocarbon years. These data indicate long residence times or long travel times from recharge areas, but provide no evidence of either modern vertical infiltration or monotonic age gradients indicating north-to-south flow. Three of these data, from water samples also having δD analyses, are depicted in Figure 1-26.

The southeastern New Mexico climate more than 10,000 years ago fostered vegetation now found only at higher elevations, as indicated by the packrat-midden studies of Van Devender (1980). Late Pleistocene climate was probably wetter and more conducive to recharge, as indicated by the concordance between the ages of packrat middens and the relatively less contaminated radiocarbon in the Rustler and Dewey Lake groundwaters described above. Fossil fauna (camels, horses, bison) from extinct spring deposits in Nash Draw near the WIPP Site are of similar age and also indicate wetter conditions than at present (Bachman, 1981).

Given the assumptions of the model of Osmond and Cowart (1976) for uranium systematics in confined hydrologic flow systems, generalized flow directions in confined Rustler groundwaters as inferred from $^{234}U/^{238}U$ relationships appear to have involved recharge from a direction with an eastward-flowing component (Figure 1-28). This is not parallel to modern flow directions inferred from potentiometric heads alone (cf. Figure 1-10). A change in flow direction back toward the west (the modern flow direction
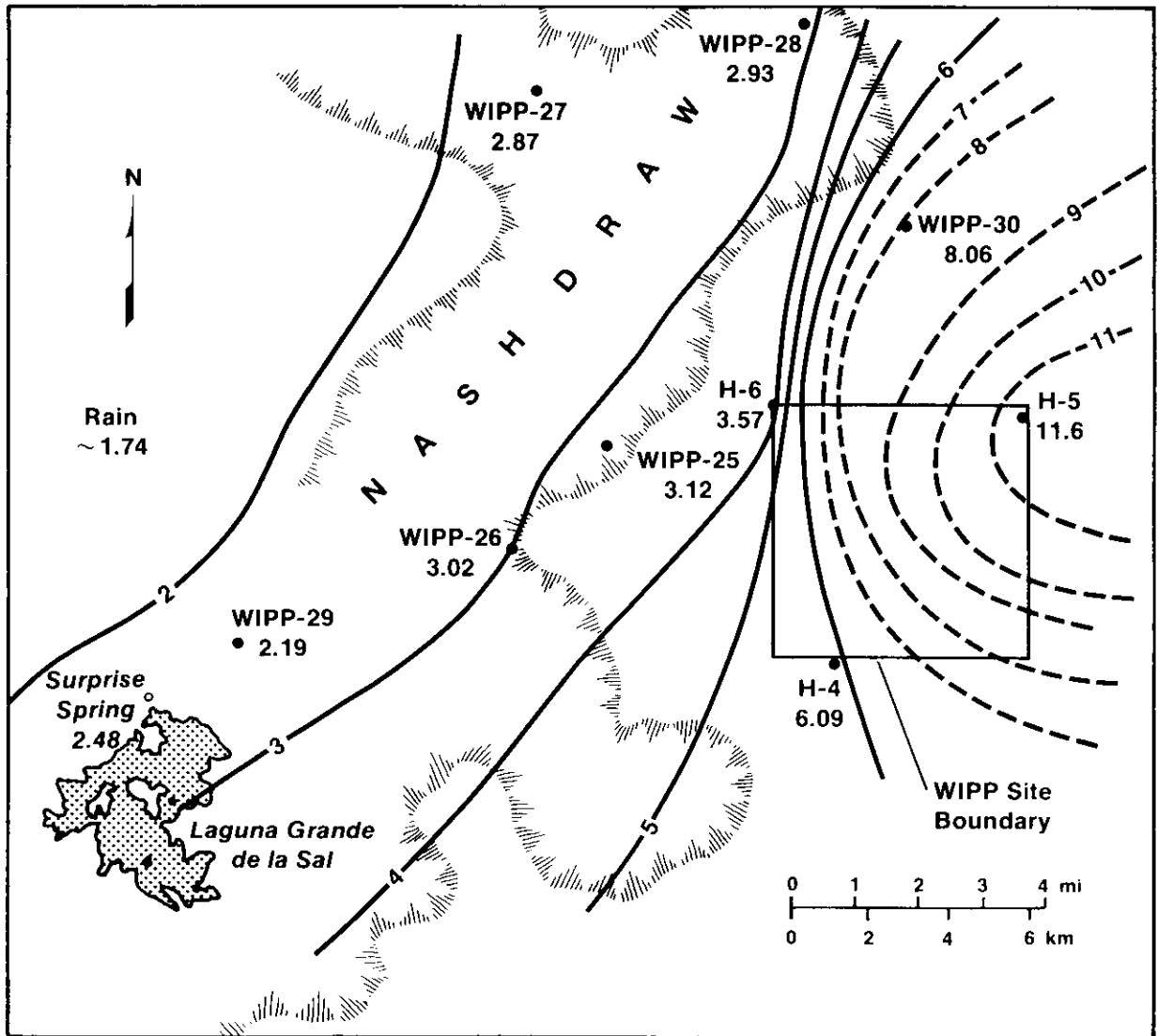
TRI-6331-49-0

Figure 1-28. Contour map of ^{234}U/^{238}U activity ratio in groundwater from the Culebra dolomite member of the Rustler Formation (Figure 5-11, from Lambert and Carter, 1987).

indicated for saturated portions of the Magenta; Mercer, 1983) during the past 10,000 to 30,000 years is likely. The activity ratio decreases westward and somewhat southward toward Nash Draw; high activity ratio values typically develop downgradient in hydrologic systems under confined, reducing conditions and are associated with long residence times. Control on contouring east of the WIPP Site is not particularly tight, due to the scarcity of wells suitable for sampling in the eastern low permeability region of the Culebra. Eastward-increasing activity ratio values are interpreted as eastward flow during Pleistocene recharge, and as mimicking an inverse-function of potentiometric head contours during that time. During the time of wetter Pleistocene conditions when the Rustler was being recharged in its outcrops in Nash Draw, the base level there was probably also being lowered by accelerated erosion and dissolution. With the onset of a drier Holocene climate and the cessation of significant recharge, the area whose base level was lowered has probably governed the local hydraulic gradient, resulting in a general southward drainage.

The proposed change in flow direction is consistent with the apparently anomalous data from borehole H-5. It is problematical to obtain either modern or ancient recharge in the vicinity of borehole H-5. In spite of the high potentiometric level there relative to the present downgradient area south and west (a condition commonly interpreted in physical hydrology as indicative of recharge), the water there contains no significant tritium and has the highest $^{234}U/^{238}U$ activity ratio (Lambert, Chapter 5). A high tritium content would be indicative of modern recharge, while a high $^{234}U/^{238}U$ activity ratio would develop in the downgradient, not the upgradient portion of a confined groundwater system, according to the model of Osmond and Cowart (1976). The transmissivity there is also extremely low (Lappin, 1988). Low permeability in the H-5 area may have inhibited subsurface drainage following the cessation of eastward flow to the area, and the high potentiometric level is suspected to be a relic of the paleoflow system.

1.4.9 Mineralogical Studies in the Culebra Member

Detailed mineralogical analyses of samples from 12 different locations along three east-west trending traverses have been carried out using a variety of quantitative techniques. Mineralogical and compositional data were obtained from both bulk matrix samples and fractures. The results of this study are in Chapter 3 and briefly summarized below.

Figure 1-29 shows the bulk mineralogy in intact cores of the Culebra along a traverse from Nash Draw (WIPP-29) to the eastern part of the WIPP Site (H-10). The mineralogy of H-7 and H-10 is typical of most cores examined at the site. The dominant mineral is a fairly pure dolomite (Ca/Mg ~ 1.05; FeO $\leq$0.23%) and comprises about 85% by weight of the bulk rock. Gypsum, calcite, and various clay minerals are observed throughout the Culebra and are distributed heterogeneously both vertically and horizontally. Fractures are observed in all cores and are lined most commonly with clay and gypsum. Clay minerals are present in all samples and comprise approximately 3 to 5% by weight of the bulk mineralogy. They occur as discrete seams along fracture surfaces or are finely dispersed throughout the matrix. The dominant clay minerals are corrensite (an ordered mixed-layer chlorite/smectite), illite, chlorite, and a serpentine-like mineral tentatively identified as amesite. On the regional scale, corrensite is the most abundant mineral observed after dolomite.

Gypsum occurs as a fracture and vug filling; all fracture surfaces examined by XRD showed the presence of nearly pure $CaSO_4 \cdot 2H_2O$. Calcite is present in significant proportions in the top part of WIPP-29 and is interpreted to be of secondary origin (Sewards, et al., Chapter 3). Microprobe analyses of microcrystalline calcite in WIPP-19 show that it is a very low-Mg calcite. Trace amounts of pyrite, magnesite, quartz, and authigenic feldspar have been observed in some cores.

A dark amorphous material is present in abundance in the Culebra samples and has been tentatively identified as organic matter. It is generally associated with clays and often
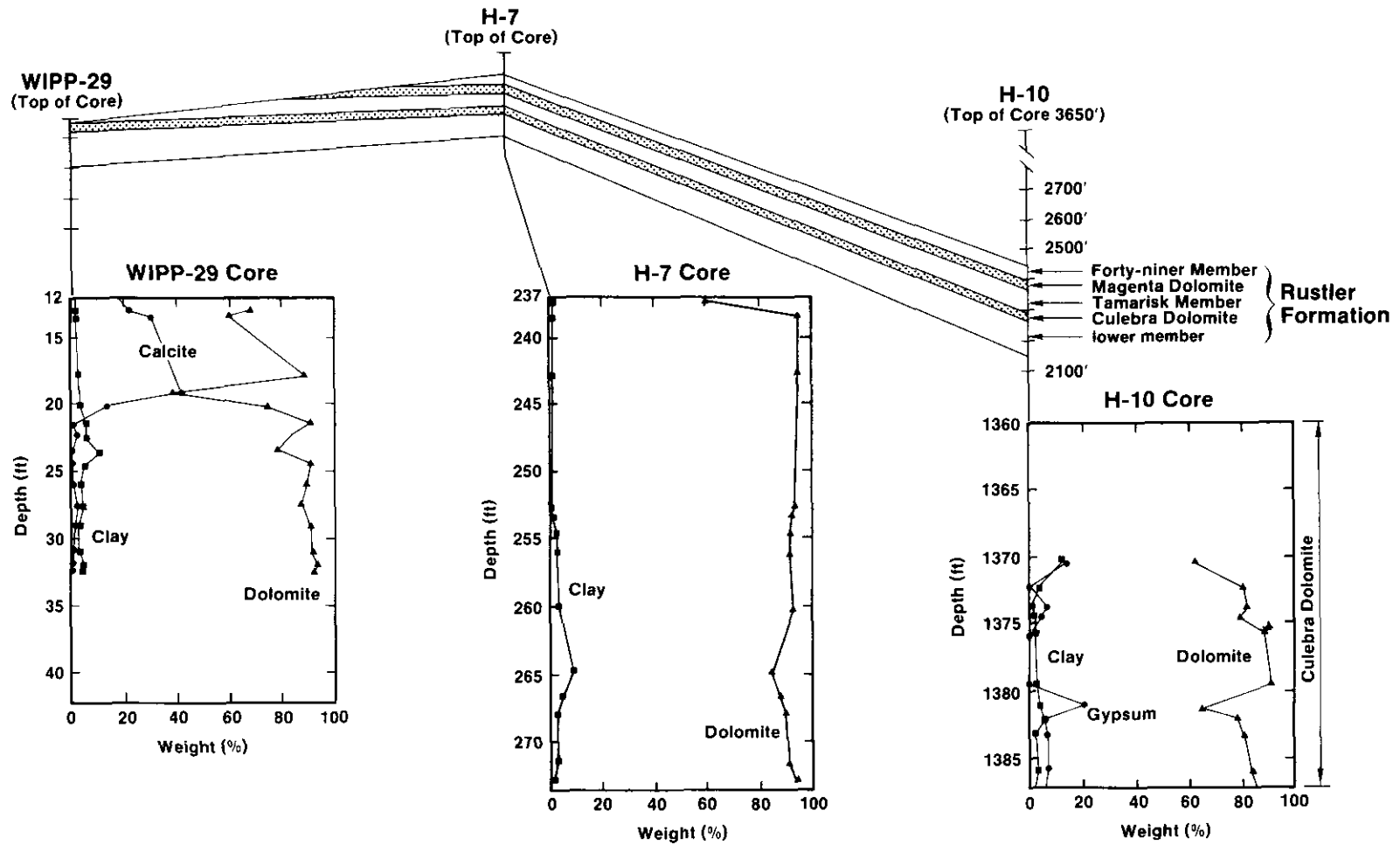
Figure 1-29. Fence diagram showing stratigraphy of the Rustler Formation and mineralogy of the Culebra member (from Sewards et al., Chapter 3).

TRI-6342-491-0

occurs in algal structures or haloes surrounding vugs whose origin has been attributed to biological activity.

1.4.10 Mineral Isotopic Studies

To evaluate further the degree of rock/water interactions in the Culebra and related rocks, supporting data have been collected on the isotopic compositions of rocks and their mineral components. These data include $\delta^{18}O$ and $\delta^{13}C$ values of dolomite and calcite, δD values of gypsum, $^{87}Sr/^{86}Sr$ ratios of both carbonates and sulfates, and whole-rock $^{234}U/^{238}U$ activity ratios.

The variations in the $^{234}U/^{238}U$ activity ratio of rock from water-bearing horizons (most rubbled) in the Culebra are minor, generally statistically indistinguishable from the theoretical secular-equilibrium value of unity (Lambert and Carter, 1987). However, water/rock interaction has given rise to significant departures of the activity ratio from unity in coexisting water, which has activity ratio values as high as 11.6 (Figure 1-28).

Despite a conclusively meteoric $\delta^{18}O/\delta D$ signature for confined groundwaters in the Culebra at the WIPP Site and in much of Nash Draw, the carbonate host mineralogy (dominantly dolomite) has generally not recrystallized in the presence of the contained water (Lambert, Chapter 5). However, secondary dolomite dissolution features (such as vugs and etch pits) are commonly developed where the Culebra carries significant amounts of water (Sewards et al., Chapter 3). The only isotopic evidence of carbonate recrystallization in equilibrium with Rustler-type water (Figure 1-30) was found in secondary calcite in a Culebra sample at WIPP-33, a borehole drilled in a collapse feature between the WIPP Site and Nash Draw. This carbonate apparently precipitated in isotopic equilibrium at ambient temperatures, involving a freshwater-type reservoir of carbon. Dolomitic aquifer rock, although partially dissolved to locally enhance the porosity, has an extremely uniform and relatively heavy isotopic composition (mean $\delta^{18}O$ = +33.4‰, 95% CL = ±1.0‰, n = 10; mean $\delta^{13}C$ = +6.1‰, 95% C = ±1.1‰, n = 10). These values are more consistent with an evaporitic origin than with diagenetic dolomitization of a biogenic limestone precursor
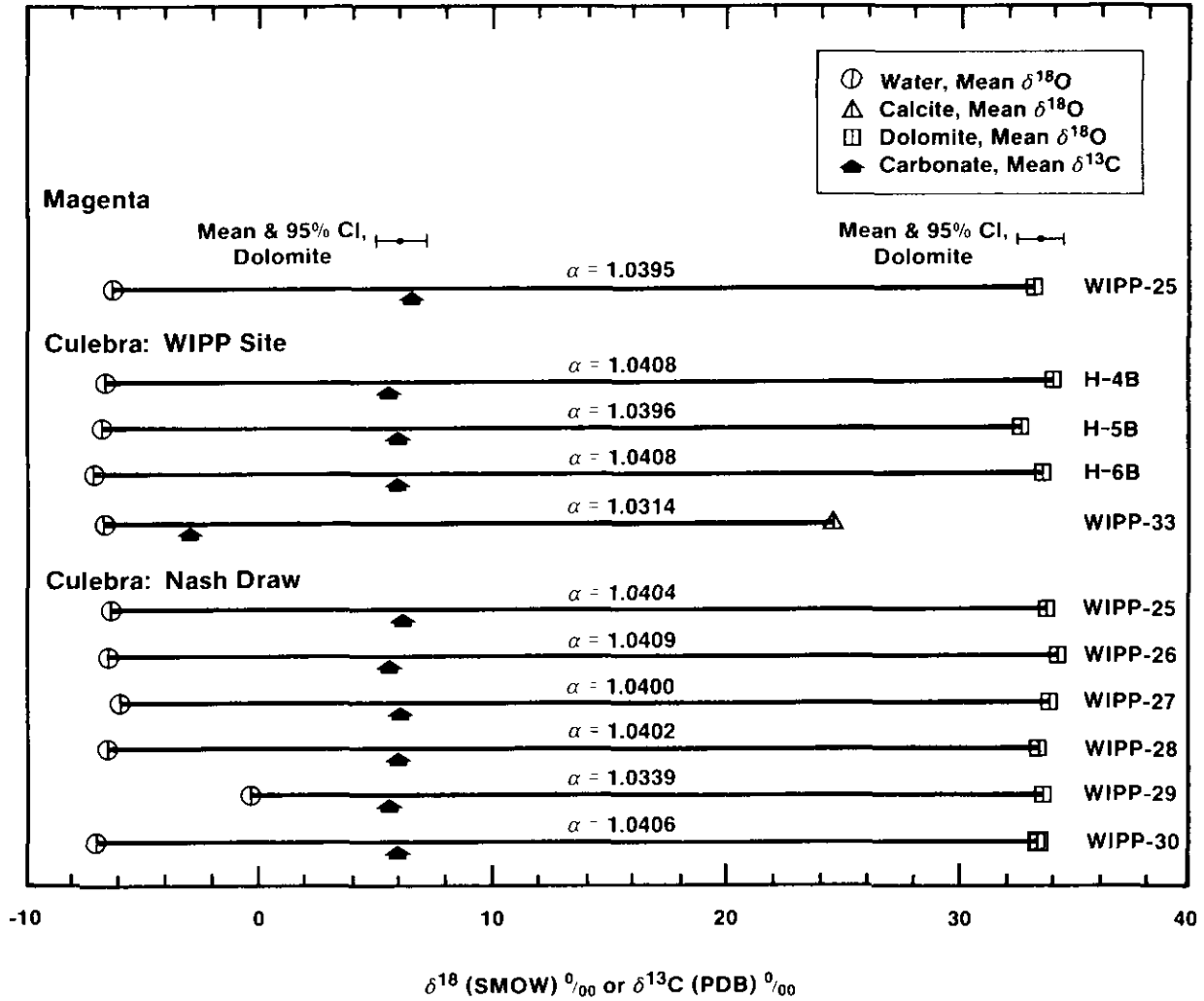
Figure 1-30. $\delta^{18}O$ values for coexisting carbonates and waters in the Rustler Formation (Figure 5-6, from Lambert and Harvey, 1987; Lambert, 1987).

(cf. Parry et al., 1970). Except for WIPP-29 Culebra, which shows both oxygen- and hydrogen-isotope shift, all the waters have a uniform $\delta^{18}O$ value of -6.6 ± 0.8‰. Calculated dolomite/water oxygen-isotope fractionation factors are too high to reflect isotopic equilibrium. Only calcite in the Culebra rubble from WIPP-33 appears to be at isotopic equilibrium with typical meteoric Rustler groundwater at ambient temperature. There is no other indication of carbonate recrystallization (reprecipitation) in the Rustler in isotopic equilibrium with meteoric Rustler groundwater. As discussed in detail by Lambert (1987), the dissolved HCO_3^- is not in $^{13}C/^{12}C$ equilibrium with the host dolomite.

$^{87}Sr/^{86}Sr$ ratios of sulfate and carbonate mineral veins, generally interpreted as the depositional record of fluid flow preferentially concentrated in fractures, are indistinguishable from those of their host rocks throughout the Rustler. This indicates a dominantly internal, not external, source for the mass transport represented by the vein fillings (Brookins and Lambert, 1988; Lambert, Chapter 5). $^{87}Sr/^{86}Sr$ ratios progressively higher in the stratigraphic section reflect a greater contribution of surface-derived cations. Rustler values, exclusive of water-bearing zones (Magenta and Culebra), are little altered by admixture of surface material relative to the tightly clustered Permian Castile/Salado values. Dew Lake veins (calcite and selenite) show a full range of mixing proportions between Rustler-type and surface-type (represented by caliche and gypsite spring deposits) cations. Aside from the Magenta and Culebra, the $^{87}Sr/^{86}Sr$ ratios of the Rustler anhydrites and gypsums ($^{87}Sr/^{86}Sr$ = 0.70694 - 0.70714) are similar to, but slightly greater than those of unaltered anhydrites interbedded with halite and polyhalite in the Salado (Figure 1-31), which have never been in contact with large amounts of meteoric water. This similarity shows that mass transport of sulfate and carbonate from surface-weathered outcrops in the recharge zone has made a limited contribution to the soluble cationic constituent of the Rustler. In contrast, veins in the Dewey Lake Red Beds containing selenite and calcite appear to have a continuum of $^{87}Sr/^{86}Sr$ ratios ($^{87}Sr/^{86}Sr$ = 0.70722 - 0.70861), representing mixing of materials derived from both Ochoan evaporites typical of the Rustler and deeper rocks, and near-surface deposits, such as caliche and gypsite spring deposits (Figure 1-31). These relationships show that the spring deposits were not derived solely and directly from
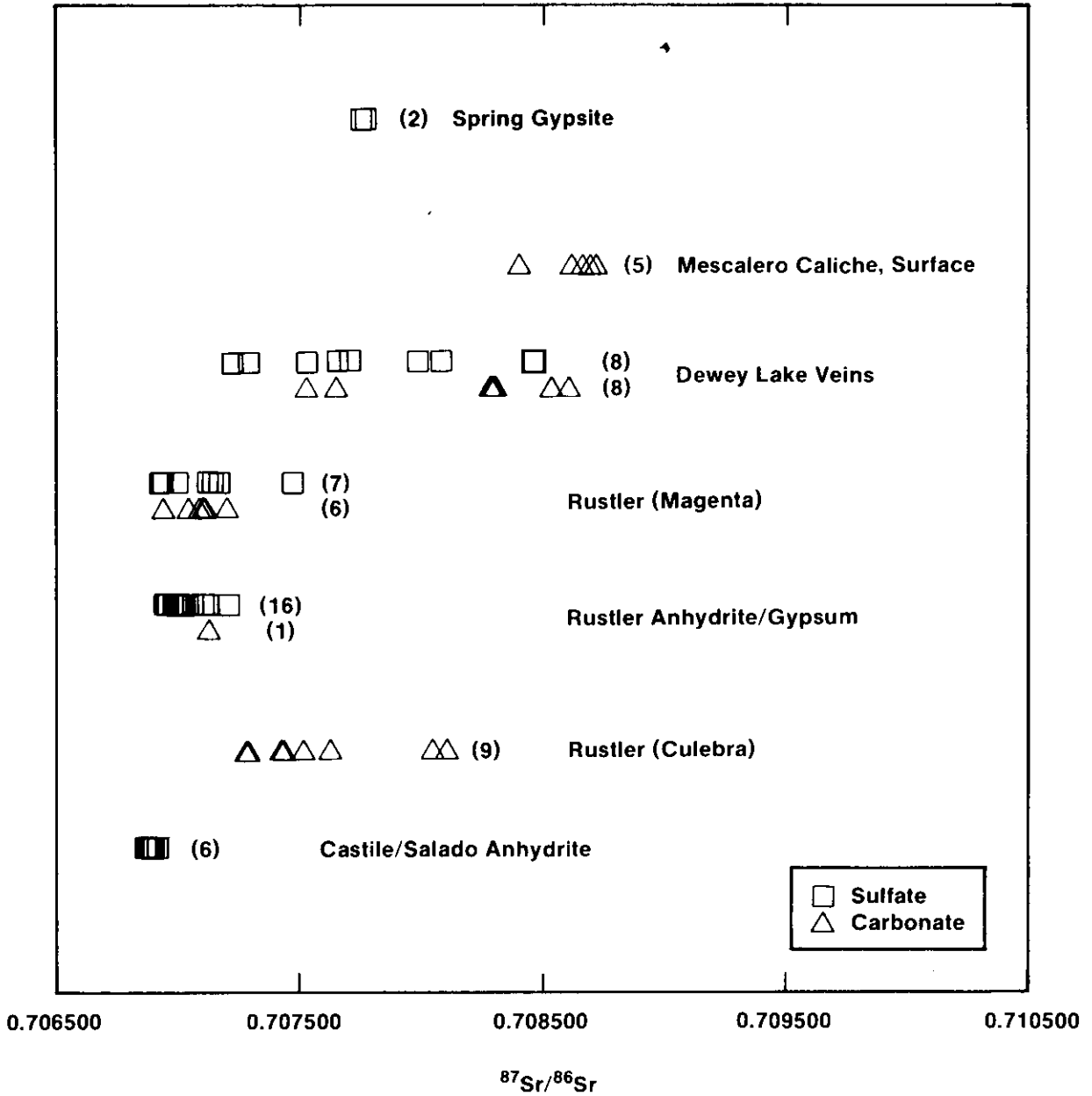
TRI-6341-58-0

Figure 1-31. $^{87}Sr/^{86}Sr$ ratios in Ochoan and related rocks (Figure 5-17; data from Brookins and Lambert [1988]).

Rustler rock dissolved and mobilized westward in the late Pleistocene (cf. Bachman, 1981), but instead require a dominant component similar to the high-[87]Sr extreme in Dewey Lake strontium.

Finally, the D/H relationships in gypsums from the Rustler and Dewey Lake Red Beds are characteristic of gypsification of anhydrite (or recrystallization of pre-existing gypsum) in the presence of meteoric water. No gypsum thus far examined bears an isotopic signature that would be expected for primary marine evaporitic sulfate ($\delta D > 0‰$). Although all gypsums examined were meteorically influenced ($\delta D < -40‰$), their δD values vary widely. Figure 1-32 plots δD values of the water of crystallization in gypsums as a function of depth. Solid lines delineate the range of gypsum compositions expected from recrystallization in the presence of a large amount of Rustler-type meteoric water (extremely high water/rock ratio). Dashed lines bound gypsum δD values expected from small amounts of such water completely scavenged during gypsification of anhydrite, and correspond to the δD field for confined Rustler waters in Figure 1-25. A few δD values are consistent with isotopic equilibrium between their waters of crystallization and large amounts of Rustler-type (Pleistocene) meteoric water. The variations in D/H ratio, both laterally and vertically, attest to differing generations of meteoric water of different isotopic compositions hydrating the sulfate or else differing water/rock ratios with an isotopically uniform reservoir contributing to the crystallographically bound water or some combination of the two. The changes in D/H ratio adjacent to a water-bearing dolomite in WIPP-34 (Figure 1-32) suggest a varying water/rock ratio at that locality, rather than multiple generations of gypsum recrystallization, although throughout the Rustler several discrete episodes may have affected the gypsum.

On a regional basis, there is no correlation of δD value with depth, suggesting a non-uniform vertical permeability throughout the Rustler/Dewey Lake section. In a given borehole core, the water/rock ratio inferred from the gypsum D/H ratio is highest, as might be expected, near the brittle, water-bearing zones in the Rustler (i.e., stratabound
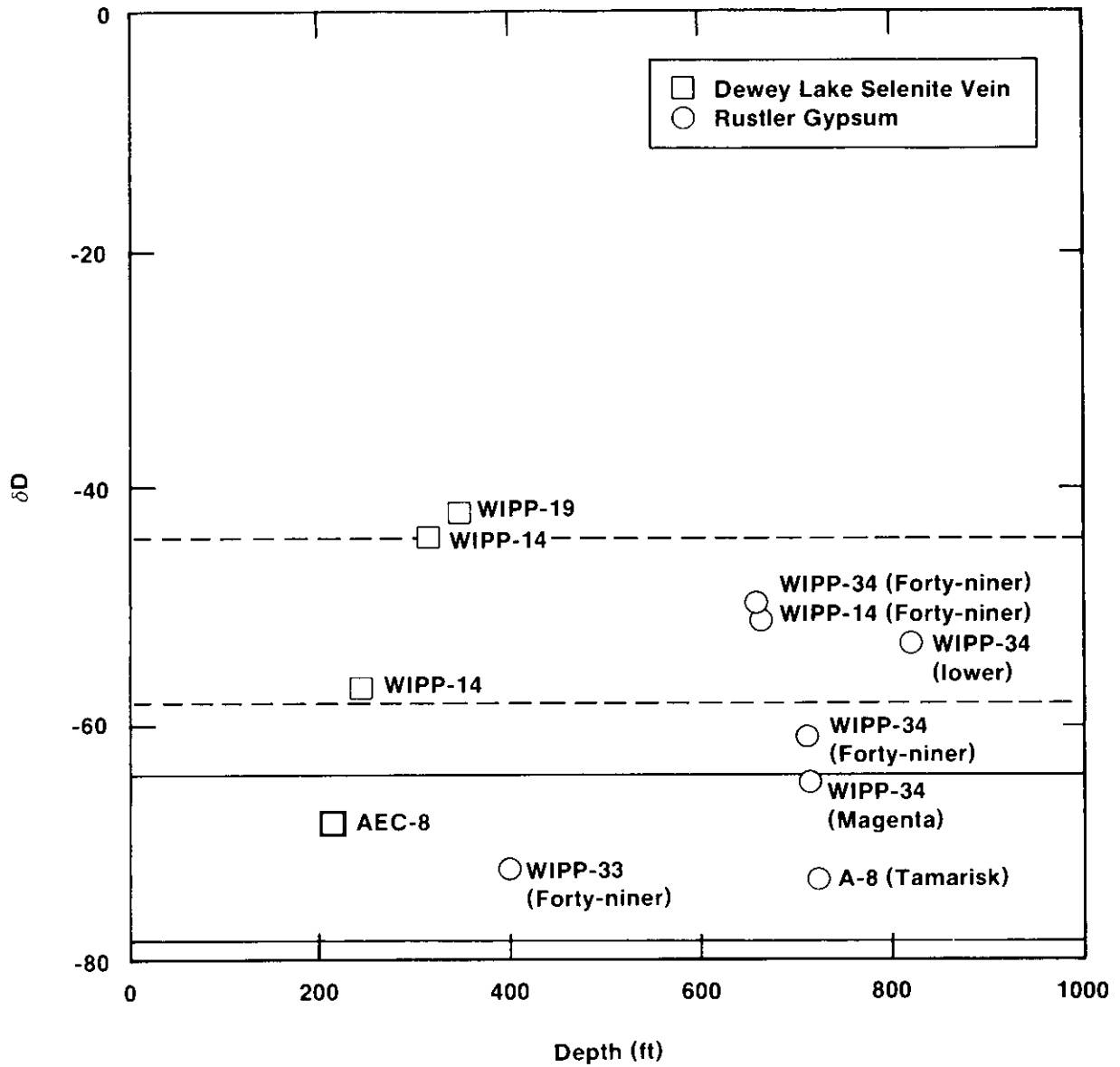
Figure 1-32. δD values of the water of crystallization in gypsums as a function of depth (Figure 19A from Lambert, Chapter 5).

TRI-6341-17-0

dolomitic layers), but diminishes with distance from such a zone. This shows that recharge has not taken place vertically from the surface. The vertical variations in D/H ratio, together with the minimal surficial component of Sr, suggest that groundwater flow within the Rustler near the WIPP Site is largely stratabound, having been recharged where near-surface exposures of water-bearing units can receive infiltration and subsequently having moved laterally.

1.5 DISCUSSION

A primary objective of this study is to determine if the spatial distribution of solutes is consistent with the hydrologic flow directions predicted independently by hydrogeologic studies assuming steady-state confined flow. Ancillary questions concern the time scale on which the Culebra dolomite may be considered confined and the time scale on which the flow within the Culebra may be considered transient.

The observed distribution of solutes in a hydrologic flow field is determined in part by the location and magnitude of solute fluxes from potential sources and to potential sinks. Section 1.5.1 describes a model for the chemical evolution of waters in the Culebra that tentatively identifies the mineralogical sources and sinks for many of the solutes. Resolution of the questions of transience and confined flow is addressed in Section 1.5.2. This involves examination of isotopic ratios and the distribution of diagnostic minerals to differentiate the independent histories of the solutes, water molecules, and mineral phases in the Culebra.

1.5.1 Processes Affecting Groundwater Composition

Two common sources of solutes in groundwater are addition of species by mixing with more saline waters and leaching or dissolution of solutes from the rock matrix. An apparent addition of solutes to groundwater will also occur during evaporation. Sinks for solutes include precipitation, coprecipitation, sorption, and ion-exchange; dilution of a concentrated solution by a dilute groundwater will also lead to an apparent loss of solutes.

Table 1-4 lists some of the processes and resulting effects that may have influenced the compositions of groundwater in the Culebra. The relative importance of these processes is discussed in the following sections.

1.5.1.1 Summary of Solute Relationships

The following solute relationships are described in the preceding sections of this chapter and in Chapter 2:

- Increases in the concentrations of Na, Cl, Ca, Mg, K, SO_4, Br, B, and Li with ionic strength; this relationship is illustrated by the "salinity factor" described in Section 1.4.3.

- The near-perfect saturation of the solutions with respect to gypsum over the entire range of ionic strength.

- The increase in the Mg/Ca ratio as the ionic strength increases (see Figure 1-12).

- The negative correlation between pH and bicarbonate alkalinity observed after the effects of salt dissolution are factored out. This relationship is most clearly indicated by the silicate/bicarbonate factor described in Section 1.4.3.

- The apparent supersaturation of dolomite; although potential loss of CO_2 gas during sampling introduces uncertainty into calculation of saturation indices of individual carbonates, the relationship between saturation indices for calcite and dolomite indicates that the degree of dolomite supersaturation increases with ionic strength (see Figure 1-20).

- The correlation of Mg with SiO_2 and the negative correlation of SiO_2 with Li and B that is observed after the effects of salt dissolution are factored out. This relationship is also clearly indicated by the silicate/bicarbonate factor.

Table 1-4. Chemical Processes That May Affect the Solute Compositions of Culebra Groundwaters

Chemical Process	Potential Effect(s) on Concentrations of Solutes in Culebra Groundwaters
Halite dissolution	Increase Na, Cl, Br, Li; decrease Cl/Br; increase solubility of carbonates and sulfates up to 3 molal ionic strength and then decrease solubility causing changes in Ca, Mg, SO_4, CO_3
Precipitation/dissolution of gypsum	Decrease/increase Ca, SO_4
Precipitation/dissolution of calcite and dolomite	Decrease/increase Ca, Mg, CO_3
Dolomitization:[1] calcite + Mg → dolomite + Ca	Decrease Mg/Ca ratio
Dedolomitization:[1] dissolution of gypsum and dolomite with concurrent precipitation of calcite.	Decrease pH, alkalinity, SO_4; must maintain Mg/Ca molar ratio < 1
Sorption/desorption by clays	Loss/gain of Li and B by solution
Mixing of connate hypersaline formation water with recharge water that has dissolved gypsum[2]	Increase Mg, Ca, K, Na, Cl; decrease SO_4, Cl/Br ratio
Incongruent dissolution of polyhalite	Increase Mg, K, SO_4; decrease Ca, Cl/Br ratio
Dissolution of silicates	Increase Si, Mg, Na
Dissolution of anhydrite with sellaite inclusions	Increase Ca, SO_4, Mg, F

1. Process may be important locally, as for example, at WIPP-33.
2. Process discussed in Chapter 4.

In Chapter 2, Siegel et al. suggest that these solute relationships are consistent with the following processes: (1) solutes are added to the Culebra brines by dissolution of evaporite minerals; (2) the solubilities of gypsum and calcite increase as the salinity increases; these minerals dissolve as chemical equilibrium is maintained between them and the groundwater; (3) equilibrium is not maintained between the waters and dolomite; sufficient Mg is added to the waters by dissolution of accessory carnallite or polyhalite so that the degree of dolomite supersaturation increases with ionic strength; and (4) clays within the fractures and rock matrix exert some control on the distribution of Li, B, Mg, and Si via sorption, ion exchange, and dissolution.

1.5.1.2 Precipitation and Dissolution of Carbonates, Sulfates, and Evaporite Salts

As discussed in Section 1.4.6, the first three of the above processes might be indicative of a partial equilibrium system in which solution/mineral equilibria shift nearly reversibly in response to increases of salinity due to dissolution of evaporite salts in rock units adjacent to the Culebra. The solubilities of gypsum, calcite, and dolomite increase with salinity up to 3 molal ionic strength and then decrease. Thus, even if the saturation indices for gypsum and calcite are near zero, the waters may still be capable of dissolving significant amounts of these phases as the salinity increases. Reaction path calculations show that addition of solutes (Mg, SO_3, K, and Cl) to the Culebra from evaporite minerals such as polyhalite and carnallite in a partial equilibrium system is consistent with the observed groundwater compositions if dolomite does not precipitate from supersaturated solutions.

The results of the reaction path calculations are in qualitative agreement with the SNORM calculations described by Bodine et al. in Chapter 4. In particular, the SNORM calculations show that the saline waters in Zone A all have appreciable $MgCl_2$, $MgSO_4$, and KCl components. This normative signature may be the result of dissolution of the assemblage halite/carnallite/polyhalite or mixing of a primitive brine with halite-dissolution water.

Isotopic studies of minerals and waters provide some support for this model. Stable-isotope compositions of carbonates indicate no recrystallization of dolomite in equilibrium

with the groundwater now found in the Culebra, but local precipitation of calcite, at the expense of dolomite, has apparently occurred in WIPP-33 Culebra. Dissolution of dolomite is possible, but would leave neither a mineralogical nor an isotopic record.

Although the reaction path models predict dissolution of gypsum in response to increases in salinity, reprecipitated gypsum appears to be quite common within the Rustler. The cationic origins of anhydrite and gypsum in the Rustler, including Culebra gypsum, are largely marine, with little contribution from surface weathering sources, as indicated by their $^{87}Sr/^{86}Sr$ ratios (Figure 1-31). Hence, the calcium sulfate was not imported by dissolution in a near-surface weathered recharge zone, but is of local origin. The variations in D/H ratios in the waters of crystallization of Rustler gypsum, however, do attest to recrystallization in the presence of meteoric water. Although most of the dissolved calcium sulfate originated locally within the evaporite section, the solid calcium sulfate hydrated in response to influx of meteoric water (Figure 1-32). Thus, the isotopic data can be reconciled with the results of the reaction path modeling if it assumed that sufficient anhydrite is hydrated to replace the gypsum that dissolves in response to the salinity increase.

1.5.1.3 Reactions Involving Silicates

The contribution of solutes from silicates is difficult to establish. In the southern part of the study area (Zone B), the salt norms indicate alkali-carbonate and/or alkali sulfate assemblages, consistent with silicate hydrolysis (Bodine et al., Chapter 4). In addition, the results of the PCAs described by Siegel et al. in Chapter 2 suggest that reactions with clay minerals may exert an observable influence on the water's minor-element chemistry throughout the study area. When the effects of solute addition associated with halite dissolution are factored out prior to the PCA, a $Mg-SiO_2$-alkalinity association is left which is negatively correlated with a pH-B-Li association. As discussed in Chapter 2, these correlations (the silicate/bicarbonate factor) are consistent with several plausible mechanisms, including uptake of Li by vacant octahedral sites in the clay lattice, sorption of

B by surface sites (SOH) of clays (reaction 1), and dissolution of a reactive amorphous Mg-rich layer $(MgSiX_{(am)})$ in corrensite (reaction 2):

$$SOH + B(OH)_4^- + H^+ \rightleftarrows SOH_2^+ B(OH)_4^- \qquad [1]$$

$$MgSiX_{(am)} + 2H_2O + 2H^+ \rightarrow Mg^{+2} + H_4SiO_4 \; . \qquad [2]$$
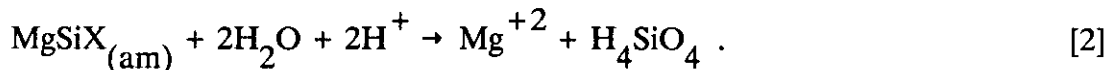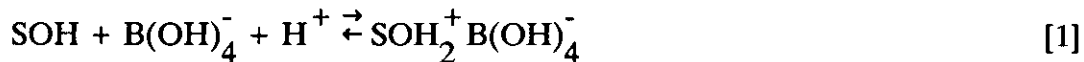
The importance of this factor is greatest in the western and southern parts of the site, where dissolution of evaporite salts may have left residues relatively enriched in clays. A survey of the literature provides ample evidence that sorption of boron and lithium and release of magnesium and silica from clays in saline waters is possible (Siegel et al., Chapter 2). However, geochemical and mineralogical evidence either supporting or contradicting this model for the WIPP is ambiguous. The PCA of minor-element data suggests that some degree of silicate hydrolysis has influenced the hydrochemistry throughout the Culebra; however, in more saline waters (Zone C) the normative salts suggestive of silicate hydrolysis are absent (Bodine et al., Chapter 4). This inconsistency may be related to the small data set used in the PCA or due to the masking of the normative signature by subsequent massive dissolution of halite and other readily soluble evaporites.

This controversy might be resolved by a systematic examination of the chemical and isotopic compositions of mineral samples from highly transmissive zones (containing core rubble rather than intact core), examination of the geochronological systematics (e.g., Rb/Sr) of the clays, more rigorous calculations of the extent of mass transfer that could result from ion exchange and sorption, and application of factor analysis to a larger data set of chemical analyses.

1.5.2 Consistency Between Solute and Isotope Distributions and Hydrologic Flow

1.5.2.1 Steady-State Versus Transient Flow

Ramey (1985) and Chapman (1988) observed that if the Culebra is a confined aquifer at steady state, present-day regional water-flow directions are not consistent with the salinity distribution at the WIPP Site, given the assumption of steady-state confined flow. These observations were based on the compositions of water samples analyzed as of 1983 by the USGS and on data gathered by the New Mexico EEG. The more extensive data set examined in this study confirms these observations. As shown in Figures 1-5, 1-6, and 1-33, Zone B (a facies with low salinity and element ratios inconsistent with halite dissolution) lies downgradient from more saline water in Zone C. Flow within Zone C (but not from Zone C to Zone B) may be consistent with progressive addition of solutes from dissolution of halite in the lower member; however, the lack of a fully coupled flow and transport model does not at this time allow quantitative mass balance calculations to be made along the hydrologic flow paths inferred from physical measurements.

The inconsistencies between the steady-state confined-flow hydrologic model and geochemical interpretations might be reconciled by considering the differences in the time scales reflected by the computed hydrologic flow field, isotope ratios, and spatial distributions of solutes and minerals. Specifically, the assumption of steady-state confined flow may be adequate on the 100-year time scale of hydrologic testing and disturbances related to the construction of the WIPP shafts. However, measurements of modern head potentials, transmissivities, and/or fluid densities do not give any direct indication of time scales on which the system might be transient. In fact, the isotopic data suggest that transient phenomena have taken place over the past 10,000 to 20,000 years in response to climatic change. Similarly, the observation that the Culebra is confined on the time scale of hydrologic testing does not ensure that vertical flux is negligible on a time scale measured in millennia. As discussed below, mineralogical and isotopic data are required to assess the
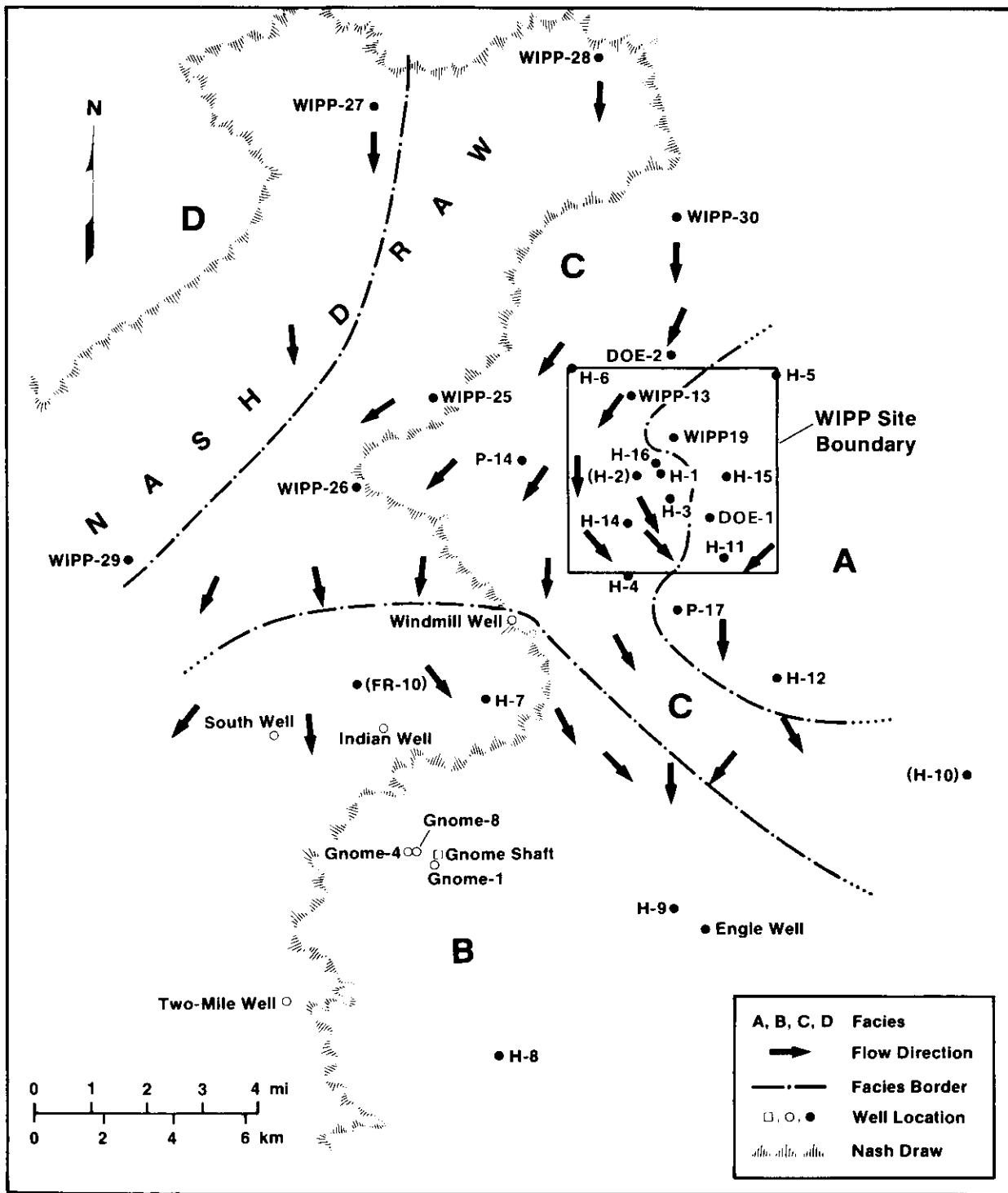
TRI-6331-77-0

Figure 1-33. Relationship between hydrological flow and hydrochemical facies of the Culebra dolomite. Compositions of waters in each zone represented by solid black circles are described in Figure 1-10. Compositions of several other wells (see Chapter 4) indicated by open circles were not included in the original data used to define the facies, but their compositions are consistent with the facies borders.

1-93

magnitude of the vertical fluxes of solutes and water into the Culebra over the 10,000-year time period of interest.

In Chapter 5, Lambert suggests that the apparent inconsistency between the steady-state hydrologic model and solute distribution pattern can be explained by a change in flow direction during the last 30,000, or perhaps 12,000 years. As discussed above, the hydrologic balance has changed since the Pleistocene, and groundwater currently flows in a southwesterly direction. Evidence for a change in flow direction consists partly of the available uranium-isotope disequilibrium data. The uranium-isotope disequilibrium model assumes reducing conditions, whereas the Eh values calculated for Culebra waters are interpreted by Myers et al. in Chapter 6 to indicate that oxidizing conditions may prevail at the present. The sensitivity of the uranium isotopic model to the disequilibria must be known before the significance of this possible inconsistency can be assessed. Even if oxidized uranium species predominate in parts of the Culebra at present, reduced species may have been abundant during the development of the observed high $^{234}U/^{238}U$ activity ratios.

1.5.2.2 The Origin of the Southern Low-Salinity Zone

In Chapter 6, Myers et al. suggest that redox conditions in the southern portion of the study area are more oxidizing than in the north. They further suggest that this is indicative of preferential vertical recharge in the south, accounting for dilution of more saline brine apparently flowing from the north. This conclusion is based primarily on the presence of detectable nitrate and lack of detectable ammonium in the south and the presence of detectable ammonium and lack of detectable nitrate to the north. However, as discussed by Robinson in Appendix 6A, these observations may be analytical artifacts related to interference by solutes in the saline brines in the northern and eastern parts of the study area. Moreover, the available radiocarbon model age in the southerly, less saline zone (Zone B, including Engle and H-9 wells), is no younger than in the northerly, more saline zone (Zone C, H-4 and H-6 wells), and thereby argues against dilution by modern vertical recharge in the south. Similarly, model ages are no older in the south, arguing against a

monotonic north-to-south, steady-state flow persisting since the Pleistocene. The one available radiocarbon age from the Dewey Lake Red Beds overlying the Rustler is consistent with this interpretation. The stable isotope characteristics of the Dewey Lake, however, are consistent with the interpretation that waters at least 12,000-16,000 years old and waters representing modern meteoric recharge in the area may be present in this unit.

Steady-state, north-to-south confined flow would not have preserved the lower-salinity zone downgradient from the saline zone (Figure 1-33). The lower-salinity zone could have arisen if the regional flow direction originally had a significant westerly component, as suggested by the generally eastward-increasing $^{234}U/^{238}U$ activity ratios discussed above. Similarities in radiocarbon age in the north and the south are consistent with water recharging both north and south parts of the WIPP area simultaneously from a near-surface Pleistocene infiltration zone in the west-northwest (Figure 1-34), groundwater at one time flowing locally subparallel rather than subnormal to the hydrochemical facies boundary between Zones B and C. Pleistocene recharge from the west-northwest is consistent with the present orientation on the Zone B/C hydrochemical facies boundary, similar radiocarbon ages in Zones B and C, eastward-increasing uranium isotope activity ratio values, and some, but not all, of the calculated modern Darcian flow vectors. This generalized paleoflow pattern during recharge is not consistent with either recharge from due north, or monotonic southward steady-state flow. A likely paleorecharge zone is nearby in surface outcrops of the Rustler Formation to the west in Nash Draw. Although it was once proposed that recharge for water now flowing in the Rustler near the WIPP Site and Nash Draw takes place as far north as Bear Grass Draw (Robinson and Lang, 1938), there is neither need nor geochemical support for such a proposal. In fact, recent work by Hunter (1985) suggests that Rustler flow from Bear Grass Draw southward toward the WIPP area may be intercepted by a major discharge zone in Clayton Basin.

A likely explanation for the less saline waters of Zone B is that at the time of influx of the present generation of Culebra groundwater in late Pleistocene time, Rustler halite was absent adjacent to the Culebra in this area, thus not providing a source of NaCl. This is
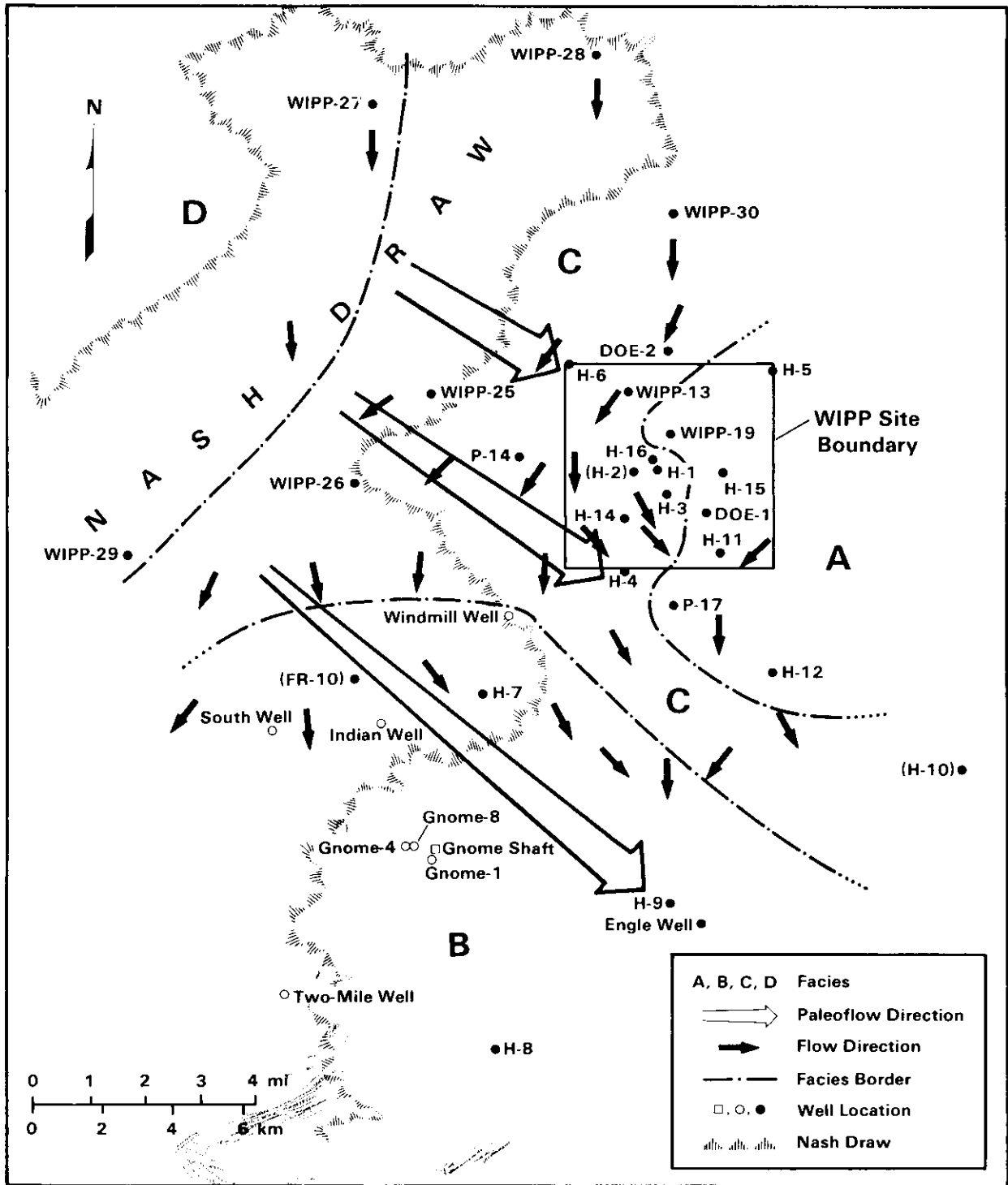
TRI-6330-78-1

Figure 1-34. Paleoflow (late Pleistocene) directions for groundwater in the Culebra member of the Rustler Formation from likely recharge areas on outcrops in Nash Draw. Paleoflow directions are superimposed on hydrochemical facies boundaries and modern flow directions interpreted from numerical modeling of physical hydrology measurements.

1-96

consistent with the present-day correlation of halite occurrence in the Rustler and the hydrochemical facies pattern (Figure 1-13). The halite might never have been deposited in the south, or pre-existing halite may have been removed by earlier dissolution during the development of the southeastern lobe of Nash Draw, which is included in Zone B. This dissolution, however, would have taken place in response to an episode of groundwater flow older than the present regime that began as early as 16,000 years ago. This older episode of dissolution could have occurred as early as 600,000 years ago, in a time of wetter climate while Nash Draw was still forming as part of the channel system of the ancestral Pecos River (Bachman, 1980). It is also conceivable that the zone of higher Culebra transmissivity south of the WIPP Site (Lappin, 1988) toward the southeastern lobe of Nash Draw is simply a manifestation of the same processes that have contributed to the widening of Nash Draw. Such processes are apparently responsible for an increasing transmissivity west of the WIPP Site toward the central axis of Nash Draw. By logical extension, it is likely that similar processes have created a "fringe" zone of increased transmissivity for some distance outward in all directions from various parts of Nash Draw (beyond its marginal scarp), including the southeastern lobe.

A karstic fringe zone along a stretch of the ancestral (Tertiary/Pleistocene) Pecos River further south was proposed by Bachman (1984) as a consequence of evaporite dissolution adjacent to the stream channel. There the thickness of the saturated zone approached 1500 ft, in which groundwater lost by upgradient seepage from the stream system dissolved halite throughout the Salado Formation and discharged downgradient. A similar mechanism may have acted on a smaller scale to dissolve evaporites adjacent to the Nash Draw stream system during the Pleistocene, contributing to the development of a marginal zone of enhanced transmissivity locally extending as far east as the WIPP Site. If the water table in the late Pleistocene (at the apparent time of latest Culebra recharge) was at an elevation (about 2977 ft) comparable to that reported for the water table that has arisen from historic potash-brine dumping in Nash Draw (Hunter, 1985), Nash Draw was a possible recharge area for the Culebra, because the base of the Culebra at known points east of Nash Draw is at lower elevations.

1.5.2.3 Zonation of Normative Solute Characteristics

The results of Bodine et al. (Chapter 4) suggest that the salt norm distribution is generally consistent with the generalized zonation of solute distributions proposed by Ramey (1985) and further developed by Siegel et al. in Chapter 2. The conceptual model reported by Bodine et al. for Rustler solute distributions involves varying degrees of dilution of primitive-diagenetic brines similar to that found in the low-permeability, halite-rich strata east of the WIPP Site (e.g., P-18 in Zone A; see Figure 1-2). P-14 Culebra water also displays a primitive-diagenetic solute norm. The diluent proposed to have infiltrated from the surface (e.g., recharge fluid) has normative solute characteristics similar to those of waters sampled from the siliciclastic alluvium in WIPP-15 (see Figure 1-2). Hydrolysis of feldspars undergoing weathering in channel deposits of the Gatuña Formation (described by Bachman, 1985) north and west of the WIPP Site is a potential source of solutes bearing a $Na-HCO_3$ or $-SO_4$ normative signature. This alkali-carbonate or -sulfate norm is preserved in Zone B, represented by waters from H-7, -8, and -9 south of the WIPP Site. Fresh waters infiltrating through this weathering zone acquired this solute assemblage, and dissolved halite and anhydrite/gypsum in the Rustler, giving norms characteristic of such dissolution (Zone C). In such dissolution brines, the alkali-carbonate or -sulfate norm may not be preserved. Increasing proportions of recharge water have mixed with the primitive water with increasing distance from P-18 and P-14. Note, however, the anomalous position of the primitive-diagenetic solute norm at P-14, which lies within Zone C rather than Zone A. This suggests that either Zone A-type solutes were at one time more widespread, or that the primitive-diagenetic norm at P-14 is more locally controlled.

The mixing/dilution model of Bodine et al. in Chapter 4 relies heavily on extensive recharge at some time (vertical, lateral, or both), especially in the southern part of the site, to provide the fluids which dilute a pre-existing, perhaps regionally pervasive, primitive-diagenetic signature. The timing of such recharge, however, is unspecified by the model. The isotopic, mineralogic, and hydrologic data discussed in other sections of this report suggest that vertical recharge to the Culebra in the WIPP area and to the east has not occurred for several thousand years.

1.5.2.4 The Degree of Hydraulic Versus Geochemical Confinement

Hydrologic testing has revealed that on the time scale of a few months the Culebra is hydrologically confined at all sites that have been sampled, except WIPP-25, WIPP-26, and WIPP-29. Generally, the hydraulic relationships suggest only limited vertical connection between the Culebra and overlying strata. Whereas hydraulic measurements can quantify short-term responses of the hydrologic flow system to transient pressure pulses such as slug- and pump-testing, geochemical measurements are more related to mass transport and rock/water interactions that take place over longer periods, up to several thousand years.

Several geochemical observations are relevant to the degree of confinement of the Culebra waters over long periods of time. First, available radiocarbon ages in the Culebra are in excess of 12,000 to 16,000 years. The three model ages (at H-6, H-4, and H-9) were determined at localities that effectively "bracket" the WIPP Site on the north and south. The lack of a statistically significant difference among these ages, and the lack of a north-south gradient in apparent age suggest either that rates of vertical infiltration at each location have been virtually identical, or that lateral flow times to each location from the surface-recharge area(s) have been virtually identical. Given the significant geological differences in the Culebra environment among the three localities, the first prospect is unlikely. The second prospect is more consistent with the available uranium-isotope and solute data, especially considering the significant differences in solutes among the three sampling localities. Similarly, the absence of a statistically significant vertical gradient in apparent age in the south (14,900 years in the Culebra at H-9 versus 14,000 years in the overlying Dewey Lake at the nearby Pocket well) is inconsistent with a significant degree of modern vertical infiltration there. In any case, groundwater has been isolated from the atmosphere for about the same length of time at all three points in the Culebra.

Second, the preservation of extensive amounts of anhydrite and a varying water/rock ratio during partial gypsification in the nondolomitic Rustler units overlying the Culebra suggest that significant amounts of water have not permeated vertically from the surface to recharge the Culebra where thick beds of overlying anhydrite are preserved. As noted by

Beauheim (1987), at two points the modern Magenta head is higher than that in the overlying Forty-niner, precluding a direct throughgoing connection between the surface and the Culebra in at least parts of the WIPP area at the present time (see Figure 1-7).

Third, strontium isotope data suggest that vertical material transport from the surface to layers underlying the Dewey Lake Red Beds has not been extensive. Even at the localities of suspected vertical solution or fracture channels (e.g., WIPP-14, WIPP-33, and WIPP-34), the $^{87}Sr/^{86}Sr$ ratios in the partially gypsified anhydrites of the Forty-niner and Tamarisk members indicate minimal admixture of surface-type strontium having a high $^{87}Sr/^{86}Sr$ ratio, a moderate amount of such admixture in the Culebra, and extensive admixture in the Dewey Lake. This stratification of strontium constitutes evidence of minimal mass transport across the Rustler/Dewey Lake contact, while allowing lateral transport of some surface-type strontium through the Culebra from its near-surface exposures.

Finally, at certain localities previously suspected to represent karst conduits (e.g., WIPP-14 and WIPP-34) the water/rock ratios in gypsiferous horizons adjacent to the water-bearing dolomites are significantly lower than in the dolomites themselves, as suggested by the D/H ratios of gypsum and of various groundwaters. Such variations in the water/rock ratio are consistent with some water having escaped from the dolomite into adjacent beds (perhaps acquiring some solutes from halite dissolution). These variations are not consistent with water migrating downward into the Culebra, during which water would first pass through a region of low water/rock ratio without having affected the gypsification of overlying anhydrite. If this were a significant mechanism of recharge to the Culebra, the stable-isotope composition of Culebra waters would exhibit a measurable shift away from meteoric values as a result of water/rock interaction in a zone of low water/rock ratio.

1.6 SUMMARY

Based on the available data on formation pressures, fluid density distribution, and transmissivities, modern flow within the Culebra at and near the WIPP Site appears to be largely

north-to-south, except in relatively low-transmissivity areas directly affected by either the high-transmissivity zone in the southeastern portion of the WIPP Site or by Nash Draw west of the WIPP Site. The amount of possible vertical flow into and out of the Culebra near the center of the WIPP Site remains indeterminate.

These present-day regional water flow directions are not consistent with the salinity distribution at the WIPP Site, given the assumption of steady-state, confined flow. Zone B, a hydrochemical facies with low salinity and element ratios inconsistent with halite dissolution, lies downgradient from more saline water in Zone C. In addition, the isotopic data presented in this report further indicate that inferences about flow direction and velocity obtained from measurements of modern head potentials and transmissivities may not be applicable to directions and velocities in the past 10,000 years, or in the next 10,000 years-- the interval of interest to regulatory agencies governing radioactive-waste repositories.

In Chapter 5, Lambert suggests that this apparent anomaly can be explained by a change in flow direction in the last 30,000, or perhaps 12,000 years. Prior to that time, the recharge direction was dominantly from the west-northwest. In Chapter 4, Bodine et al. suggest that solute distribution is derived by mixing of (perhaps originally widespread) primitive-diagenetic brines now found mostly in the low-permeability, halite-rich strata east of the WIPP Site, with recharge water that has infiltrated from the surface and dissolved halite and anhydrite/gypsum. The isotopic, mineralogic, and hydrologic data discussed in other chapters of this report, however, suggest that vertical material transport into the Culebra in the WIPP area and to the east and south has not occurred to a significant degree for several thousand years (see Chapter 5). The SNORM results are not inconsistent with the isotopic results if the recharge component proposed in Chapter 4 moved from its paleorecharge area (Rustler outcrops in Nash Draw), where it acquired its alkali-carbonate/sulfate signature, thence laterally (stratabound) toward the east-southeast, preserving isotopic indicators of age (radiocarbon) and paleoflow direction (uranium). Such a paleoflow direction from nearby paleorecharge areas could also have resulted in the

preservation of the northwest-southeast orientation of the hydrochemical facies transition zone between Zones B and C.

Waters in the Culebra are undersaturated with respect to halite and anhydrite and saturated with respect to gypsum. Evaluation of water/carbonate (calcite and dolomite) equilibria is hindered by uncertainties in pH related to potential loss of CO_2 gas during sample collection. A model for the chemical evolution of water in the Culebra proposed by Siegel et al. in Chapter 2 suggests that dissolution of salt and concomitant changes in mineral solubilities constitute an important irreversible process affecting water chemistry. Na, Cl, Mg, K, and SO_4 are added to the Culebra by dissolution of evaporite salts in adjacent strata. Equilibrium is maintained with gypsum and calcite, but dolomite supersaturation increases as the salinity of the water increases. Isotopic studies of minerals and waters provide some support for this model.

Controls on the distribution of minor and trace elements are more problematical. For waters of lower ionic strength, the contribution of solutes from silicates may be more important. The results of the PCA described by Siegel et al. in Chapter 2 suggest that reactions with clay minerals may exert an observable influence on the distribution of SiO_2, Mg, Li, and B throughout the entire study area.

1.7 REFERENCES

Allison, G. B. 1982. "The Relationship between ^{18}O and Deuterium in Water in Sand Columns undergoing Evaporation." *Journal of Hydrology*, Vol. 55:163-169.

Allison, G. B., W. J. Stone, and M. W. Hughes. 1985. "Recharge in Karst and Dune Elements of a Semi-arid Landscape as Indicated by Natural Isotopes and Chloride." *Journal of Hydrology*, Vol. 76:1-25.

Bachman, G. O. 1980. *Regional Geology and Cenozoic History of the Pecos Region, Southeastern New Mexico.* Open File Report 80-1099. Denver, CO: US Geological Survey.

Bachman, G. O. 1981. *Geology of Nash Draw, Eddy County, New Mexico.* Open File Report 81-31. Denver, CO: US Geological Survey.

Bachman, G. O. 1984. *Regional Geology of the Ochoan Evaporites, Northern Part of the Delaware Basin.* Circular 184. Socorro, NM: Bureau of Mines and Mineral Resources.

Bachman, G. O. 1985. *Assessment of Near-Surface Dissolution at and near the Waste Isolation Pilot Plant (WIPP), Southeastern New Mexico.* SAND84-7178. Albuquerque, NM: Sandia National Laboratories.

Barr, G. E., S. J. Lambert, and J. A. Carter. 1979. "Uranium Isotope Disequilibrium in Groundwaters of Southeastern New Mexico and Implications Regarding Age-Dating of Waters." *Proceedings of the International Symposium on Isotope Hydrology.* Vol 2. STI/PUB/493. Vienna, Austria: International Atomic Energy Agency. 645-660.

Beauheim, R. L. 1987. *Interpretations of Single-Well Hydraulic Tests Conducted at and near the Waste Isolation Pilot Plant (WIPP) Site, 1983-1987*. SAND87-0039. Albuquerque, NM: Sandia National Laboratories.

Bodine, M. W., Jr., and B. F. Jones. 1986. *The Salt Norm: A Quantitative Chemical-Mineralogical Characterization of Natural Waters*. Water Resources Investigation Report 86-4086. Reston, VA: US Geological Survey.

Brookins, D. G., and S. J. Lambert. 1987. "K-Ar and Rb-Sr Age Determinations from Clay Minerals and Related Minerals from the WIPP (Waste Isolation Pilot Plant), Southeastern New Mexico." *Isochron/West* No. 49:4-7.

Brookins, D. G., and S. J. Lambert. 1988. "WIPP Site Studies: Secondary Selenite Veins in the Rustler Formation and Dewey Lake Red Beds." *Materials Research Society Symposium Proceedings*. Vol. 112:233-241.

Brookins, D. G., J. K. Register, and H. Krueger. 1980. "Potassium-Argon Dating of Polyhalite in Southeast New Mexico." *Geochimica et Cosmochimica Acta*, Vol. 44:635-637.

Chapman, J. B. 1988. *Chemical and Radiochemical Characteristics of Groundwater in the Culebra Dolomite, Southeastern New Mexico*. EEG-39. Santa Fe, NM: New Mexico Environmental Evaluation Group.

Craig, H., L. I. Gordon, and Y. Horibe. 1963. "Isotopic Exchange Effects in the Evaporation of Water, I: Low-Temperature Experimental Results." *Journal of Geophysical Research*, Vol. 68:5079-5087.

Deer, W. A., R. A. Howie, and J. Zussman. 1962. *Rock-Forming Minerals.* Vol. 3, *Sheet Silicates.* Vol. 4, *Framework Silicates.* Vol. 5, *Non-Silicates.* London: Longman.

Evans, G. V., R. L. Otlet, R. A. Downing, R. A. Monkhouse, and G. Rae. 1979. "Some Problems in the Interpretation of Isotope Measurements in United Kingdom Aquifers." *Proceedings of the International Symposium on Isotope Hydrology,* Vol. 2. STI/PUB 493. Vienna, Austria: International Atomic Energy Agency. 679-706.

Fleischer, M. 1987. *Glossary of Mineral Species.* Tucson, AZ: the Mineralogical Record, Inc.

Haug, A., V. A. Kelly, A. M. LaVenue, and J. F. Pickens. 1987. *Modeling of Ground-Water Flow in the Culebra Dolomite at the Waste Isolation Pilot Plant (WIPP) Site.* SAND86-7167. Albuquerque, NM: Sandia National Laboratories.

Helgeson, H. C. 1968. "Evaluation of Irreversible Reactions in Geochemical Processes Involving Minerals and Aqueous Solutions. I. Thermodynamic Relations." *Geochimica et Cosmochimica Acta.* Vol. 32:853-877.

Hunter, R. L. 1985. *A Regional Water Balance for the Waste Isolation Pilot Plant (WIPP) Site and Surrounding Area.* SAND84-2233. Albuquerque, NM: Sandia National Laboratories.

Isaacson, R. E., L. E. Brownell, R. W. Nelson, and E. L. Roetman. 1974. "Soil-Moisture Transport in Arid Site Vadose Zones." *Proceedings of the International Symposium on Isotope Hydrology:*97-114.

Lambert, S. J. 1978. "Geochemistry of Delaware Basin Groundwaters." *Geology and Mineral Deposits of Ochoan Rocks in Delaware Basin and Adjacent Areas.* Ed. G. S. Austin. Circular 159. Socorro, NM: New Mexico Bureau of Mines and Mineral Resources. 33-38.

Lambert, S. J. 1983. *Dissolution of Evaporites in and Around the Delaware Basin, Southeastern New Mexico and West Texas.* SAND82-0461. Albuquerque, NM: Sandia National Laboratories.

Lambert, S. J. 1987. *Feasibility Study: Applicability of Geochronologic Methods Involving Radiocarbon and Other Nuclides to the Groundwater Hydrology of the Rustler Formation.* SAND86-1054. Albuquerque, NM: Sandia National Laboratories.

Lambert, S. J., and J. A. Carter. 1984. *Uranium-Isotope Disequilibrium in Brine Reservoirs of the Castile Formation, Northern Delaware Basin, Southeastern New Mexico. 1: Principles and Methods.* SAND83-0144. Albuquerque, NM: Sandia National Laboratories.

Lambert, S. J., and J. A. Carter. 1987. *Uranium-Isotope Systematics in Groundwaters of the Rustler Formation, Northern Delaware Basin, Southeastern New Mexico.* SAND87-0388. Albuquerque, NM: Sandia National Laboratories.

Lambert, S. J., and D. M. Harvey. 1987. *Stable-Isotope Geochemistry of Groundwaters in the Delaware Basin of Southeastern New Mexico.* SAND87-0138. Albuquerque, NM: Sandia National Laboratories.

Lambert, S. J., and K. L. Robinson. 1984. *Field Geochemical Studies of Groundwaters in Nash Draw, Southeastern New Mexico.* SAND83-1122. Albuquerque, NM: Sandia National Laboratories.

Lappin, A. R. 1988. *Summary of Site-Characterization Studies Conducted from 1983 Through 1987 at the Waste Isolation Pilot Plant (WIPP) Site, Southeastern New Mexico.* SAND88-0157. Albuquerque, NM: Sandia National Laboratories.

LaVenue, A. M., A. Haug, and V. A. Kelley. 1988. *Numerical Simulation of Ground-Water Flow in the Culebra Dolomite at the Waste Isolation Pilot Plant (WIPP) Site.* SAND88-7002. Albuquerque, NM: Sandia National Laboratories.

Mercer, J. W. 1983. *Geohydrology of the Proposed Waste Isolation Pilot Plant Site, Los Medaños Area, Southeastern New Mexico.* Water Resources Investigation Report 83-4016. Albuquerque, NM: US Geological Survey.

Mercer, J. W. and B. R. Orr. 1979. *Interim Data Report on the Geohydrology of the Proposed Waste Isolation Pilot Plant Site, Southeast New Mexico.* Water Resources Investigation Report 79-98. Albuquerque, NM: US Geological Survey.

Nativ, R., and D. A. Smith. 1987. "Hydrogeology and Geochemistry of the Ogallala Aquifer, Southern High Plains." *Journal of Hydrology*, Vol. 91:217-253.

Osmond, J. K., and J. B. Cowart. 1976. "The Theory and Uses of Natural Uranium Isotopic Variations in Hydrology." *Atomic Energy Review*, Vol. 14:621-679.

Parry, W. T., C. C. Reeves, Jr., and J. W. Leach. 1970. "Oxygen and Carbon Isotope Composition of West Texas Lake Carbonates." *Geochimica et Cosmochimica Acta*, Vol. 34:825-830.

Plummer, L. N. 1984. "Geochemical Modeling: A Comparison of Forward and Inverse Methods." *Proceedings First Canadian/American Conference on Hydrogeology.* Ed. B. Hitchen and E. I. Wallick. Worthington, Ohio: National Water Well Association.

Plummer, L. N., D. L. Parkhurst, G. W. Fleming, and S. A. Dunkle. 1988. "PHRQPITZ - A Computer Program for Geochemical Calculations in Brines." Water Resources Investigation unpublished report. Reston, VA: US Geological Survey.

Powers, D. W., S. J. Lambert, S. E. Shaffer, L. R. Hill, and W. D. Weart, ed. 1978. *Geological Characterization Report, Waste Isolation Pilot Plant (WIPP) Site, Southeastern New Mexico*. SAND78-1596. Albuquerque, NM: Sandia National Laboratories.

Ramey, D. S. 1985. *Chemistry of Rustler Fluids*. EEG-31. Santa Fe, NM: New Mexico Environmental Evaluation Group.

Randall, W. S., M. E. Crawley, and M. L. Lyon. 1988. *Annual Water Quality Data Report for the Waste Isolation Pilot Plant*. DOE-WIPP 88-006. Carlsbad, NM: Waste Isolation Pilot Plant Project Office.

Register, J. K., and D. G. Brookins. 1980. "Rb-Sr Isochron Age of Evaporite Minerals from the Salado Formation (Late Permian), Southeastern New Mexico." *Isochron/West*, No. 29.

Robinson, K. L. 1988. *Analysis of Solutes in Groundwaters from the Rustler Formation at and near the WIPP Site*. SAND86-0917. Albuquerque, NM: Sandia National Laboratories.

Robinson, T. W., and W. B. Lang. 1938. "Geology and Ground-Water Conditions of the Pecos River Valley in the Vicinity of Laguna Grande de la Sal, New Mexico, with Special Reference to the Salt Content of the River Water. *New Mexico State Engineer*. 77-100.

Snyder, R. P. 1985. *Dissolution of Halite and Gypsum, and Hydration of Anhydrite to Gypsum, Rustler Formation, in the Vicinity of the Waste Isolation Pilot Plant, Southeastern New Mexico*. Open File Report 85-229. Denver, CO: US Geological Survey.

Statistical Analysis System Institute. 1982. *SAS User's Guide: Statistics*.

Uhland, D. W., and W. S. Randall. 1986. *Annual Water Quality Data Report*. DOE-WIPP-86-006. Carlsbad, NM: Waste Isolation Pilot Plant Project Office.

Uhland, D. W., W. S. Randall, and R. C. Carrasco. 1987. *Annual Water Quality Data Report, March, 1987*. DOE-WIPP-87-006. Carlsbad, NM: Waste Isolation Pilot Plant Project Office.

United States Department of Energy and the State of New Mexico. 1988. "Agreement for Consultation and Cooperation between Department of Energy and the State of New Mexico on the Waste Isolation Pilot Plant: Updated April 18, 1988." Appendix II:3. On file at the Waste Management and Transportation Library, Sandia National Laboratories, Albuquerque, New Mexico.

Van Devender, T. R. 1980. "Holocene Plant Remains from Rocky Arroyo and Last Chance Canyon, Eddy County, New Mexico." *The Southwestern Naturalist*, Vol. 25:361-372.